

UNIVERSIDADE FEDERAL DO RIO GRANDE – FURG

PÓS-GRADUAÇÃO EM OCEANOGRAFIA BIOLÓGICA

Idade, crescimento e mudanças ontogenéticas
no uso de habitat da tartaruga-oliva
(*Lepidochelys olivacea*) no litoral de Sergipe

ROBERTA PETITET

Tese apresentada ao Programa de Pós-graduação em Oceanografia Biológica da Universidade Federal do Rio Grande - FURG, como requisito parcial à obtenção do título de doutor.



Rio Grande
Janeiro/2017

AGRADECIMENTOS

Primeiramente agradeço a minha família, que por mais longe que eles estão, sempre me apoiaram naquilo que eu acreditava. À minha mãe, que por mais que ela quisesse que eu voltasse para casa, me apoiou. Às minhas irmãs pela amizade incondicional. Ao meu pai, por ter me dado a força necessária para eu ter coragem de ganhar o mundo. E todo o resto de minha família pelo apoio.

Ao meu orientador Leandro Bugoni, pelo companheirismo e simplicidade. Apesar de ter enlouquecido comigo em alguns momentos, sempre acreditou em mim.

Ao pessoal do TAMAR de Sergipe que me deu todo apoio e ajuda durante as coletas e minhas idas à Pirambu. Muito obrigada Jaque, Beto, Nêne, Mari (s), Adriano, Buíu e César.

À Larisa Avens, pela sua simplicidade e força de vontade de me ajudar em todos os momentos que pedi ajuda.

Ao George Zug, pela sua simplicidade e me ajudado com os dados do primeiro capítulo de minha tese.

À Hannah Vander Zanden, por ter me ajudado no terceiro capítulo da tese.

À Fundação Mamíferos Aquáticos, pela ajuda nas coletas de amostras de úmeros.

Aos técnicos de laboratório, Leo e Claudio, por estarem sempre dispostos a me ajudar!!

À minha banca de acompanhamento Edu, Kinas e Manuel, que me ajudaram nessa jornada. E também à Silvina Botta e Agnaldo Martins pelas considerações relevantes durante a defesa da tese.

A todos os meus amigos cassineiros por me apoiarem nessa minha jornada!!

Muito obrigada Mari, Vane, Marcinha, Jony, Camila, Renatones, Baila, Dé, Diogão, Lú, Leo (de novo), Cilene, Lula!!

A uma pessoa muito especial que apareceu no final do doutorado, mas que fez toda diferença, Nicholas, que me deu força e acreditou em mim. Se não fosse ele acho que não teria tido a calma e concentração que tive no final.

E a todas as outras pessoas que me ajudaram durante esse período de pesquisa e estudo: MUITO OBRIGADO!!!

ÍNDICE

RESUMO.....	2
ABSTRACT.....	4
INTRODUÇÃO.....	6
OBJETIVOS.....	19
Objetivo geral.....	19
Objetivos específicos.....	19
HIPÓTESES.....	20
MATERIAL E MÉTODOS (versão resumida).....	21
Área de estudo.....	21
Métodos de amostragem.....	22
Determinação de idade.....	22
Uso de habitat.....	26
Especialização individual e consistência temporal.....	27
Análise estatística.....	28
SÍNTESE DOS RESULTADOS.....	28
Determinação de idade.....	28
Uso de habitat.....	29
Especialização individual e consistência temporal.....	30
CONCLUSÃO.....	31
BIBLIOGRAFIA CITADA.....	32
APÊNDICE I.....	43
APÊNDICE II.....	83
APÊNDICE III.....	132

LISTA DE APÊNDICES

APÊNDICE I – Age and growth of olive ridley sea turtles *Lepidochelys olivacea* in the main Brazilian nesting ground

APÊNDICE II – High habitat use plasticity by female olive ridley sea turtles (*Lepidochelys olivacea*) revealed by stable isotope analysis in multiple tissues

APÊNDICE III – Individual specialization and temporal consistency in resource use by olive ridley sea turtles (*Lepidochelys olivacea*) inferred by stable isotope analysis in humerus growth layers

RESUMO

A tartaruga-oliva, *Lepidochelys olivacea*, é a espécie de tartaruga marinha mais abundante, entretanto ainda classificada globalmente como vulnerável na lista de espécies ameaçadas de extinção. No entanto, pouco recurso é direcionado para a pesquisa desta espécie e, além disso, o seu ciclo de vida ocorrendo predominantemente no ambiente oceânico, dificulta seu estudo. No presente estudo realizou-se a determinação da idade de tartarugas-oliva encontradas encalhadas mortas no litoral de Sergipe, nordeste do Brasil, e áreas adjacentes pelo uso da técnica de esqueletocronologia no úmero. Ainda, elucidou-se o uso de habitat desta espécie no Brasil através da análise de isótopos estáveis (AIE) de carbono e nitrogênio (C e N) em múltiplos tecidos (células vermelhas, soro, epiderme e carapaça). E, por fim aplicou-se a AIE nas linhas de crescimento do úmero, a fim de determinar a consistência temporal e especialização individual da população de tartarugas-oliva do nordeste do Brasil. As tartarugas-oliva encontradas encalhadas mortas tiveram uma faixa etária entre 14 e 26 anos, maturando por volta dos 16 anos de idade. A AIE em múltiplos tecidos demonstrou que antes de se reproduzir esta espécie habita uma variedade de áreas de alimentação, tanto em águas oceânicas quanto também em águas neríticas, em uma escala de semanas a meses. Por sua vez, a AIE nas linhas de crescimento do úmero também demonstrou essa variedade de habitats, porém em uma escala temporal anual, ao longo de vários anos. Portanto, essa plasticidade gera uma alta variação individual dentro da mesma população tornando a população de tartaruga-oliva do nordeste do Brasil uma população generalista com indivíduos especialistas. Entretanto, devido a essa gama de

habitats utilizados pela população e suas principais ameaças, i.e. a captura incidental na pesca de arrasto no ambiente nerítico e a pesca de espinhel pelágico no ambiente oceânico, ocorrendo ao longo de todo o ciclo anual e ao longo da vida das tartarugas, é necessário estabelecer ações de conservação nas áreas de concentração dessas pescarias para reduzir a mortalidade.

PALAVRAS-CHAVE: conservação, consistência temporal, especialização individual, marca de crescimento esquelética, maturação, uso de habitat.

ABSTRACT

Olive ridley sea turtle, *Lepidochelys olivacea*, is the most abundant sea turtle species, but it is still globally classified as vulnerable in the list of threatened species. However, limited funds are directed to the research of this species and, due to its life cycle occurring predominantly in the oceanic environment, makes study difficult. In the current study age estimation of olive ridley sea turtles stranded dead on the coast of Sergipe state, northeastern Brazil, and adjacent areas had been carried out through the skeletochronology technique in the humerus bone. It also elucidated the use of habitat of this species in northeastern Brazil through stable isotope analysis (SIA) of carbon and nitrogen (C and N) in multiple tissues (red cells, serum, epidermis and scute). SIA in humerus growth lines was carried out in order to determine the temporal consistency and individual specialization of individuals composing the olive ridley population at northeastern Brazil. Olive ridleys stranded dead had age range between 14 and 26 years old, with an age at sexual maturity about 16 years old. SIA in multiple tissues has shown that before breeding, this species inhabits a variety of feeding areas, both in oceanic as well as in neritic waters, on a time scale from week to months. In humerus growth lines, on their turn, SIA also demonstrated a variety of habitats each year, along several years. This plasticity generates a high individual variation within the population, and consequently the olive ridley population of northeastern Brazil could be classified as a generalist population with specialist individuals. Moreover, the variety of habitats used by the population, and the main threats, i.e. bycatch in trawling fisheries in the neritic waters and longline fisheries in oceanic waters, occurring throughout

the annual cycle and its life, it is necessary to establish conservation actions focused on the reduction of mortality.

KEYWORDS: conservation, habitat use, individual specialization, maturation, skeletal growth mark, temporal consistency.

INTRODUÇÃO

Lepidochelys olivacea, conhecida popularmente como tartaruga-oliva, é a tartaruga mais abundante dentre as sete espécies de tartarugas marinhas existentes (Reichart, 1993). Esta espécie pertence à família Cheloniidae e é a de menor tamanho dentre as outras espécies da mesma família, com tamanho máximo de comprimento curvilíneo da carapaça (CCC) de 83,0 cm (Silva *et al.*, 2007). Seu nome comum é dado devido à cor “oliva” da carapaça (Fig. 1). A identificação desta espécie é relativamente fácil, pois a tartaruga-oliva possui de 5 a 9 pares de escudos laterais e centrais (Fig. 1).



Figura 1: Vista dorsal da tartaruga-oliva (*Lepidochelys olivacea*) demonstrando a disposição dos escudos da carapaça.

Fonte: <http://www.tamar.org.br/tartaruga.php?cod=21>

Esta espécie tem distribuição circunglobal, principalmente em águas quentes e tropicais (Reichart, 1993). A maior colônia de desova desta espécie no Oceano Atlântico sul se localiza no Gabão, oeste da África, seguido pelas colônias no Suriname/Guiana Francesa, Brasil e, por fim, colônias menores como em Angola e República do Congo (Metcalf *et al.*,

2015). No Brasil, a principal área de desova localiza-se no estado de Sergipe, na região nordeste do país, com mais de 6000 ninhos por ano na região (Fig. 2; Castilhos *et al.*, 2011).



Figura 2: Tartaruga-oliva (*Lepidochelys olivacea*) desovando na Praia de Pirambu, estado de Sergipe.

O ciclo de vida da tartaruga-oliva é classificado como ‘tipo 3’, de desenvolvimento oceânico (Bolten, 2003). Quando os neonatos emergem do ninho, entram no oceano e nadam continuamente até chegar no ambiente oceânico, onde passam a maior parte de seu ciclo de vida (Plotkin, 2007). Não é conhecido o uso de habitat de neonatos e juvenis desta espécie, porém os escassos registros indicam que o estágio juvenil ocorre somente no ambiente oceânico (Fig. 3; Plotkin, 2007). No Oceano Atlântico sul, juvenis são capturados incidentalmente na pesca de espinhel pelágico, entre as latitudes 10°N e 10°S (Sales *et al.*, 2008), semelhante às tartarugas-oliva do Oceano Pacífico (Polovina *et al.*, 2004). Quando maturam, as tartarugas-oliva deslocam-se para a costa para se reproduzir. No Brasil não é conhecida a idade de maturação desta espécie, mas no Oceano Pacífico ocidental as

tartarugas migram para áreas costeiras onde reproduzem por volta de 13 anos de idade (Zug *et al.*, 2006). No Brasil, o menor tamanho de tartaruga-oliva desovante é de 62,5 cm de CCC (Silva *et al.*, 2007), porém a faixa de tamanho das tartarugas encontradas encalhadas mortas é de 43,0 a 78,0 cm CCC (média \pm DP = 65,9 \pm 5,7 cm CCC). Entretanto, há uma variação entre indivíduos quanto ao tamanho de maturidade sexual como também há uma variação na idade de maturação sexual (Avens *et al.*, 2015).

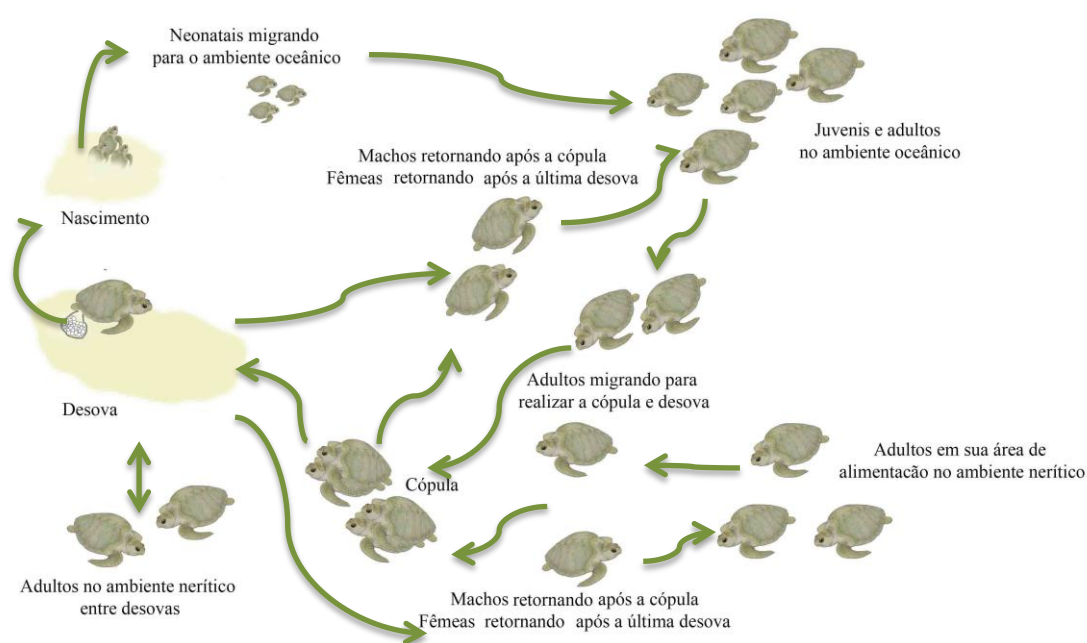


Figura 3: Ciclo de vida proposto para a tartaruga-oliva (*Lepidochelys olivacea*) que desova em Sergipe, Brasil, a partir de informações prévias sobre a espécie e do presente estudo

A tartaruga-oliva tem duas estratégias de desova: uma delas é conhecida como *arribada*, na qual milhares de fêmeas emergem ao mesmo tempo do oceano para desovar (Pritchard, 2007). Não é conhecido o estímulo inicial para que estas tartarugas saiam sincronizadamente para realizar a desova. A *arribada* somente ocorre em poucas praias no Suriname, Costa

Rica e México, além de Orissa, Índia, no Oceano Índico (Pritchard, 2007); a outra estratégia de reprodução é a desova de tartarugas-oliva solitárias, quando as fêmeas emergem do oceano para desovar não sincronizadamente, i.e. independentes umas das outras, como ocorre nas outras espécies de tartarugas marinhas. As tartarugas-oliva que realizam a *arribada* desovam duas vezes a cada temporada de reprodução, com quatro ou mais semanas de intervalo, e têm alta fidelidade ao sítio de desova (Bernardo & Plotkin, 2007). Por sua vez, as solitárias também desovam duas vezes a cada temporada, mas com um intervalo de duas semanas, e menor fidelidade ao sítio de desova (Bernardo & Plotkin, 2007). No Brasil, esta espécie realiza a desova solitária entre os meses de novembro e março, apesar de também ocorrerem algumas desovas durante os outros meses do ano, em menor quantidade (Silva *et al.*, 2007). Diferente do padrão da espécie, as tartarugas-oliva no Brasil desovam com intervalo de 22 dias (~3 semanas) e possuem alta fidelidade ao sítio de desova, retornando para desovar em média a ~5 km de distância do ninho anterior (Matos *et al.*, 2012).

Após a temporada de reprodução esta espécie realiza migração pós-reprodutiva, para locais bastantes diversos dependendo do indivíduo (Silva *et al.*, 2011). Na Austrália, Guiana Francesa e Oman (África), após a temporada de reprodução, as tartarugas-oliva permanecem, primeiramente, em águas neríticas, alimentam-se sobre a plataforma continental (Whiting *et al.*, 2007; Rees *et al.*, 2012; Plot *et al.*, 2015). Ao contrário, na população do Oceano Pacífico tropical oriental, adultos desta espécie parecem utilizar mais áreas de alimentação do ambiente oceânico do que do ambiente nerítico, após se

reproduzirem (Plotkin, 2010). No nordeste brasileiro esta espécie utiliza tanto o ambiente oceânico quanto o ambiente nerítico, ao sul ou ao norte da praia de reprodução (Silva *et al.*, 2011; Di Benedetto *et al.*, 2015). Plot *et al.* (2015) propuseram que estes diferentes padrões de migração pós-nidificação, entre populações de tartarugas-oliva no mundo, são devido às diferentes condições ambientais nas áreas adjacentes aos sítios reprodutivos.

Durante a temporada reprodutiva as tartarugas-oliva utilizam os ambientes neríticos próximos da praia de reprodução; após a última desova os indivíduos migram para áreas de alimentação, em ambiente oceânico e/ou nerítico (Fig. 3; Silva *et al.*, 2011). Foram identificadas áreas de alimentação de tartarugas-oliva na plataforma continental ao norte da praia de reprodução em frente aos estados do Pará, Rio Grande do Norte, Pernambuco e Alagoas e, ao sul, em frente ao estado do Espírito Santo (Silva *et al.*, 2011). Ainda, foram apontadas áreas de alimentação no ambiente oceânico (Silva *et al.*, 2011).

Pouco se sabe sobre a dieta da tartaruga-oliva, apesar de que, em geral, é uma espécie onívora e oportunista (Colman *et al.*, 2014). Na costa oeste do México, adultos alimentam-se em maior quantidade de salpas, e a curta plataforma continental do local favorece tal dieta, embora peixes também façam parte da dieta, seguidos em menor volume os moluscos e crustáceos (Montenegro-Silva *et al.*, 1986). Em alto mar no Oceano Pacífico, juvenis alimentam-se de itens pelágicos, como os pirossomos e salpas (Polovina *et al.*, 2004). No Oceano Atlântico, no nordeste brasileiro, adultos de tartaruga-oliva alimentam-se primariamente de peixes, seguido de crustáceos e moluscos, porém dentre 30 tartarugas encalhadas mortas na

praia, somente 14 continham itens em seu estômago (Colman *et al.*, 2014).

Idade e tamanho são componentes críticos da história de vida de um animal, além de serem parâmetros chave para estimar o crescimento somático e a idade de maturação de uma determinada população (Bernardo, 1993). Idade de maturação é uma característica pouco conhecida da demografia de populações de tartarugas marinhas em geral (Bjorndal *et al.*, 2013). No entanto é um parâmetro que deve ser estimado mais rigorosamente para inferir reais riscos de extinção para esses répteis (TEWG, 2009).

Determinação de idade, taxa de crescimento e idade de maturação são parâmetros essenciais para a análise de viabilidade populacional (do inglês, *population viability analysis* – PVA). PVA utiliza dados da história de vida de animais para descrever a probabilidade de extinção de uma dada população ou espécie, projetando-a para o futuro (Boyce, 1992; Beissinger & Westphal, 1998; Brook *et al.*, 2000). Essa análise tem especial importância para espécies ameaçadas de extinção, podendo auxiliar em estratégias de manejo e conservação, sob diferentes cenários.

Marcação-recaptura e acompanhamento em cativeiro podem gerar parâmetros demográficos de idade, idade de maturação e taxa de crescimento. Entretanto, a primeira exige um trabalho de campo intensivo de longa duração, enquanto o segundo, as informações geradas não são comparáveis com populações selvagens. A técnica de esqueletocronologia tem a grande vantagem de obter esses mesmos parâmetros demográficos de modo rápido. Além disso, esta técnica permite analisar a taxa de crescimento do indivíduo por ano, podendo gerar trajetórias e detectar mudanças

ontogenéticas em diferentes características biológicas e ecológicas (Snover *et al.*, 2007). A esqueletocronologia é baseada em marcas de crescimento em estruturas ósseas. O princípio básico desta técnica é que o crescimento ósseo é cíclico e tem periodicidade anual, na qual a formação de osso cessa ou desacelera antes da nova formação (Castanet *et al.*, 1993).

Essa técnica vem sendo aperfeiçoada ao longo do tempo, após Zug *et al.* (1986) apresentarem o primeiro trabalho que aplicou a técnica em tartarugas-cabeçuda (*Caretta caretta*) e utilizou elementos ósseos do crânio e dos membros dianteiros (úmero). A partir deste estudo foi constatado que o úmero é o osso mais útil para esse tipo de técnica, devido à maior relação entre osso denso e osso reabsorvido (Zug *et al.*, 1986). No entanto, para a tartaruga-de-couro (*Dermochelys coriacea*) os ossículos dos olhos demonstraram ser mais eficazes devido à alta reabsorção óssea que ocorre nos úmeros desta espécie (Avens *et al.*, 2009). Essa técnica já foi aplicada para diversas espécies de tartarugas marinhas, como a tartaruga-cabeçuda (Snover & Hohn, 2004; Snover *et al.*, 2007; Petitet *et al.*, 2012), a tartaruga-de-kemp *Lepidochelys kempii* (Snover & Hohn, 2004), tartaruga-verde (*Chelonia mydas*) (Goshe *et al.*, 2010; Snover *et al.*, 2011), tartaruga-de-pente (*Eretmochelys imbricata*) (Snover *et al.*, 2013; Silva *et al.*, 2015), tartaruga-de-couro (Avens *et al.*, 2009) e tartaruga-oliva (Zug *et al.*, 2006).

A validação da técnica de esqueletocronologia para tartarugas marinhas, ou seja, a demonstração que uma linha de crescimento refere-se a um ano de vida do animal, foi feita somente para algumas espécies: tartaruga-cabeçuda (Snover & Hohn, 2004), tartaruga-verde (Snover *et al.*, 2011), tartaruga-de-kemp (Snover & Hohn, 2004) e tartaruga-de-pente

(Snover *et al.*, 2013). Essa validação pode ser realizada com espécimes de idade conhecida provenientes de cativeiro (Snover & Hohn, 2004), análise de incremento marginal para descrever o padrão de deposição de marca de crescimento (Snover *et al.*, 2013) e marcação com tetraciclina, antibiótico que destaca a marcação da linha de crescimento no momento da injeção (Snover *et al.*, 2011).

A partir da deposição das linhas de crescimento anualmente é possível identificar mudanças ontogenéticas e/ou simplesmente mudanças na dieta e de habitat (Vander Zanden *et al.*, 2013). A taxa de crescimento é um *proxy* para essas mudanças, principalmente quando ocorre a maturação e, portanto, quando a taxa de crescimento somático diminui (Avens *et al.*, 2015).

Isótopos estáveis de elementos como carbono ($\delta^{13}\text{C}$) e nitrogênio ($\delta^{15}\text{N}$) permitem o estudo de conectividade migratória entre ambientes isotopicamente distintos e/ou diferenças na dieta (Ceriani *et al.*, 2014). Animais migratórios, como as tartarugas marinhas, utilizam sequencialmente uma variedade de habitats durante seu ciclo de vida (Bolten, 2003). Cada habitat pode ter seu próprio perfil de composição isotópica de carbono e nitrogênio (Post, 2002) e, portanto, a partir da análise de isótopos estáveis (AIE) é possível estudar a conectividade entre esses ambientes (Ceriani *et al.*, 2014). Deste modo, a técnica permite estudar a ecologia e demografia de espécies migratórias (Rubenstein & Hobson, 2004).

A proporção entre os isótopos estáveis leves e pesados, de carbono e nitrogênio encontrada em diversos tecidos, representa a dieta do animal no momento em que o tecido foi sintetizado (Hobson, 1999). A partir da análise de diferentes tecidos, com diferentes tempos de formação (ou regeneração),

é possível obter informações de padrões de migração e relações tróficas durante os diversos estágios de desenvolvimento dos animais (Hobson, 1999).

Cada habitat pode ter valores característicos de isótopos estáveis, caracterizando assim um “padrão” de valores de $\delta^{13}\text{C}$ e $\delta^{15}\text{N}$, da base da cadeia alimentar até o predador de topo (Post, 2002). No entanto, o valor de $\delta^{13}\text{C}$ entre o consumidor e sua dieta mudam pouco, em uma escala de c. 1‰, enquanto o $\delta^{15}\text{N}$ muda numa escala de c. 3–5‰; tais valores são denominados fatores de discriminação trófico (Peterson & Fry, 1987; Post 2002). Deste modo, devido à baixa variabilidade nos valores de $\delta^{13}\text{C}$ entre níveis tróficos, estes são utilizados como marcadores de habitat (longitudinalmente) durante a síntese de determinado tecido, enquanto os valores de $\delta^{15}\text{N}$ são utilizados como *proxy* de nível trófico (Post, 2002).

A amostragem de tecidos com diferentes taxas de renovação de um mesmo indivíduo para a AIE nos permite entender a utilização de recursos em escalas temporais diferentes (Martínez del Rio *et al.*, 2009). Assinaturas isotópicas referem-se ao tempo em que determinado tecido foi sintetizado, podendo ser permanentes – como em tecidos metabolicamente inertes (penas, pelos, unhas, escamas dérmicas) – ou temporárias – em tecidos metabolicamente ativos (sangue, pele, músculo). Dentre os tecidos ativos, cada tecido possui uma taxa de renovação (*i.e.* o tempo em que os elementos químicos obtidos através da dieta são integrados ao tecido), podendo variar de dias, meses, até anos. Em tartarugas-cabeçuda juvenis a taxa de renovação da epiderme, para o $\delta^{13}\text{C}$ e $\delta^{15}\text{N}$, é por volta de 45 dias para ambos os elementos, enquanto a carapaça tem uma taxa de renovação

de 50 dias para $\delta^{13}\text{C}$ e 16 dias para o $\delta^{15}\text{N}$ (Reich *et al.*, 2008). As células vermelhas e o plasma têm uma taxa de renovação similar para o $\delta^{13}\text{C}$ (~40 dias) enquanto que para o $\delta^{15}\text{N}$ o primeiro renova em 36 dias e o segundo em 22 dias (Reich *et al.*, 2008). Estes são os poucos trabalhos sobre taxa de renovação (i.e. tempo de síntese) de tecidos em tartarugas marinhas, enquanto outros abordam a diferença entre os valores isotópicos na dieta e nos tecidos do consumidor, denominado de FDT, e restritos a tartarugas-verde e tartarugas-de-couro (Seminoff *et al.*, 2006; Reich *et al.*, 2008; Seminoff *et al.*, 2009). Assim sendo, os habitats utilizados, a contribuição dos alimentos na dieta e o nível trófico podem ser inferidos em diferentes tempos antes da amostragem (DeNiro & Epstein, 1978, 1981; Hobson, 1999).

A AIE em tartarugas-cabeçuda vem sendo realizada para o entendimento da conectividade migratória da espécie no Japão, oceano Atlântico norte e mar Mediterrâneo (Hatase *et al.*, 2002; Revelles *et al.*, 2007; Vander Zanden *et al.*, 2016). Entretanto, para a tartaruga-oliva existe um único trabalho com IE em úmero (Biasatti 2004), enquanto estudos de uso de habitat somente foram realizados com técnicas de telemetria de adultos e juvenis até então (Polovina *et al.*, 2004; Whiting *et al.*, 2007; Plotkin, 2010; Silva *et al.*, 2011; Chambault *et al.*, 2016). No entanto, esses trabalhos demonstram uma variação individual para esta espécie quanto ao uso de habitat e, conseqüentemente, as áreas de alimentação.

A variação individual pode levar a uma especialização individual que consiste em um indivíduo utilizar um subconjunto dos recursos utilizado pela população (Bolnick *et al.*, 2003). O termo “indivíduo especialista” é definido como um indivíduo do qual o nicho é substancialmente mais estreito do que o

nicho da população (Bolnick *et al.*, 2003). A expressão “especialização individual” designa tanto a predominância de indivíduos especialistas na população como também o nível em que a dieta dos indivíduos é restrita, em comparação com o nicho de sua população (Bolnick *et al.*, 2003).

Esse fenômeno é reportado para vários táxons de vertebrados e invertebrados (Bolnick *et al.*, 2003). A largura total do nicho (do inglês, *total niche width*, TNW), que é a variância no tipo ou tamanho de presas capturadas pela população, pode ser dividida em dois componentes: componente dentro do indivíduo (do inglês, *within-individual component*, WIC), e que consiste na variância de recursos da dieta do mesmo indivíduo; e componente entre os indivíduos (do inglês, *between-individual component*, BIC), definido como a variância da dieta entre os indivíduos de uma população (Bolnick *et al.*, 2003). Assim, o nível de especialização individual é avaliado pela relação WIC/TNW que, quanto mais próximo do valor ‘0’ indica indivíduos especialistas, enquanto valores próximos de ‘1’, indicam indivíduos generalistas (Bolnick *et al.*, 2002). Deste modo, a partir desses índices, é possível classificarmos as populações como especialistas, generalistas com indivíduos generalistas ou, ainda, generalistas com indivíduos especialistas (Fig. 4; Bearhop *et al.*, 2004; Vander Zanden *et al.*, 2013).

Isótopos estáveis de carbono e nitrogênio em tecidos amostrados ao longo do tempo, como por exemplo, carapaça de tartarugas marinhas (Vander Zanden *et al.*, 2010, 2013; Pajuelo *et al.*, 2016), barbatanas de baleias (Schell *et al.*, 1989), bigodes de lontras e focas (Newsome *et al.*, 2009) e dentes de lobo-marinho (Albernaz *et al.*, 2017) podem determinar a classificação de uma população, já que as linhas ou camadas de crescimento

do tecido inerte representam diferentes períodos da vida do organismo. Além disso, pode-se inferir se há consistência temporal na contribuição da dieta e uso de habitat, podendo ser calculadas a partir dos valores de WIC (Vander Zanden *et al.*, 2013). A AIE em linhas de crescimento do osso do úmero em tartarugas marinhas pode permitir a determinação desses índices, porém existe apenas dois trabalhos com essa abordagem, em tartaruga-cabeçuda no Oceano Atlântico norte, utilizando somente o $\delta^{15}\text{N}$ (Avens *et al.*, 2013; Ramirez *et al.*, 2015).

Inferências sobre o uso de habitat e contribuição das presas na dieta ao longo do tempo de um mesmo indivíduo permitem estimar quais as ameaças potenciais em cada ambiente visitado pelo indivíduo. A tartaruga-oliva utiliza o ambiente oceânico e nerítico, sofrendo ameaças em ambos (Sales *et al.*, 2008; Silva *et al.*, 2011).

Antes do estabelecimento das bases do projeto TAMAR (ICMBio) na região nordeste do Brasil a grande ameaça a *L. olivacea* era a coleta de ovos e o abate de fêmeas para consumo (Castilhos *et al.*, 2011), porém atualmente são atividades proibidas e fiscalizadas. Desta forma, a atual ameaça a esta espécie é a captura incidental em pescarias, tanto de arrasto que ocorre perto da costa, em frente ao estado de Sergipe, quanto na pescaria de espinhel pelágico, que ocorre no ambiente oceânico (Sales *et al.*, 2008; Silva *et al.*, 2011). Em um estudo de telemetria com as tartarugas-oliva desovantes no estado de Sergipe, foi demonstrada uma sobreposição elevada entre as áreas utilizadas para permanência durante o período de nidificação e a atuação da pesca de arrasto de camarão (Silva *et al.*, 2011).

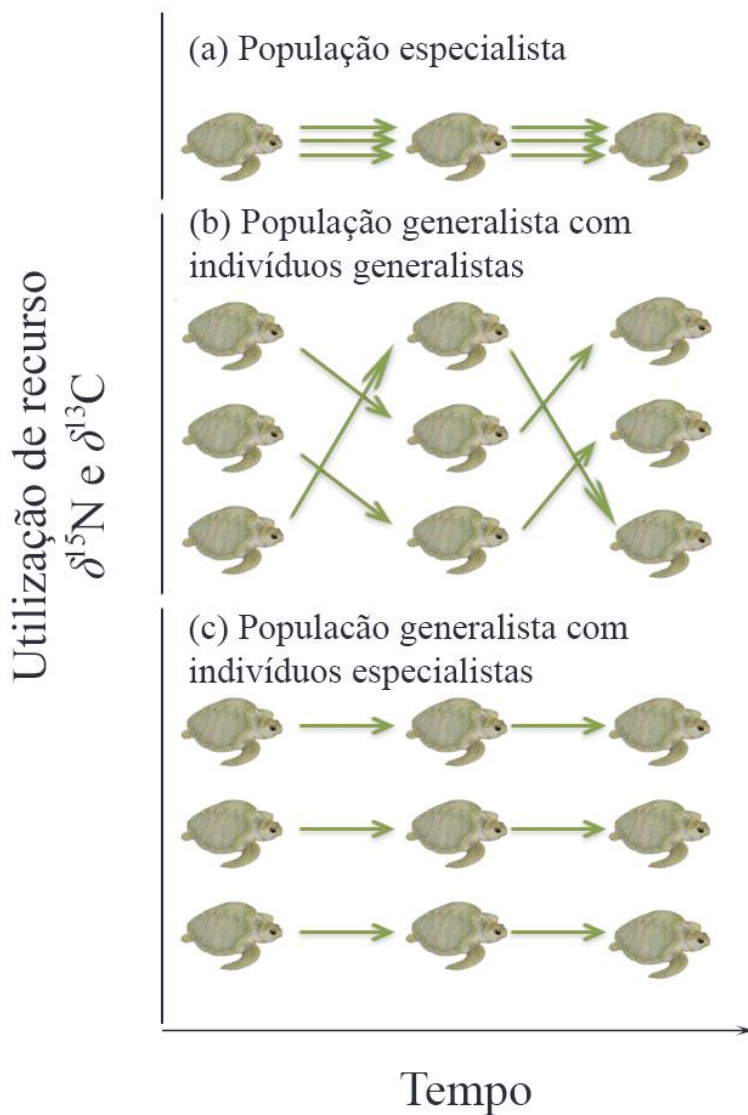


Figura 4: Modelo conceitual de utilização de recursos baseado em valores de $\delta^{13}\text{C}$ e $\delta^{15}\text{N}$ de três tipos de população (a, b e c). As setas indicam a alimentação dos indivíduos ao longo do tempo, e cada tartaruga representa valores de $\delta^{13}\text{C}$ ou $\delta^{15}\text{N}$ de um determinado tecido amostrado sucessivamente. Figura modificada de Vander Zanden *et al.* (2010).

Adicionalmente, há frequentemente o encontro de fêmeas de tartarugas-oliva encalhadas mortas nesta região, com ovos em seus ovidutos, indicando que estavam no processo de reprodução (Castilhos *et al.*, 2011). Na pesca de espinhel pelágico dirigida a atuns e tubarões, há um alto número

de juvenis e adultos de tartaruga-oliva capturados incidentalmente no ambiente oceânico (Sales *et al.*, 2008). Entre os anos de 2001 e 2005, 1386 tartarugas marinhas foram capturadas e 81 foram identificadas como tartaruga-oliva nesta pescaria, a maioria em águas oceânicas adjacentes ao nordeste brasileiro (Sales *et al.*, 2008). A mortalidade pela pesca contribui, assim, para que esta espécie apesar de ser a mais abundante dentre as espécies de tartarugas marinhas, permaneça na lista vermelha da União Internacional para a Conservação da Natureza (em inglês, *International Union for Conservation of Nature – IUCN*) (IUCN, 2016) como “vulnerável”, e também na lista de espécies ameaçadas do Ministério do Meio Ambiente (MMA, 2014) como “em perigo”.

OBJETIVOS

Objetivo geral

Determinar o padrão de crescimento e identificar mudanças ontogenéticas no uso de habitat da tartaruga-oliva que desovam no litoral de Sergipe.

Objetivos específicos

- ✓ Estimar as classes de idade de *L. olivacea* encontradas encalhadas mortas em Sergipe;
- ✓ Estimar a idade de primeira maturação;
- ✓ Gerar uma curva de crescimento com as faixas de idade das tartarugas;
- ✓ Determinar o uso de habitat de *L. olivacea* encontradas em Sergipe a partir da análise de isótopos estáveis em múltiplos tecidos (epidérmico, plasma

sanguíneo, células vermelhas e carapaça), comparado com o das potenciais presas (músculo);

- ✓ Determinar possíveis alterações ontogenéticas na dieta e no uso de habitat em decorrência do recrutamento, a partir dos padrões de isótopos estáveis (IE) no colágeno de linhas de crescimento dos úmeros.

HIPÓTESES

- ✓ As tartarugas encalhadas no litoral de Sergipe terão intervalo de idade compatível com indivíduos adultos, já que são encontradas tartarugas com o intervalo de tamanho referentes a adultos desovantes;
- ✓ A curva de crescimento inicialmente indicará um crescimento mais acelerado, correspondente ao período de desenvolvimento dos juvenis, estabilizando-se quando as tartarugas alcançarem em torno de 60 cm de CCC e iniciarem a primeira reprodução;
- ✓ Quanto ao uso de habitat inferido pelos isótopos estáveis, nos tecidos e nas linhas de crescimento de formação recente dos adultos, serão referentes a itens alimentares neríticos, enquanto nos tecidos de adultos sintetizados há bastante tempo, serão compatíveis com itens do ambiente pelágico.
- ✓ O colágeno ao longo das linhas de crescimento no úmero das tartarugas-oliva adultas do litoral de Sergipe será sintetizado a partir de itens alimentares dos ambientes nerítico e oceânico, variando entre indivíduos, devido ao tempo de permanência nos habitats. Para as linhas correspondentes ao período juvenil, os valores isotópicos serão

compatíveis com o ambiente oceânico, pois os indivíduos juvenis não permanecem próximo à costa;

- ✓ Baseado em valores de isótopos estáveis a população de tartarugas-oliva de Sergipe será caracterizada como generalista com indivíduos especialistas, devido à grande variação individual nos habitats para onde deslocam-se após a reprodução e à dieta oportunista.

MATERIAL E MÉTODOS (versão resumida)

Área de estudo

A amostragem do presente estudo foi realizada na costa do estado de Sergipe e sul do estado de Alagoas, ao longo de 173 km de praia, entre 10°31'S e 11°25'S, monitorado pelo TAMAR-ICMBio (Programa Brasileiro de Conservação de Tartarugas Marinhas) em parceria com a Fundação Mamíferos Aquáticos (FMA). Nessa área localizam-se três bases do TAMAR-ICMBio: Ponta dos Mangues, Pirambu e Abaís (Fig. 5).

No estado de Sergipe localiza-se a principal área de reprodução de tartarugas-oliva solitárias do Brasil, com cerca de 6000 ninhos a cada estação de reprodução (Silva *et al.*, 2007). Na praia de Pirambu ocorre a maior quantidade de desovas em comparação com as praias adjacentes (Silva *et al.*, 2007). A reprodução nesta área ocorre entre os meses de setembro e março, porém durante o ano ocorrem desovas eventuais (Silva *et al.*, 2007).

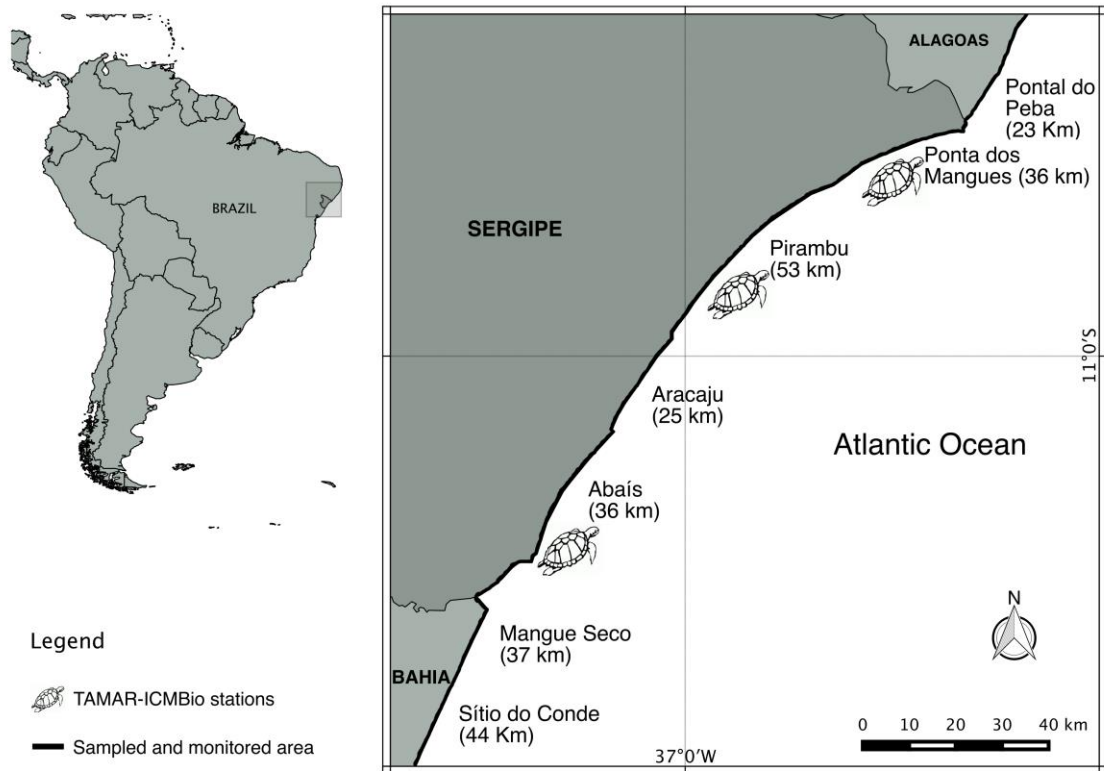


Figura 5: Área de amostragem do presente estudo. As tartarugas indicam as estações do TAMAR-ICMBio, ao longo da praia onde foram feitas as coletas de úmero de tartarugas-oliva (*Lepidochelys olivacea*). Na área de Pirambu foram coletados os tecidos para análise de isótopos estáveis (AIE) de tartarugas-oliva desovantes.

Métodos de amostragem

Determinação de idade

A coleta de úmeros de tartarugas-oliva, encontradas encalhadas mortas, ocorreu entre os anos de 2010 e 2012 e todas as tartarugas tiveram seu CCC medido com fita flexível. Somente tartarugas com aparência saudável foram amostradas como, por exemplo, tartarugas sem tumores externos. Foram coletados, ainda, 14 neonatos de tartaruga-oliva encontrados mortos após emergirem de seus ninhos.

O processamento para análise de esqueletocronologia foi realizado baseado em Avens & Goshe (2007) e Petit et al. (2012) (para maiores detalhes ver Apêndice I). No presente trabalho foi considerado que uma linha de crescimento refere-se a um ano de vida do animal, baseado na validação realizada com *L. kempii* (Snover & Hohn, 2004). A primeira linha de crescimento refere-se ao primeiro ano de vida do animal, denominada “*annulus*”, que é uma linha difusa, depositada no centro do osso, enquanto que as linhas mais recentes são melhor definidas e depositam-se ao longo da circunferência do úmero, de dentro para a fora (Fig. 6; Zug et al., 1986; Snover & Hohn, 2004). Uma linha de crescimento é composta por uma área clara (que indica crescimento ativo do osso) e uma área escura (que representa um crescimento retido), denominado, em inglês, de “*line of arrested growth*” (LAG) (Fig. 6; Snover & Hohn, 2004). A identificação de uma linha de crescimento é realizada a partir da constatação que esta completou a volta na circunferência do osso do úmero (Castanet & Smirina, 1990). No entanto há derivações nessa interpretação, como linhas duplas, “*split lines*” e linhas acessórias (Fig. 7; Castanet & Smirina, 1990).

Nos animais mais velhos ocorre a reabsorção óssea no centro do osso e, deste modo, a primeira linha de crescimento, *annulus*, é perdida (Parham & Zug, 1998). Assim, é necessário gerar um fator de correção para estimar a idade das tartarugas mais velhas a partir das tartarugas que possuem a “*annulus*” (Parham & Zug, 1998). Os indivíduos amostrados neste estudo foram classificados como adultos, baseado no tamanho (CCC) das fêmeas desovantes na área de estudo, e na constatação de que nenhuma possuía a “*annulus*”.

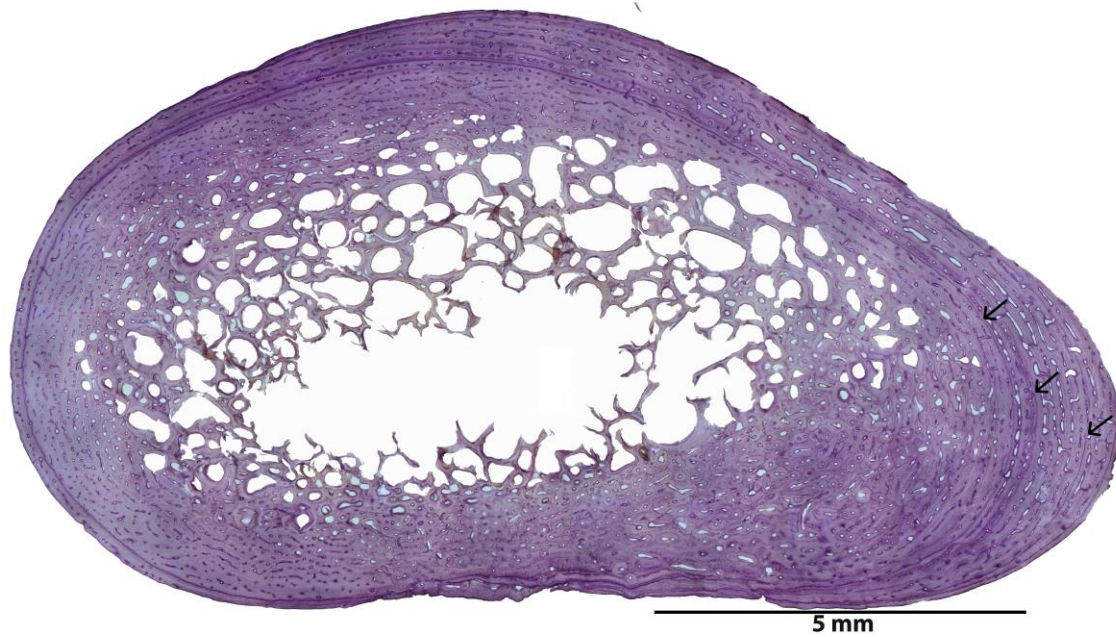


Figura 6: Secção corada do úmero de uma tartaruga-oliva (*Lepidochelys olivacea*), as setas indicam as linhas de crescimento.

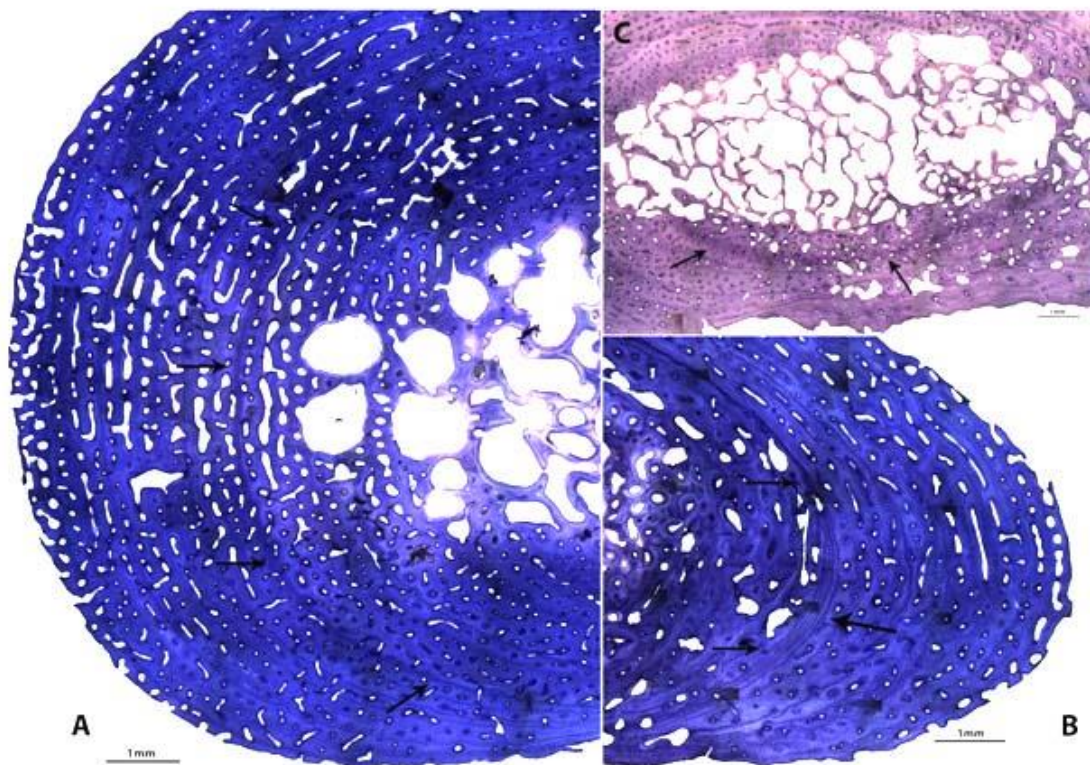


Figura 7: Secção do osso do úmero coradas de tartarugas-cabeçudas (*Caretta caretta*). As setas indicam linhas duplas em (A), “Split lines” em (B) e primeira linha de crescimento, “annulus” em (C).

Para tanto, foram utilizados indivíduos juvenis de tartarugas-oliva provenientes do Pacífico norte central, de Zug *et al.* (2006), para gerar o fator de correção para as tartarugas-oliva do presente estudo. Foram aplicados dois modelos, de regressão linear e de função de potência, entre o diâmetro das linhas de crescimento observadas e o número da linha de crescimento correspondente a idade dos animais juvenis. Posteriormente, o diâmetro das linhas de crescimento foi substituído pelo diâmetro da área de reabsorção dos animais mais velhos e, assim, calculados quantas linhas de crescimento foram perdidas nesta área (mais detalhes ver Apêndice I). Por fim, no presente estudo, a idade das tartarugas-oliva foi determinada através da soma das linhas de crescimento observadas no úmero e das linhas de crescimento estimadas a partir da área de reabsorção. A partir dos dados de tamanho e idade, foram aplicados os modelos de crescimento de Schnute e de von Bertalanffy (Schnute, 1981; von Bertalanffy, 1957).

A taxa de crescimento foi baseada no retrocálculo de Snover *et al.* (2007) e na hipótese de proporcionalidade corporal (“*Body proportional hipotesis*”) de Francis (1990). Foi calculada a taxa de crescimento, por linha de crescimento, gerando uma trajetória para cada indivíduo amostrado.

As tartarugas marinhas maturam em idades e tamanhos diferentes, portanto cada indivíduo possui uma idade e tamanho de primeira maturação (Avens *et al.*, 2013). No entanto, na deposição das linhas de crescimento é possível identificar uma linha chamada de “*rapprochement*”, cuja diminuição na taxa de crescimento e aumento da espessura entre as linhas indica o momento de maturação daquele indivíduo (Avens *et al.*, 2015). Deste modo, a idade de maturação da tartaruga-oliva foi estimada a partir do modelo de

crescimento de von Bertalanffy e da linha “*rapprochement*”.

Uso de habitat

Durante a estação de reprodução, o TAMAR-ICMBio realiza monitoramento noturno à procura de fêmeas desovantes ao longo de 12 km de praia em Pirambu. Nesse local, em parceria com o TAMAR-ICMBio, durante o mês de novembro de 2013, foram coletadas amostras de sangue (células vermelhas – CV e soro), epiderme e queratina da carapaça de tartarugas-oliva desovantes para a AIE. Em conjunto com a coleta de material biológico destas tartarugas vivas, também foi realizada a biometria (CCC) de cada animal, novamente somente de animais aparentemente saudáveis.

Na mesma época de coleta de tecidos das tartarugas-oliva foram coletadas presas potenciais da espécie, selecionadas a partir de um estudo anterior de dieta (Colman *et al.*, 2014). Estas presas foram provenientes do *bycatch* da pesca de arrasto que ocorre na área e foram classificadas como presas neríticas, incluindo crustáceos e peixes demersais. Para as presas oceânicas foram utilizados valores isotópicos de uma espécie de organismo gelatinoso (*Velella velella*) proveniente da Ilha da Trindade, Espírito Santo, localizada a 1160 km da costa.

O uso de habitat das tartarugas-oliva foi analisado a partir da comparação de valores isotópicos dos tecidos das tartarugas com os valores isotópicos dos músculos das potenciais presas, ou de presas inteiras, baseado em modelos de mistura (MM) no pacote “*IsotopeR*” (Hopkins III *et al.*, 2012). Modelos de mistura estimam a contribuição de fontes alimentares potenciais, com valores isotópicos conhecidos, para o valor isotópico

encontrado no tecido do consumidor. Foram utilizados os isótopos de $\delta^{13}\text{C}$ e $\delta^{15}\text{N}$ como *proxy* do habitat e do nível trófico, respectivamente (Post, 2002). Para o MM, foi utilizado o fator de discriminação trófico de tartarugas-cabeçuda juvenis (Reich *et al.*, 2008), espécie também carnívora e com fase juvenil oceânica, pois para a tartaruga-oliva esse valor não é conhecido (Apêndice II).

Especialização individual e consistência temporal

Antes do processamento para esqueletocronologia, foi coletada uma seção do úmero de 1 mm de espessura para AIE. Desta seção foram extraídas amostras das linhas de crescimento de 20 úmeros que compunha a amostra utilizada para esqueletocronologia, utilizando-se broca de dentista. A especialização individual e consistência temporal foram mensuradas baseadas no WIC, BIC e TNW (Bolnick *et al.*, 2003). Para o cálculo desses índices foi utilizada a variância dos valores isotópicos de $\delta^{13}\text{C}$ e $\delta^{15}\text{N}$ das linhas de crescimento dentro de cada indivíduo (WIC), entre os indivíduos (BIC) e a amplitude de nicho total da população (TNW) (Vander Zanden *et al.*, 2013). Os índices WIC e WIC/TNW são referentes à consistência temporal e nível de especialização individual, respectivamente (Bolnick *et al.*, 2003; Vander Zanden *et al.*, 2013, Apêndice III). Além disso, para o cálculo desses índices a amostra foi dividida em dois grupos de idades (mais novos e mais velhos) buscando agrupar os organismos anteriores e posteriores ao recrutamento. Em conjunto, foram aplicados MMs e utilizados os valores isotópicos de presas coletadas na área de estudo, conforme citado na seção anterior. Os MMs foram utilizados para obter informações de uso de habitat

entre os ambientes oceânico e nerítico, baseado nas prováveis contribuições das presas/fontes alimentares. Os MMs também foram construídos para representar dois momentos, um para os indivíduos mais novos e outro para os indivíduos mais velhos. O FDT para osso de tartaruga não é conhecido e, assim, foi utilizado o valor padrão de ca 3‰ para $\delta^{15}\text{N}$ e ca 1‰ para o $\delta^{13}\text{C}$ (Peterson & Fry, 1987; Post, 2002).

Análise estatística

As inferências tiveram enfoque bayesiano (Ellison, 2004) nas análises de linhas perdidas, retrocálculo, taxa de crescimento, modelo de crescimento e MM isotópicos. Para os índices de especialização individual e consistência temporal, foi utilizado enfoque clássico, por inferência frequentista. Todas as análises foram realizadas no software R (R Core Team, 2014) e no programa JAGS (<http://mcmc-jags.sourceforge.net> [acessado 4 de Fevereiro de 2015]).

SÍNTESE DOS RESULTADOS

Determinação de idade

As 68 tartarugas-oliva que tiveram úmeros coletados tiveram CCC entre 58,0 e 77,0 cm (média \pm DP: 69,1 \pm 4,56 cm). Estes tamanhos referem-se a um intervalo de idade de 14 a 26 anos. Baseado no menor tamanho de tartarugas-oliva desovantes em Sergipe de 62,5 cm CCC (Silva *et al.*, 2007), a amostra foi, portanto, composta por indivíduos adultos. Entretanto, somente 25 indivíduos tiveram maturação confirmada, todas fêmeas, devido à presença de ovos em seus ovidutos.

A função de potência obteve o melhor ajuste para o cálculo de linhas

perdidas na área de reabsorção do úmero. O número de LAGs observadas em cada úmero foi entre 3 e 9, enquanto que o número de LAGs estimado em cada área de reabsorção foi de 11 a 17. A média da idade de maturação estimada a partir do modelo de crescimento de von Bertalanffy foi de 14 anos (10–16 anos), enquanto pela linha de maturação (*rapprochement*) foi de 16,6 anos (13–21 anos).

A taxa de crescimento foi inversamente correlacionada à idade, ou seja, quanto mais velho o animal menor a taxa de crescimento. O modelo de crescimento demonstrou um crescimento com taxa homogênea, devido à amostra ser composta exclusivamente por indivíduos já adultos.

Uso de habitat

Um total de 46 fêmeas adultas vivas de tartaruga-oliva foi amostrado, com intervalo de tamanho entre 64,0 e 76,0 cm de CCC (média \pm DP = 71,4 \pm 3,10 cm). Os valores de $\delta^{13}\text{C}$ nos diferentes tecidos tiveram uma ordem crescente, com CVs < soro < carapaça < epiderme, enquanto que para $\delta^{15}\text{N}$ foi carapaça < CVs < epiderme < soro.

Os MMs demonstraram alta contribuição de organismos gelatinosos para a síntese dos tecidos da epiderme e CVs, seguido de uma pequena contribuição de peixes demersais e uma contribuição insignificante de crustáceos. No entanto, para a carapaça e o soro, o MM demonstrou uma alta contribuição de peixes demersais, seguido de uma contribuição menor de gelatinosos e uma contribuição baixa de crustáceos. A maioria das amostras obteve esse padrão quanto às contribuições das presas, porém dois indivíduos demonstraram altos valores de $\delta^{13}\text{C}$ e baixos valores de $\delta^{15}\text{N}$,

indicando que possivelmente esses indivíduos habitaram o ambiente nerítico durante todo o tempo de síntese dos diversos tecidos.

Especialização individual e consistência temporal

A subamostra de 20 indivíduos de tartarugas-oliva que tiveram isótopos estáveis analisados nas linhas de crescimento do úmero possuía tamanho de 58,0 a 77,0 cm de CCC, representando animais de 14 a 23 anos de idade. Até cinco LAGs foram amostradas de cada úmero, totalizando 82 LAGs. Estas LAGs referiam-se a um intervalo de tamanho retrocalculado de 50,6 a 77,0 cm de CCC, correspondente a um intervalo de idade retrocalculada de 12 a 23 anos. Dentre os indivíduos, somente seis foram confirmadas como fêmeas sexualmente maduras.

Os valores de $\delta^{13}\text{C}$ das LAGs variaram entre $-20,96\text{‰}$ e $-11,94\text{‰}$ (média \pm DP = $-15,45 \pm 1,35\text{‰}$) e os valores de $\delta^{15}\text{N}$ entre $7,34\text{‰}$ e $14,21\text{‰}$ (média \pm DP = $10,73 \pm 1,47\text{‰}$). Os animais mais jovens tiveram um maior intervalo de valores de $\delta^{13}\text{C}$ do que os animais mais velhos. Os valores de $\delta^{15}\text{N}$ aumentaram com a idade.

O MM demonstrou uma contribuição alta de organismos gelatinosos para a síntese do colágeno do osso de indivíduos mais novos, seguido por uma contribuição menor de crustáceos e peixes demersais. Entretanto, para os indivíduos mais velhos, apesar da fonte com maior contribuição também ter sido os organismos gelatinosos, crustáceos tiveram uma contribuição elevada para este grupo, seguido de uma pequena contribuição de peixes demersais.

O WIC calculado a partir dos valores de $\delta^{13}\text{C}$ e $\delta^{15}\text{N}$, utilizado como

proxy para a consistência temporal no uso de recursos, foi menor para os indivíduos mais velhos do que para os indivíduos mais novos. A relação WIC/TNW dos valores de $\delta^{13}\text{C}$ e também de $\delta^{15}\text{N}$, *proxy* para especialização individual, foi baixa para ambos os grupos de indivíduos.

CONCLUSÃO

A faixa etária de tartarugas-oliva encalhadas mortas no litoral de Sergipe foi maior (14 a 26 anos) do que no Pacífico (7 a 24 anos). Da mesma forma a estimativa de idade de maturação foi de 16,6 anos para o presente estudo e 13 anos no Oceano Pacífico, e é nessa idade (16,6 anos) que a taxa de crescimento diminui e estabiliza na população do Brasil. Portanto, esta população de tartaruga-oliva do Brasil pode levar em torno de 16 anos para se recuperar de eventual redução populacional. Esta estimativa coincide com um aumento abrupto no número de ninhos desta espécie na área de estudo, que também ocorreu cerca de 16 anos após o início da proteção de ovos, filhote e fêmeas nas praias de desova de Sergipe, iniciada em 1982 pelo TAMAR-ICMBio (Silva *et al.*, 2007). Entretanto, atualmente a tartaruga-oliva é ameaçada por outros impactos nos ambientes que utiliza, o que causa a grande mortalidade de adultos na região (Castilhos *et al.*, 2011). A AIE demonstrou que esta espécie utiliza tanto as águas neríticas como as águas oceânicas após se reproduzir. No ambiente nerítico adjacente à área de amostragem a pesca de arrasto sobrepõe-se com habitats ocupados pelas tartarugas entre as desovas (Silva *et al.*, 2010). Já no ambiente oceânico, não só as adultas, mas também as juvenis são capturadas incidentalmente pela pesca de espinhel pelágico (Sales *et al.*, 2008).

Além dessa variação no uso de habitat ao longo do desenvolvimento ontogenético, há um alto nível de variação individual que indica que a população de tartaruga-oliva do nordeste brasileiro é uma população generalista, com indivíduos especialistas. Quando adultas as tartarugas podem ocupar tanto os ambientes neríticos quanto os oceânicos, ou uma mistura destes dois ambientes. Portanto, é essencial um melhor entendimento sobre o ciclo de vida desta espécie durante o ano todo, visando subsidiar planos de conservação e diminuir a mortalidade de adultos próximo e também distante das áreas de reprodução.

Portanto, é essencial um melhor entendimento sobre as diversas fases do ciclo de vida desta espécie, em particular durante os estágios menos conhecidos, com o período juvenil e o período do ano em que estão distantes das áreas de desova, visando subsidiar planos de conservação e diminuir a mortalidade de adultos próximo e também distante das áreas de reprodução.

BIBLIOGRAFIA CITADA

- Albernaz, TL, Secchi, ER, Oliveira, LR & Botta, S. 2017. Ontogenetic and gender-related variation in the isotopic niche within and between three species of fur seals (genus *Arctocephalus*). *Hydrobiologia*, 787:1213–139.
- Avens, L & Goshe, LR. 2007. Comparative skeletochronological analysis of Kemp's ridley (*Lepidochelys kempii*) and loggerhead (*Caretta caretta*) humeri and scleral ossicles. *Mar. Biol.*, 152:1309–1317.
- Avens, L, Taylor, JC, Goshe, LR, Jones, TT & Hastings, M. 2009. Use of skeletochronological analysis to estimate the age of leatherback sea

- turtles *Dermochelys coriacea* in the western North Atlantic. *Endang. Species Res.*, 8:165–177.
- Avens, L, Goshe, LR, Pajuelo, M, Bjorndal, KA, MacDonald, BD, Lemons, GE, Bolten, AB & Seminoff, JA. 2013. Complementary skeletochronology and stable isotope analyses offer new insight into juvenile loggerhead sea turtle oceanic stage duration and growth dynamics. *Mar. Ecol. Prog. Ser.*, 491:235–251.
- Avens, L, Goshe, LR, Coggins, L, Snover, ML, Pajuelo, M, Bjorndal, KA & Bolten, AB. 2015. Age and size at maturation and adult stage duration for loggerhead sea turtles in the western North Atlantic. *Mar. Biol.*, 162:1749–1767.
- Bearhop, S, Adams, CE, Waldron, S, Fuller, RA & Macleod, H. 2004. Determining trophic niche width: a novel approach using stable isotope analysis. *J. Anim. Ecol.*, 73:1007–1012.
- Beissinger, SR & Westphal, MI. 1998. On the use of demographic models of population viability in endangered species management. *J. Wildl. Manage.*, 62:821–841.
- Bernardo, J. 1993. Determinants of maturation in animals. *Trends Ecol. Evol.*, 8:166–173.
- Bernardo, J & Plotkin, PT. 2007. An evolutionary perspective in the *arribada* phenomenon and reproductive behavioral polymorphism of olive ridley sea turtle (*Lepidochelys olivacea*). In: Plotkin, PT (ed) *Biology and conservation of ridley sea turtles*. Johns Hopkins University Press, Baltimore, MD, Chap 4:9–87.
- Biasatti, DM. 2004. Stable carbon isotopic profiles of sea turtle humeri:

- implications for ecology and physiology. *Palaeogeogr. Palaeoclimatol. Palaeoecol.*, 206:203–216.
- Bjorndal, KA, Parsons, J, Mustin, W & Bolten, AA. 2013. Threshold to maturity in a long-lived reptile: interactions of age, size, and growth. *Mar. Biol.*, 160:607–616.
- Bolnick, DI, Yang, LH, Fordyce, JA, Davis, JM & Svanback, R, 2002. Measuring individual-level resource specialization. *Ecology*, 83:2936–2941.
- Bolnick, DI, Svanback, R, Fordyce, JA, Yang, LH, Davis, JM, Hulseley, CD & Forister, ML. 2003. The ecology of individuals: incidence and implications of individual specialization. *Am. Nat.*, 161:1–28.
- Bolten, AB. 2003. Active swimmers-passive drifters: the oceanic stage of loggerheads in the Atlantic system. In: Bolten AB, Witherington BE (eds) *Loggerhead sea turtles*. Smithsonian Institution, Washington, DC, Chap 4:63–78.
- Boyce, MS. 1992. Population viability analysis. *Annu. Rev. Ecol. Syst.*, 23:481–506.
- Brook, BW, O’Grady, JJ, Chapman, AP, Burgman, MA, Akçakaya, HR & Frankham, R. 2000. Predictive accuracy of population viability analysis in conservation biology. *Nature*, 404:385–387.
- Castanet, J & Smirina, E. 1990. Introduction to the skeleto-chronological method in amphibians and reptiles. *Ann. Sci. Nat. Zool.*, 13 ser. 11:191–196.
- Castanet, J, Francillon-Vieillot, H, Meunier, FJ & De Ricqlès, A. 1993. Bone and individual aging. In: Hall BBK (ed) *Bone: bone growth*, Vol 7. CRC Press, Boca Raton, FL, chap 9:245–283.

- Castilhos, JC, Coelho, AC, Argolo, JF, Santos, EAP, Marcovaldi, AM, SANTOS, ASS & Lopez, M. 2011. Avaliação do estado de conservação da tartaruga marinha *Lepidochelys olivacea* (Eschscholtz 1829) no Brasil. *Biodiv. Bras.*, 1:28–36.
- Ceriani, SA, Roth, JD, Ehrhart, LM, Quintana-Ascencio, PF & Weishampel, JF. 2014. Developing a common currency for stable isotope analyses of nesting marine turtles. *Mar. Biol.*, 161:2257–2268.
- Chambault, P, Thoisy, B, Heerah, K, Conchon, A, Barrioz, S, Reis, V, Berzins, R, Kelle, L, Picard, B, Roquet, F, Le Maho, Y & Chevallier, D. 2016. The influence of oceanographic features on the foraging behavior of the olive ridley sea turtle *Lepidochelys olivacea* along the Guiana coast. *Prog. Oceanogr.*, 142:58–71.
- Colman, LP, Sampaio, CLS, Weber, MI & Castilhos, JC. 2014. Diet of olive ridley sea turtles, *Lepidochelys olivacea*, in the waters of Sergipe, Brazil. *Chelonian Conserv. Biol.*, 13: 266–271.
- DeNiro, MJ & Epstein, S. 1978. Influence of diet on the distribution of carbon isotopes in animals. *Geochim. Cosmochim. Acta*, 42:495–506.
- DeNiro, MJ & Epstein, S. 1981. Influence of diet on the distribution of nitrogen isotopes in animals. *Geochim. Cosmochim. Acta*, 45:341–351.
- Di Benedetto, APM, Moura, JF & Siciliano, S. 2015. Feeding habits of the sea turtles *Caretta caretta* and *Lepidochelys olivacea* in south-eastern Brazil. *Mar. Biodiv. Rec.*, 8:1–5.
- Ellison, AM. 2004. Bayesian inference in ecology. *Ecol. Lett.*, 7:509–520.
- Francis, RICC. 1990. Back-calculation of fish length: a critical review. *J. Fish. Biol.*, 36:883–902.

- Goshe, LR, Avens, L, Scharf, FS & Southwood, AL. 2010. Estimation of age at maturation and growth of Atlantic green turtles (*Chelonia mydas*) using skeletochronology. *Mar. Biol.*, 157:1725–1740.
- Hatase, H, Takai, N, Matsuzawa, Y, Sakamoto, W, Omuta, K, Goto, K, Arai, N & Fujiwara, T. 2002. Size-related differences in feeding habitat use of adult female loggerhead *Caretta caretta* around Japan determined by stable isotope analyses and satellite telemetry. *Mar. Ecol. Prog. Ser.*, 233:273–281.
- Hobson, KA. 1999. Tracing origins and migration of wildlife using stable isotopes: a review. *Oecologia*, 120:314–326.
- Hopkins-III, JB, Ferguson, JM. 2012. Estimating the diets of animals using stable isotopes and a comprehensive Bayesian mixing model. *PLoS ONE*, 7:e28478
- IUCN. 2014. *The IUCN red list of threatened species*. Version 2016-2. <www.iucnredlist.org>. Downloaded on 04 December 2016.
- Martínez del Rio, C, Wolf, N, Carleton, SA & Gannes, LZ. 2009. Isotopic ecology ten years after a call for more laboratory experiments. *Biol. Rev.*, 84:91–111.
- Matos, L, Silva, ACCD, Casitinhos, JC, Weber, MI, Soares, LS & Vicente, L. 2012. Strong site fidelity and longer internesting interval for solitary nesting olive ridley sea turtles in Brazil. *Mar. Biol.*, 159: 1011–1019.
- Metcalfe, K, Agamboué, PD, Augowet, E, Boussamba, F, Cardiec, F, Fay, M, Formia, A, Kema Kema, JR, Kouerey, C, Mabert, BDK, Maxwell, SM, Minton, G, MOUNGUENGUI MOUNGUENGUI, GA, Moussounda, C, Moukoumou, N, Manfoumbi, JC, Nguema AM, Nzegoue, J, Parnell, RJ,

- Plessis, P, Sounguet, GP, Tilley, D, Verhage, S, Viljoen, W, White, L, Witt, MJ & Godley, BJ. 2015. Going the extra mile: ground-based monitoring of olive ridley turtles reveals Gabon hosts the largest rookery in the Atlantic. *Biol. Conserv.*, 190:14–22.
- MMA (Ministério do Meio Ambiente). 2014. Répteis - *Lepidochelys olivacea* (Eschscholtz, 1829) - Tartaruga-oliva. In: *Lista de espécies da fauna Brasileira ameaçadas de extinção*. www.icmbio.gov.br/portal/biodiversidade/fauna-brasileira/lista-de-especies/6630-especie-6630 (acessado em 4 de dezembro de 2016).
- Montenegro-Silva, BC, Gonzalez, NGB & Guerrero, AM. 1986. Estudio del contenido estomacal de la tortuga marina *Lepidochelys olivacea*, en la costa de Oaxaca, México. *An. Inst. Cienc. Mar. Limnol. Univ. Nac. Auton. Mex.*, 13:121–132.
- Newsome, SD, Tinker, MT, Monson, DH, Oftedal, OT, Ralls, K, Staedler, MM, Fogel, ML & Estes, JA. 2009. Using stable isotopes to investigate individual diet specialization in California sea otters (*Enhydra lutris nereis*). *Ecology*, 90:961–974.
- Pajuelo, M, Bjorndal, KA, Arendt, MD, Foley, AM, Schroeder, BA, Witherington, BE & Bolten, AB. 2016. Long-term resource use and foraging specialization in male loggerhead turtles. *Mar. Biol.*, 163:235.
- Parham, JF & Zug, JR. 1998. Age and growth of loggerhead sea turtles of coastal Georgia: an assessment of skeletochronological age-estimates. *Bull. Mar. Sci.*, 61:287–304.
- Peterson, BJ & Fry, B. 1987. Stable isotopes in ecosystem studies. *Ann. Rev. Ecol. Syst.*, 18:298–320.

- Petit, R, Secchi, ER, Avens, L & Kinas, PG. 2012. Age and growth of loggerhead sea turtles in southern Brazil. *Mar. Ecol. Prog. Ser.*, 456:255–268.
- Plot, V, Thoisy, B & Georges, JY. 2015. Dispersal and dive patterns during the post-nesting migration of olive ridley turtles from French Guiana. *Endang. Species Res.*, 26:221–234.
- Plotkin, PT. 2007. Introduction. In: Plotkin PT (ed) *Biology and conservation of ridley sea turtles*. Johns Hopkins University Press, Baltimore, MD, p 3–5.
- Plotkin, PT. 2010. Nomadic behaviour of the highly migratory olive ridley sea turtle *Lepidochelys olivacea* in the eastern tropical Pacific Ocean. *Endang. Species Res.*, 13:33–40.
- Polovina, JJ, Balazs, GH, Howell, EA, Parker, DM, Sekil, MP & Dutton, PH. 2004. Forage and migration habitat of loggerhead (*Caretta caretta*) and olive ridley (*Lepidochelys olivacea*) sea turtles in the central north Pacific Ocean. *Fish. Oceanogr.*, 13:36–51.
- Post, DM. 2002. Using stable isotopes to estimate trophic position: models, methods, and assumptions. *Ecology*, 83:703–718.
- Pritchard, PCH. 2007. *Arribadas* I have known. In: Plotkin, PT (ed) *Biology and conservation of ridley sea turtles*. Johns Hopkins University Press, Baltimore, MD, Chap 1:7–21.
- R Core Team. 2014. *R: a language and environment for statistical computing*. R Foundation for Statistical Computing, Vienna. www.R-project.org.
- Ramirez, MD, Avens, L, Jeminoff, JA, Goshe, LR & Heppell, SS. 2015. Patterns of loggerhead turtle ontogenetic shifts revealed through isotopic analysis of annual skeletal growth increments. *Ecosphere*, 6:1–17

- Rees, AF, Al-Kiyumi, A, Broderick, AC, Papathanasopoulou, N & Godley, BJ. 2012. Conservation related insights into the behaviour of the olive ridley sea turtle *Lepidochelys olivacea* nesting in Oman. *Mar. Ecol. Prog. Ser.*, 450:195–205.
- Reich, KJ, Bjorndal, KA & Martínez del Rio, C. 2008. Effects of growth and tissue type on the kinetics of ^{13}C and ^{15}N incorporation in a rapidly growing ectotherm. *Oecologia*, 155:651–663.
- Reichart, HA. 1993. *Synopsis of biological data on the olive ridley sea turtle Lepidochelys olivacea (Eschscholtz, 1982) in the western Atlantic*. NOAA Tech. Memo. NMFS- SEFSC-336.
- Revelles, M, Cardona, L, Aguilar, A, Borrell, A, Fernández, G & San Félix, M. 2007. Stable C and N isotope concentration in several tissues of the loggerhead sea turtle *Caretta caretta* from the western Mediterranean and dietary implications. *Sci. Mar.*, 71:87–93.
- Rubenstein, DR & Hobson, KA. 2004. From birds to butterflies: animal movement and stable isotopes. *Trends Ecol. Evol.*, 19:256–263.
- Sales, G, Giffoni, BB & Barata, PCR. 2008. Incidental catch of sea turtles by the Brazilian pelagic longline fishery. *J. Mar. Biol. Assoc. UK*, 88:853–864.
- Schell, DM, Saupe, SM & Haubenstock, N. 1989. Bowhead whale (*Balaena mysticetus*) growth and feeding as estimated by $\delta^{13}\text{C}$ techniques. *Mar. Biol.*, 103:433–443.
- Schnute, J. 1981. A versatile growth model with statistically stable parameters. *Can. J. Fish. Aquat. Sci.*, 38:1128–1140.
- Seminoff, JA, Jones, TT, Eguchi, T, Jones, DR & Dutton PH. 2006. Stable

- isotope discrimination ($\delta^{13}\text{C}$ and $\delta^{15}\text{N}$) between soft tissues of the green sea turtle *Chelonia mydas* and its diet. *Mar. Ecol. Prog. Ser.*, 308:271–278.
- Seminoff, JA, Jones, TT, Eguchi, T, Hastings, M & Jones, DR. 2009. Stable carbon and nitrogen isotope discrimination in soft tissues of the leatherback turtle (*Dermochelys coriacea*): insights for trophic studies of marine turtles. *J. Exp. Mar. Biol. Ecol.*, 381:33–41.
- Silva, ACCD, Castilhos, JC, Lopez, GG & Barata, PCR. 2007. Nesting biology and conservation of the olive ridley sea turtle (*Lepidochelys olivacea*) in Brazil, 1991/1992 to 2002/2003. *J. Mar. Biol. Assoc. UK*, 87:1047–1056.
- Silva, ACCD, Castilhos, JC, Santos, EAP, Brondízio, LS & Bugoni, L. 2010. Efforts to reduce sea turtle bycatch in the shrimp fishery in northeastern Brazil through a co-management process. *Ocean. Coast. Manage.*, 53:570–576.
- Silva, ACCD, Santos, EAP, Oliveira, FLC, Weber, MI, Batista, JAF, SERAFINI, TZ & Castilhos, JC. 2011. Satellite-tracking reveals multiple foraging strategies and threats for olive ridley turtles in Brazil. *Mar. Ecol. Prog. Ser.*, 443:237–247.
- Silva, LM. 2014. Mudanças ontogenéticas na dieta e no uso de habitat e estimativa de idade e crescimento da tartaruga-de-pente, *Eretmochelys imbricata*. *Dissertação de Mestrado, Fundação Universidade Federal do Rio Grande, Brasil*, 131 p.
- Snover, ML & Hohn, AA. 2004. Validation and interpretation of annual skeletal marks in loggerhead (*Caretta caretta*) and Kemp's ridley (*Lepidochelys kempii*) sea turtles. *Fish. Bull.*, 102:682–692.

- Snover, ML, Avens, L & Hohn, AA. 2007. Back-calculating length from skeletal growth marks in loggerhead sea turtles *Caretta caretta*. *Endang. Species Res.*, 3:95–104.
- Snover, ML, Hohn, AA, Goshe, LR & Balazs, GH. 2011. Validation of annual skeletal marks in green sea turtles *Chelonia mydas* using tetracycline labeling. *Aquat. Biol.*, 12:197–204.
- Snover, ML, Balazs, GH, Murakawa, SKK, Hargrove, SK, Rice, MR & Seitz, WA. 2013. Age and growth rates of Hawaiian hawksbill turtles (*Eretmochelys imbricata*) using skeletochronology. *Mar. Biol.*, 160:37–46.
- TEWG (Turtle Expert Working Group). 2009. *An assessment of the loggerhead turtle population in the western north Atlantic Ocean*. NOAA Tech. Memo. NMFS-SEFSC-575.
- Vander Zanden, HB, Bjorndal, KA, Reich, KJ & Bolten, AB. 2010. Individual specialists in a generalist population: results from a long-term stable isotope series. *Biol. Lett.*, 6:711–714.
- Vander Zanden, HB, Bjorndal, KA & Bolten, AB. 2013. Temporal consistency and individual specialization in resource use by green turtles in successive life stages. *Oecologia*, 173:767–777.
- Vander Zanden, HB, Bolten, AB, Tucker, AD, Hart, KM, Lamont, MM, Fujisaki, I, Reich, KJ, Addison, DS, Mansfield, KL, Phillips, KF, Pajuelo, M & Bjorndal, KA. 2016. Biomarkers reveal sea turtles remained in oiled areas following the *Deepwater Horizon* oil spill. *Ecol. Appl.*, 26:2145–2155.
- von Bertalanffy, L. 1957. Quantitative laws in metabolism and growth. *Q. Rev.*

Biol., 32:217–231.

Whiting, SD, Long, JL & Coyne, M. 2007. Migration routes and foraging behaviour of olive ridley turtles *Lepidochelys olivacea* in northern Australia. *Endang. Species Res.*, 3:1–9.

Zug, GR, Wynn, AH & Ruckdeschel, C. 1986. Age determination of loggerhead sea turtles, *Caretta caretta*, by incremental growth marks in the skeleton. *Smithson. Contrib. Zool.*, 427:1–34.

Zug, GR, Chaloupka, M & Balazs, GH. 2006. Age and growth in olive ridley sea turtles (*Lepidochelys olivacea*) from the north-central Pacific: a skeletochronological analysis. *Mar. Ecol.*, 27:263–270.

APÊNDICE I

**Age and growth of olive ridley sea turtles *Lepidochelys olivacea* in the
main Brazilian nesting ground**

Roberta Petitet, Larisa Avens, Jaqueline C. Castilhos, Paul G. Kinas, Leandro
Bugoni

PUBLICADO NO PERIÓDICO *MARINE ECOLOGY PROGRESS SERIES*

Vol. 541: 205–218, 2015

Age and growth of olive ridley sea turtles *Lepidochelys olivacea* in the main Brazilian nesting ground

Roberta Petit^{1,2,*}, Larisa Avens³, Jaqueline C. Castilhos⁴, Paul G. Kinas⁵,
Leandro Bugoni¹

¹Laboratório de Aves Aquáticas e Tartarugas Marinhas, Instituto de Ciências Biológicas, Universidade Federal do Rio Grande (FURG), Campus Carreiros, Avenida Itália s/n, CP 474, 96203-900 Rio Grande, RS, Brazil

²Programa de Pós-Graduação em Oceanografia Biológica, Instituto de Oceanografia, Universidade Federal do Rio Grande (FURG), Campus Carreiros, Avenida Itália s/n, CP 474, 96203-900 Rio Grande, RS, Brazil

³Southeast Fisheries Science Center, Center for Coastal Fisheries and Habitat Research, NOAA National Marine Fisheries Service, 101 Pivers Island Road, Beaufort, NC 28516, USA

⁴Fundação Centro Brasileiro de Proteção e Pesquisa das Tartarugas Marinhas, Reserva Biológica de Santa Isabel s/n, Centro, 49190-000 Pirambu, SE, Brazil

⁵Laboratório de Estatística Ambiental, Instituto de Matemática, Estatística e Física, Universidade Federal do Rio Grande (FURG), CP 474, Avenida Itália s/n, CP 474, 96203-900 Rio Grande, RS, Brazil

ABSTRACT: Olive ridleys *Lepidochelys olivacea* are the most abundant sea turtles in the world, and their early life and adulthood offshore distributions make them less prone to anthropogenic coastal threats. However, primary use of oceanic habitat also results in olive ridley life history being the least studied of all sea turtle species. Here, age at maturation and growth rates of 68 olive ridleys washed ashore dead in northeastern Brazil were estimated through skeletochronological analysis of humerus bones. Turtles ranged from 58.0 to 77.0 cm in curved carapace length (CCL), with estimated ages between 14 and 26 yr old. As the sample comprised mostly adults, it was necessary to apply a correction factor from skeletochronological analysis of north-central Pacific olive ridley sea turtles to estimate the number of skeletal growth marks potentially lost at the bone's core. Mean age at sexual maturation was estimated to be 16 yr for a mean size at sexual maturation of 66.0 cm CCL. Growth models fit to the data showed a clear plateau of growth at 15 yr old, which likely coincides with the time when turtles begin directing energy toward reproduction instead of somatic growth. The olive ridley population in the study area is threatened in oceanic and neritic waters by longline and trawl fisheries, respectively. Despite this current threat, the number of nests has increased sharply for the past 16 yr, a time frame coincident with initiation of conservation actions on the beaches in 1982 and which corresponds with the mean age at maturity found in the current study.

KEY WORDS: Growth rate · Line of arrested growth · LAG · Life history · Maturation · Reptile · Skeletochronology · Skeletal growth mark

Resale or republication not permitted without written consent of the publisher

INTRODUCTION

Age and size are critical components of an animal's life history and key parameters to estimate somatic growth rates and age at maturation of a given popu-

lation (Bernardo 1993). Age at sexual maturation is one of the most significant data gaps in our knowledge of sea turtle demography (Bjorndal et al. 2013) and a parameter that must be estimated more rigorously to realistically infer extinction risks for sea tur-

*Corresponding author: rpellet@hotmai.com

tles (TEWG 2009). Generally, growth rate is related to age at sexual maturation for slow-growing animals; as the animal reaches maturity, growth rate starts to decrease over time, which reflects a switch in resource allocation to reproduction, rather than to somatic growth (Kozłowski 1992). Environmental conditions can also affect growth rates such that ectotherms from cold environments grow more slowly but reach larger sizes than at high temperatures (Kozłowski et al. 2004). Age determination, growth rates and particularly age-at-maturity data are essential parameters for population viability analysis (PVA). PVA uses measured or inferred life history data to predict the probability risk of extinction of a given population and project it forward using stochastic computer simulation for threatened species (Boyce 1992, Beissinger & Westphal 1998, Brook et al. 2000). The accuracy of parameters used in the models is a key aspect of precise PVA modeling (Brook et al. 2000).

Despite their importance, age and growth data are difficult to collect due to the complex pattern of migration exhibited by sea turtles throughout their life cycle, and therefore, many questions still remain. Although mark-recapture and captive growth studies can allow age and growth rate estimation, the former is related only to a short period of the overall sea turtle life cycle and the latter does not allow comparison with wild populations (Avens & Snover 2013, Bjørndal et al. 2013). Skeletochronological analysis is a type of age determination method involving skeletal growth mark counts, and in sea turtles, the method has been applied primarily to humerus bones and less often in scleral ossicles (Zug et al. 1986, Zug & Parham 1996). Furthermore, somatic growth rates can be estimated from each skeletal growth mark pair using the back-calculation method described by Snover et al. (2007a), enabling calculation of growth trajectories and consequently allowing detection of possible ontogenetic shifts based on growth rate oscillations (Snover et al. 2010).

Olive ridley sea turtles *Lepidochelys olivacea* spend most of their life cycle in oceanic waters, and are therefore classified as development type 3, oceanic developmental pattern (Bolten 2003). Olive ridley hatchlings emerge from nests, enter the sea, traverse the neritic zone and reach the oceanic zone where they spend their early and late juvenile stages until maturity (Reichert 1993). After maturation, this species recruits to the natal beaches to breed, followed by migration back to foraging grounds (Reichert 1993). This species displays 2 types of reproductive strategies: female turtles nest individually, and/or together in

groups comprising thousands of turtles (1000–500 000 animals), known as 'arribadas' (Plotkin 2007). Both solitary and arribada nesters typically have 2 clutches every nesting season, but the former has an interesting interval of 2 wk, while for the latter it seems to be 4 wk or more (Bernardo & Plotkin 2007).

Olive ridleys occur nearly circumglobally in tropical oceans (Reichert 1993). There are few studies of habitat use of juvenile olive ridleys, but in the Pacific Ocean, Polovina et al. (2004) demonstrated use of oceanic habitat from 15° to 26°N, with a water temperature regime between 23 and 28°C. In the western South Atlantic Ocean, off the northern Brazilian coast, Sales et al. (2008) reported that olive ridleys ranging from 35 to 80 cm in curved carapace length (CCL) were incidentally captured in the pelagic longline fishery mostly between 10°N and 10°S. Although this size range encompasses late juveniles and adult stages, most captured turtles were juveniles, based on the smaller size of olive ridleys nesting in Brazil (62.50 cm CCL) (Silva et al. 2007, Sales et al. 2008). This suggests that oceanic waters adjacent to northern Brazil are likely to be important habitats for juvenile olive ridleys (Sales et al. 2008). In contrast, adults in the same area seem to utilize both oceanic and neritic areas after the nesting season. Silva et al. (2011) demonstrated that post-nesting migrations of olive ridley occur in 3 different directions: while some individuals migrate to oceanic waters, others move to neritic waters northward or southward to feed. In Australia, French Guiana and Oman, following the nesting season, olive ridleys remain primarily in neritic areas and forage over the continental shelf (Whiting et al. 2007a, Rees et al. 2012, Plot et al. 2015). In contrast, in the eastern tropical Pacific Ocean, adults of this species seem to utilize more oceanic than neritic feeding grounds after nesting seasons (Plotkin 2010). Plot et al. (2015) proposed that these different patterns of post-nesting migration in olive ridley populations worldwide are due to environmental conditions in the areas adjacent to the reproductive sites.

In the South Atlantic Ocean, the largest nesting population of olive ridleys occurs in Gabon (Africa) followed by Suriname/French Guiana and Brazil, and smaller populations occur in Angola and the Republic of Congo (Metcalfe et al. 2015). Within Brazil, Sergipe state in the northeast hosts the main nesting area for olive ridley sea turtles in the country, and the species is threatened by incidental mortality in the trawl fishery in this region (Silva et al. 2007, 2010). Since 1990, the number of trawl vessels has increased in areas close to olive ridley nesting beaches,

where adult males and females reside during reproductive seasons (Silva et al. 2010, 2011). This overlap causes increased mortality of adults, the life stage essential for persistence of sea turtle populations (Wallace et al. 2008). From 1994 to 1999, 283 sea turtles stranded dead on a small section (163 km) of the beach, and 56.9% were olive ridley sea turtles in the size range of adult nesting females (Silva et al. 2010). However, threats are not restricted to the neritic zone, as off the northeastern Brazilian coast, longline fisheries incidentally capture mostly olive ridley and leatherback (*Dermochelys coriacea*) sea turtles (Sales et al. 2008).

As the olive ridley is regarded as the most abundant sea turtle in the world, this species is not ranked as a 'conservation priority', and consequently, funding for research is scarce (Plotkin 2007). Additionally, its mainly oceanic distribution during early life and adulthood impedes access to individuals for study as compared to other, more coastal sea turtle species. As a result, few studies of this species have been conducted and published (Plotkin 2007). To date, only one age-determination study of olive ridley sea turtles has been reported: Zug et al. (2006) estimated the age of 26 specimens from the north-central Pacific through skeletochronology analysis of humerus bones. Turtles in the sample ranged from 20.5 to 64.4 cm in straight carapace length (SCL), and ages were estimated to be between 7.3 and 24.1 yr old (Zug et al. 2006). As olive ridleys from the north-central Pacific mature at 53 cm

SCL, a mean of 13 yr of age at first maturation was estimated (Zug et al. 2006).

In the current study, we estimate the age structure of olive ridley sea turtles stranded dead on the coast of Sergipe state in northeastern Brazil using skeletochronological analysis of humerus bones. In addition, size-at-age data yielded by the analysis are used to generate a growth curve to estimate age at first maturation and somatic growth rates for the first time for this major olive ridley population.

MATERIALS AND METHODS

Study area

Sampling took place along the coast of Sergipe state and south coast of Alagoas state in northeast Brazil, along 173 km of beach, between 10° 31' S and 11° 25' S, which is monitored by TAMAR-ICMBio (the Brazilian Sea Turtle Conservation Programme) in partnership with the Fundação Mamíferos Aquáticos (FMA). In the study area, there are 3 TAMAR-ICMBio stations (Ponta dos Mangues, Pirambu and Abais beaches). Monitoring occurs along the whole Sergipe state coast, in addition to Pontal do Peba, in Alagoas state (Fig. 1). Despite being located in 2 states, the coastlines of both areas are contiguous and as a result are treated as a single area in this study. Sergipe state is the main Brazilian reproductive area for olive ridley

sea turtles, where 77% of Brazilian nests occur (6000 nests yr⁻¹) (Castilhos et al. 2011). Olive ridley sea turtles are known to form 'arribadas' (large nesting aggregations) (Pritchard 2007); however, at this location they are solitary nesters. Although breeding occurs mainly between September and March, olive ridley sea turtle nesting is observed all year round in low numbers (Silva et al. 2007). In 1982, when TAMAR-ICMBio began working in Sergipe state, almost all eggs were collected for human consumption; however, poaching decreased gradually over the years after the TAMAR-ICMBio station was established (Silva et al. 2007). While the number of nests has currently increased (Silva et al. 2007), trawl fishery activity is a significant threat in the area, causing high mortality of olive ridley adults (Silva et al. 2010).

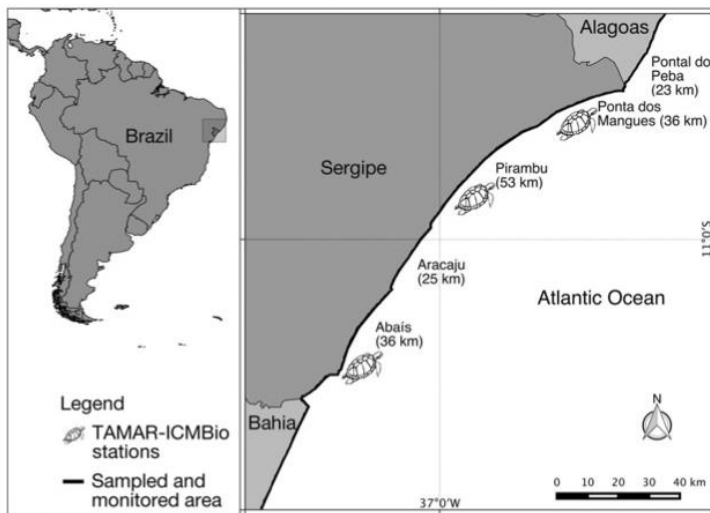


Fig. 1. Sampling locations of olive ridley sea turtles *Lepidochelys olivacea* stranded dead on the coast of Sergipe and Alagoas states, northeastern Brazil. Numbers in km indicate the extension of monitored coastal areas. Beaches in Alagoas were monitored from the nearby stations in Sergipe

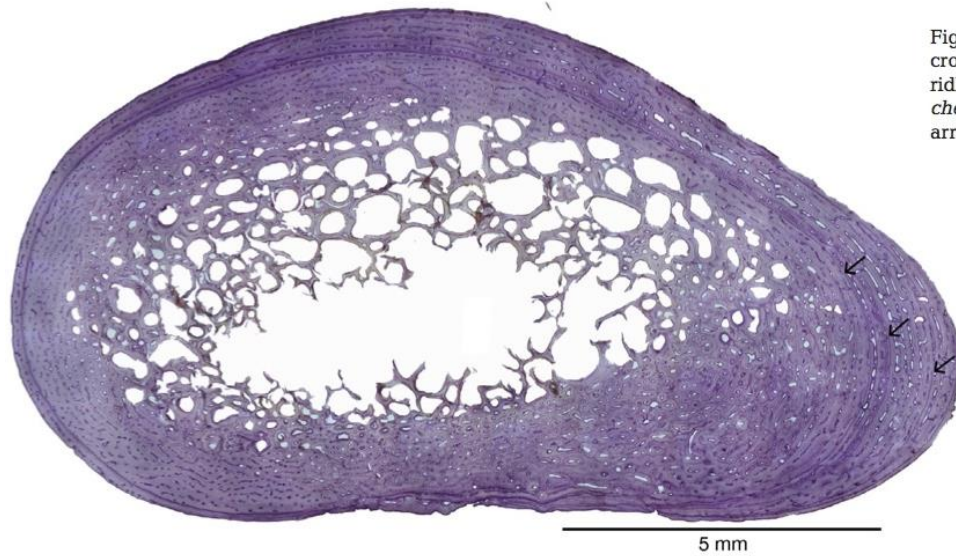


Fig. 2. Humerus (stained cross-section) from olive ridley sea turtle *Lepidochelys olivacea*. Black arrows: lines of arrested growth (LAGs)

Sample collection and preparation

From July 2010 to October 2012, humeri of olive ridleys stranded dead on the beach were collected for skeletochronological analysis. For every turtle, CCL was measured (Bolten 1999) with a flexible metric tape measure (± 0.1 cm). When possible, sex, presence of tags, formed eggs and tumor presence was recorded; if a turtle had a tumor, the sample was discarded. In addition, humeri of 14 fully developed hatchlings that failed to emerge from the nest surface and died at Pirambu beach were sampled.

Humerus bone samples were frozen and then transported to the Laboratório de Aves Aquáticas e Tartarugas Marinhas at the Universidade Federal do Rio Grande (FURG) in southern Brazil. Humeri were cleaned, measured and histologically processed according to methods detailed in Avens & Goshe (2007) and Petit et al. (2012), which resulted in a calibrated digital image of each entire processed humerus cross-section at 4 \times magnification (Fig. 2 & 3).

Age estimation

Each composite cross-section was analyzed as in Petit et al. (2012). A skeletal growth mark consists of a lightly stained area followed by a dark line of arrested growth (LAG), which appeared both as defined or diffuse (Zug et al. 1986). The interpretation of these LAGs was based on Castanet & Smirina (1990) and Snover & Hohn (2004). An axis parallel to the dorsal edge of the humerus was used to measure

the resorption core, width of each LAG and humerus diameter, using ImageJ v.1.48 software.

The first growth mark is called the annulus and differs from others in that it is a diffuse band closest to the center of the bone; subsequent, more discrete LAGs are deposited along the outer circumference. Commonly, the annulus appears in young vertebrates only, because in large animals, resorption of older inner lines occurs as the individual develops and matures (Zug et al. 1986). The majority of sampled humeri were from adult olive ridleys, based on the size range of mature females from the main nesting area in Sergipe state (Silva et al. 2007), or the presence of eggs in the oviducts for stranded fe-

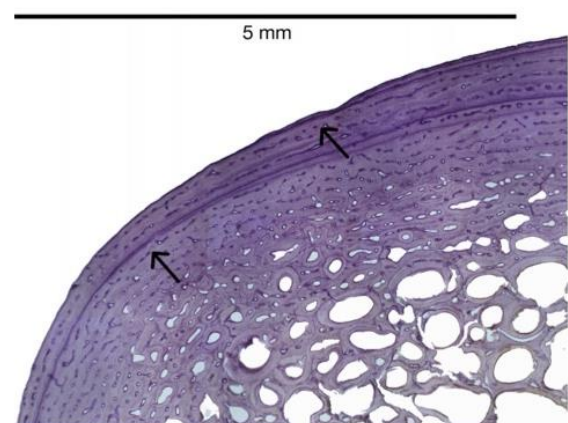


Fig. 3. Higher magnification of a portion of a humerus stained section from olive ridley sea turtle *Lepidochelys olivacea*. Arrows indicate where the lines of arrested growth (LAGs) are splitting

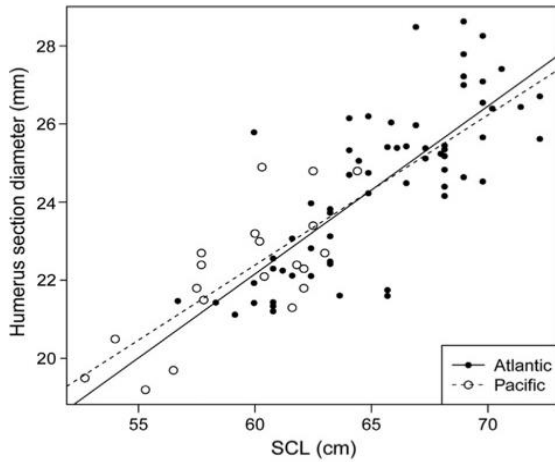


Fig. 4. Relationship between humerus section diameter (HSD) and straight carapace length (SCL) of olive ridley sea turtles *Lepidochelys olivacea* sampled in the Atlantic and Pacific Oceans. Solid line is the model ($SCL = a + b \cdot HSD$) fitted to the data set of olive ridleys from northeastern Brazil only. Dashed line is the same model, but data set is from olive ridleys from the Pacific, stranded at Hawaii archipelago

males. Because our sample did not contain juvenile turtles, annuli could not be found. Therefore, a correction factor was applied to estimate the number of lost LAGs in the resorption core of each section. This correction factor was based on data from olive ridley

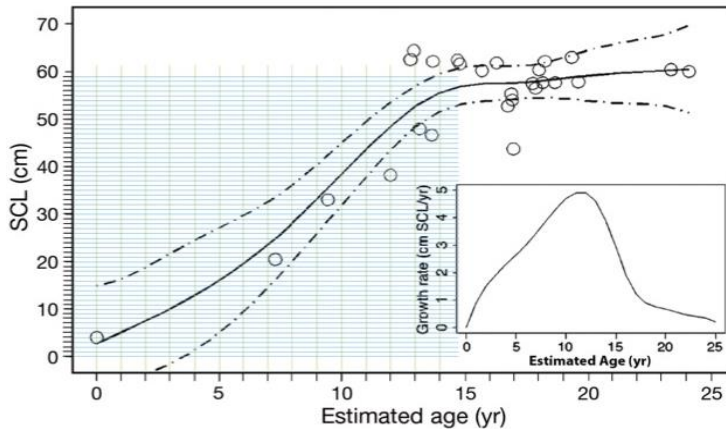


Fig. 5. Growth model fitted to size-at-age data of olive ridley sea turtles *Lepidochelys olivacea* from the Pacific Ocean, from Zug et al. (2006). Shaded area is the grid overlaid to extract the size-at-age data to estimate lost lines of arrested growth (LAG) of olive ridleys from the Atlantic. Adapted from Zug et al. (2006). SCL = straight carapace length. Dashed lines are the 95 % interval of growth model. Open dots are the estimated age and inset shows growth rates of olive ridley sea turtles from Zug et al. (2006)

turtles from the north-central Pacific Ocean, as reported in Zug et al. (2006). As populations are different between the Pacific and Atlantic basins, it was first necessary to determine whether turtles from the 2 populations have a similar growth. Thus, a linear model between humerus section diameter (HSD) vs. SCL was fitted, one for Pacific Ocean data (Zug et al. 2006) and another for Atlantic Ocean data (present study). Comparison of both linear models revealed that the 2 turtles groups exhibit very similar growth patterns, as the relationships were not significantly different (Fig. 4; $p = 0.652$).

Thereafter, a data set of size-at-age extracted from the growth model fitted to 26 specimens (20.5–64.4 cm SCL) along with the known mean hatchling size (~4 cm SCL) from the north-central Pacific Ocean were used to develop the correction factor. A grid was overlaid onto a growth model fitted (generalized smoothing spline model) to estimate SCL at discrete year intervals (Zug et al. 2006) (Fig. 5). Year was used as a proxy for LAG number, starting with the first year LAG (Fig. 5), and SCL was substituted into the relationship SCL vs. HSD provided by Zug et al. (2006) to yield an estimate of LAG diameter at size ($HSD = 0.332 + 0.385SCL$). Two models were then fit to the LAG diameter:LAG number pairs to characterize the relationship: the first model was a linear regression ($y = a + bx$) and the second model was a power function ($y = ax^b$), where y is the LAG diameter, x is the LAG number, a and b are the estimated parameters. Finally, we used the estimated parameters (a and b) and substituted resorption core diameter (y_{core}) for LAG diameter for each turtle in the sample to estimate the number of LAGs potentially lost to resorption (x_{core}). The age estimate for each turtle was therefore a combination of the number of growth layers observed in the outermost region of the bone section (x_{obs}), plus the predicted number of resorbed growth layers in the resorption core of the humerus ($x = x_{core} + x_{obs}$). As carapace measures were based in CCL, this measurement was converted to SCL based on the equation from Whiting et al. (2007b) (range: 65.0–75.2 cm CCL, $n = 85$; $SCL = 0.818CCL + 9.244$; $R^2 = 0.91$).

Age estimation was based on the assumption that 1 LAG represents 1 yr of age, as has been validated by known age specimens and marginal

increment analysis for the phylogenetically close Kemp's ridley *Lepidochelys kempii* (Snover 2002, Snover & Hohn 2004), and a marginal increment analysis to describe the pattern of skeletal growth mark deposition of a tropical sea turtle species, the hawksbill sea turtle *Eretmochelys imbricata* (Snover et al. 2013). Additionally, the pattern of annual LAG deposition has also been validated for 2 other sea turtle species: loggerhead *Caretta caretta* and green turtle *Chelonia mydas* (Klinger & Musick 1992, Coles et al. 2001, Snover et al. 2011) with known age specimen and tetracycline labeling, respectively. For the olive ridley, validation is difficult because they spend most of their life cycle in the oceanic zone. However, although the Kemp's ridley has a different life cycle from the olive ridley, the 2 species are closely related, having diverged only 2.5–3.5 million yr ago (Bowen et al. 1998). In addition, the 2 ridley sea turtle species share many characteristics: they are the smallest of all sea turtle species, with similar minimum female nesting size (~60 cm SCL) (Reichert 1993, Zug et al. 1997, Silva et al. 2007), and both species exhibit arribadas (Pritchard 2007). Therefore, it is likely that the olive ridley sea turtle deposits 1 LAG each year of life, as assumed in the current study.

Growth model

Schnute's growth model was fitted to the olive ridley sea turtles' size-at-age, as was done for loggerhead sea turtles in Petit et al. (2012). It is a general model that includes Pütter, von Bertalanffy, Richards, Gompertz and logistic growth models as special cases. The model proposed by Schnute (1981) is appropriate for the purpose of the present study, as the available size-at-age data for olive ridley sea turtles describes only 2 stages of their life cycle, hatching and adults; therefore, the flexibility of this growth model to accommodate this is an advantage. Schnute's generic equation with 5 parameters is detailed in Schnute (1981) and Petit et al. (2012).

Growth rates

Growth rates were calculated based on the back-calculation method (Snover et al. 2007a) and incorporating the body proportional hypothesis (BPH) from Francis (1990). Four equations were fitted to check the best relationship between carapace length (in cm, SCL) and HSD (mm) (excluding hatchlings) as in Petit et al. (2012) for loggerhead sea turtles. The

mean hatchling carapace length used was 4.03 ± 0.17 (SD) cm SCL and the mean hatchling humerus diameter was 2.20 ± 0.02 mm. Then we used the BPH equation to back-calculate carapace length from the interior LAGs, as in the equation provided by Francis (1990) and Petit et al. (2012).

Annual somatic growth rates were calculated from each pair of successive LAG diameter measurements for each olive ridley in the sample, based on the assumption that 1 LAG represents 1 yr of age. In addition, as the sample comprised mostly adults, many olive ridley humerus sections showed LAGs spaced very closely together at the outer edge (Fig. 3). Such a decrease in LAG spacing corresponds to a decrease in growth rates, as a consequence of the onset of sexual maturity (Francillon-Vieillot et al. 1990, Guarino et al. 2008), when a turtle becomes anatomically and endocrinally capable of copulating and producing viable eggs (Caillouet et al. 2011). This phenomenon in the bones is termed 'rapprochement', and refers to the first decreasing interval between LAGs, previously observed in humeri of adult-sized turtles (Goshe et al. 2010, Snover et al. 2013, Avens et al. 2015) (Fig. 3). Therefore, size and age associated with the rapprochement LAG for a turtle were estimated when this line could be identified, as a proxy for estimated size at sexual maturation (SSM) and age at sexual maturation (ASM).

Statistical analysis

Inference was performed within a Bayesian statistical framework (Ellison 2004). In Bayesian analysis, estimates of unknown parameters are given as probability distributions denoted 'posteriors' (Gelman et al. 2003). We used non-informative priors for all estimated parameters and models fitted. Samples from the posterior distributions were drawn by Markov chain Monte Carlo (MCMC) and sampling importance resampling (SIR) (Gelman et al. 2003, Skare et al. 2003). In MCMC, a Markov chain is set up in such a fashion that the posterior is its long-run equilibrium distribution, while SIR aims at drawing a random sample from a target distribution. We used SIR only for the Schnute's growth model due to difficulties in obtaining acceptable convergence with MCMC.

All analyses were performed with R software (R Core Team 2014), and the JAGS program (<http://mcmc-jags.sourceforge.net> [accessed on 4 February 2015]) to specify models and perform the Bayesian analysis (Gilks et al. 1994). The R code for all ap-

Table 1. Values of Bayesian fits from power function model and linear regression between the diameter of the line of arrested growth (LAG) versus LAG number of olive ridley sea turtles *Lepidochelys olivacea* sampled in the Pacific Ocean by Zug et al. (2006). *a*, *b* and σ represent the posterior mean; values in brackets are 95% probability intervals. DIC = deviance information criterion; a smaller DIC indicates a better model fit

Parameter	Power function $y = ax^b$	Linear regression $y = a + bx$
<i>a</i>	0.27 [0.08–0.44]	0.17 [–0.02 to 0.36]
<i>b</i>	1.06 [0.93–1.18]	1.50 [1.44–1.55]
σ	0.34 [0.32–0.43]	0.81 [0.57–1.18]
DIC	1.30	37.58

plications is available in the Supplement at www.int-res.com/articles/suppl/m451p205_supp.pdf. Model selection was based on the deviance information criterion (DIC), in which the smallest values indicate the best fit (Spiegelhalter et al. 2002).

RESULTS

Age estimation

Age estimates for a total of 68 turtles with CCL between 58.0 and 77.0 cm (mean \pm SD: 69.1 \pm 4.56 cm) or SCL between 56.7 and 72.2 cm (mean \pm SD: 65.8 \pm 3.73 cm) were between 14 and 26 yr. The

sample comprised 25 females, 5 males and 38 turtles of undetermined sex, of which a sub-sample of 17 females was classified as sexually mature by the presence of formed eggs in the oviduct (n = 10) or detection of tags previously applied when the turtle had nested (n = 7). The power function model provided the best fit for the LAG diameter:LAG number relationship, according to the lower DIC value (Table 1). From the data set of Zug et al. (2006), the correction factor equation to estimate the number LAGs lost to resorption took the form:

$$LAG \text{ diameter (mm)} = 0.26 \times (LAG \text{ number})^{1.05} \quad (1)$$

Thus, within the equation, resorption core diameter values (y_{core}) were substituted for LAG diameters to provide the number of lost LAGs in the resorption area (x_{core}). The LAGs effectively observed in each humerus ranged from 3 to 9, while the estimated lost LAGs in the resorption core ranged from 11 to 16. LAG deposition patterns were similar to those of other sea turtle species, with a light band of fast bone growth followed by a dark line of slow growth, and the majority of the humerus sections presented split and double LAGs (Zug et al. 1986, Castanet & Smirina 1990) (Fig. 3).

Growth model

Schnute's growth model fitted well to size-at-age data for olive ridley sea turtles in the current study (Fig. 6a), generating a curve similar to size-at-age data from the Pacific (Fig. 5). The curve had an

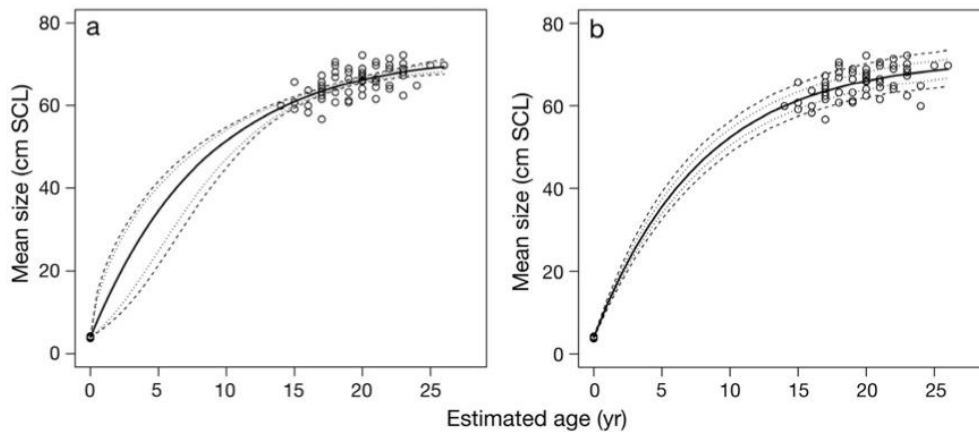


Fig. 6. Bayesian fit of (a) Schnute's (1981) and (b) von Bertalanffy growth models to estimated age vs. size (straight carapace length, SCL) of olive ridley sea turtles *Lepidochelys olivacea* sampled in the Atlantic Ocean along northeastern Brazil. Black solid line is the curve generated from Schnute's model; dashed and dotted lines are probability intervals of 95% and 80%, respectively

Table 2. Bayesian fit of Schnute's (1981) and von Bertalanffy growth models for straight carapace length (SCL) and estimated age data of olive ridley sea turtles *Lepidochelys olivacea* sampled in northeastern Brazil. Estimated parameters are posterior means; values in brackets are 95% probability intervals. DIC = deviance information criterion to guide model selection; a smaller DIC indicates a better fit. nd = no data

Parameter	Schnute's model	Parameter	von Bertalanffy model
a	0.19 [0.09–0.31]	y_0	4.03 [3.93–4.14]
b	0.18 [–0.92 to 1.18]	k	0.13 [0.02–0.16]
y_1	4.03 [3.93–4.13]	y_∞	71.71 [68.12–76.25]
y_2	68.42 [66.75–70.35]	σ	0.05 [0.04–0.06]
σ	0.05 [0.04–0.06]	nd	nd
DIC	–407.8	DIC	347.2

inflection point (τ_i, y_i) and became S-shaped. The values of parameters a and b were similar to parameters of a von Bertalanffy growth model (von Bertalanffy 1957). The von Bertalanffy growth model requires a sample from all size classes ranging from hatchlings to old adults encompassing asymptotic size. Despite that our sample was restricted to mostly adults and 14 hatchlings, the von Bertalanffy model also fitted well, but the curve did not have an inflection point (Fig. 6b). The von Bertalanffy growth model equation took the form:

$$y_\tau = y_\infty [1 - \exp(-k(\tau - y_0))] \quad (2)$$

where y_τ is the size of the specimen at age τ ; in this case the size was the SCL in cm; k is the intrinsic growth rate and y_0 is the hypothetical age when length is equal to 0. Although both the Schnute's and von Bertalanffy growth models had similar parameter values (Table 2), Schnute's model had a smaller DIC than the von Bertalanffy model, suggesting that the former model had a better fit than the latter. As the von Bertalanffy model, in addition to the Pütter, Richards, Gompertz and logistic models, are special cases of the generalized growth model proposed by Schnute (1981), it was expected that Schnute's model would have a better fit than von Bertalanffy's. In addition, as the von Bertalanffy growth model is simpler than Schnute's, it calculated the age at maturation of olive ridleys from Eq. (2). The growth model fits demonstrated a gradual

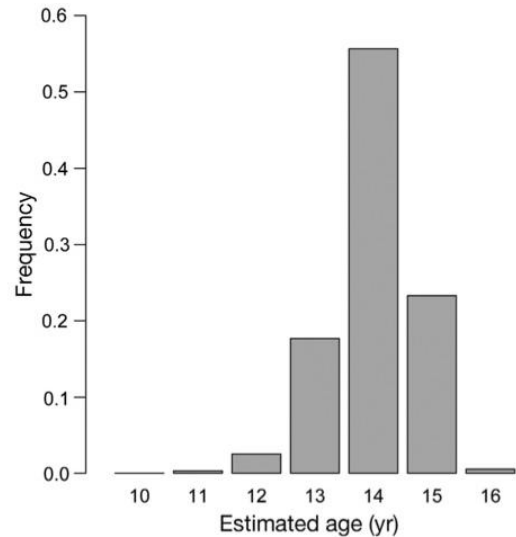


Fig. 7. Estimated distribution for age at maturation for olive ridley sea turtles *Lepidochelys olivacea* sampled in northeastern Brazil

decrease in growth at around 60 cm SCL, which corresponds with the lower end of the size range of olive ridleys recorded nesting at the main reproductive area in Brazil where humerus samples were obtained (Silva et al. 2007). For this size, mean age was estimated to be 14 yr, with a probability interval between 10 and 16 yr old. However, olive ridley sea turtles were estimated to have a 79% of probability of maturing at 14–15 yr of age (Fig. 7).

Table 3. Bayesian fit of 4 models for straight carapace length (SCL) vs. humerus section diameter (HSD) of olive ridley sea turtles *Lepidochelys olivacea* sampled in northeastern Brazil. In each model, L is SCL and D is HSD; L_{op} = carapace length at hatching; D_{op} = humerus diameter at hatching. Estimated parameters are posterior means; values in brackets are 95% probability intervals. DIC = deviance information criterion to select among models; a smaller DIC indicates a better fit

Model	Estimated parameters				DIC
	a	b	c	σ	
$L = L_{op} + b(D - D_{op})^c$		2.36 [2.12–2.70]	0.57 [0.46–0.64]	0.041 [0.035–0.049]	234.1
$L = L_{op} + b(D - D_{op})$		2.73 [2.69–2.76]		3.57 [3.01–4.25]	369.4
$L = a + bD^c$	16.91 [3.44–28.51]	4.38 [2.51–7.88]	0.76 [0.61–0.87]	2.53 [2.14–3.02]	323.5
$L = a + bD$	30.59 [22.80–39.82]	1.42 [1.04–1.73]		2.52 [2.13–3.01]	323.3

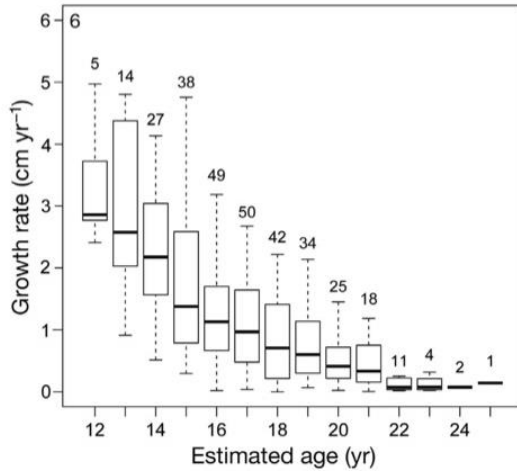


Fig. 8. Relationship between estimated age and annual growth rate based on back-calculated lengths from each growth mark diameter from each olive ridley sea turtle *Lepidochelys olivacea* sampled. Boxes are the range of growth rates; horizontal lines inside boxes are the means; vertical dashed lines are SD; numbers above boxes are sample sizes (i.e. numbers of lines of arrested growth or LAGs) corresponding with each age indicated along the x-axis

Growth rates

The best fit for back calculation was the equation which incorporated L_{op} , D_{op} and the constant c (Table 3). Therefore, this equation was used in the BPH equation from Francis (1990) and from Petitet et al. (2012) to calculate growth rates. The growth rate between each LAG pair showed a decrease from the inner LAG to the outer LAG (Fig. 8), suggesting that as turtles get older, growth rate decreases. The sample showed only growth rates from LAGs related to age estimates between 12 and 25 yr old. Although this range encompasses only the adult stage, it is clear that growth rates associated with early ages at maturation (12 yr) are higher than those corresponding with mean age at maturation (14–15 yr), when growth rates slow down (Fig. 8).

In 60 olive ridley humeri, the rapprochement LAG was identified, and the range of ages inferred by this approach was from 13 to 21 yr old (mean \pm SD: 16.6 ± 1.80 yr), while estimated SCL varied between 56.1 and 68.6 cm (mean \pm SD: 63.3 ± 3.34 cm) or CCL between 57.5 and 72.6 cm (mean \pm SD: 66.0 ± 3.34 cm). The number of years after rapprochement (= period after maturation) ranged from 1 to 7 yr, in which growth rates decreased and became gradual (Fig. 9). The sub-sample of 17

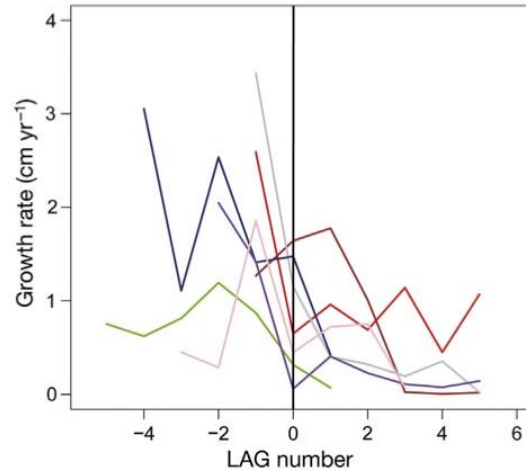


Fig. 9. Growth rates from 6 turtles from the sub-sample of 17 matured females of olive ridley *Lepidochelys olivacea*. Each line represents 1 individual; the line of arrested growth (LAG) 0 refers to the rapprochement (maturation) represented by the black straight line in the middle of the graph

mature females had ASM estimates between 15 and 21 yr old (mean \pm SD: $18 \text{ yr} \pm 1.53 \text{ yr}$), at SSMs between 60.8 and 68.5 cm SCL (mean \pm SD: 65.5 ± 2.78 cm) or 63.0 and 72.5 cm CCL (mean \pm SD: 68.8 ± 3.40 cm).

DISCUSSION

Age estimation

We present the first study of age estimation for olive ridleys from the Atlantic Ocean, based on skeletochronological analysis and estimated for olive ridleys sized 56.7–72.2 cm SCL and ranging in age from 14–26 yr old. As the correction factor for lost LAGs applied was based on data from the north-central Pacific Ocean for turtles 7.3–24 yr old and 20.5–64.4 cm SCL in size (Zug et al. 2006), similar ages were expected for turtles of similar sizes in our samples from the Atlantic. However, there were some Atlantic olive ridleys in our sample of similar size or smaller whose age estimates were either younger or older than turtles from the Pacific. These discrepancies may have been in part due to methodological differences between the 2 studies; whereas Zug et al. (2006) analyzed undecalcified and unstained humerus cross-sections, the current study examined decalcified, thin-sectioned, stained hume-

rus cross-sections. Goshe et al. (2009) showed that in larger animals, the skeletochronological method without staining humerus sections might underestimate age due to the presence of closely spaced LAGs. As our sampling comprised mostly adults, with sections depicting double and split LAGs (Castanet et al. 1993, Snover & Hohn 2004, Petit et al. 2012), without staining, it would be impossible to read all lines (Figs. 2 & 3). However, for juveniles, there was no significant difference in the number of visible LAGs between stained and unstained bones (Goshe et al. 2009). As a result, use of the correction factor based on a data set of juveniles from Zug et al. (2006) was appropriate for the present study.

The frequency of growth mark deposition can potentially vary between and within individuals due to the influence of favorable and unfavorable environmental conditions, access to resources, abiotic factors and genetic contribution (Bjorndal et al. 2003, Petit et al. 2012). Formerly it was assumed that growth mark deposition in ectotherms was linked to variations in growth rates caused by seasonal fluctuations in temperature (Patnaik & Behera 1981). However, studies of tropical cold-blooded species, i.e. reptiles and amphibians, have demonstrated annual deposition of growth marks despite the absence of seasonal influences in the environment. Pal et al. (2009) and Zug & Rand (1987) showed annual deposition of LAGs in long bones (humerus, femur and third toe) from tropical lizards, fan-throated lizard *Sitana ponticeriana* and green iguana *Iguana iguana*, respectively. Scholz et al. (2010) demonstrated LAGs with seasonal growth pattern in a tropical amphibian, the West African caecilian *Geotrypetes seraphini*, which they interpreted as annually deposited marks. Although these are terrestrial animals, analyses have also supported deposition of annual LAGs in humeri of hawksbill and green sea turtles from the tropical Hawaiian archipelago (Snover et al. 2011, 2013). In addition to the more tropical sea turtle species, olive ridley humerus sections are also similar to those of loggerheads and Kemp's ridleys, which despite being temperate sea turtle species also have been demonstrated to exhibit annual LAG deposition (Klinger & Musick 1992, Coles et al. 2001, Snover & Hohn 2004). Given that olive ridley humerus sections in the present study showed LAG deposition characteristics similar to other sea turtles, this indicates that olive ridley bone growth may also have an annual cyclic pattern (Fig. 2).

The olive ridley, as well as the leatherback sea turtle, is more oceanic than other sea turtle species.

After hatching, olive ridleys spend all early life and late juvenile phases in the oceanic zone, after which they mature and recruit to nearshore areas for mating and nesting (Reichert 1993). The duration of the 'lost years', which is the period from hatchlings entering the sea until recruitment (Musick & Limpus 1996), is still unknown for these species. However, as the present study estimated a mean age of 14 yr old (range 10–16 yr) for the first maturation by the von Bertalanffy growth model, it can be estimated that the 'lost years' period for olive ridley sea turtle spans at least ~10 yr. After this time, they recruit to natal beaches, breed and/or nest, and migrate to a neritic or oceanic foraging ground (Plotkin 2010, Silva et al. 2011, Plot et al. 2015). The mean age at maturation estimated for olive ridleys in this study (~14 yr old) was similar to north-central Pacific olive ridleys (~13 yr old), despite that the minimum size for nesting females on Pacific Ocean beaches is 53 cm SCL (Zug et al. 2006), while for Atlantic Ocean beaches it is around 60 cm SCL or 62.50 cm CCL (Silva et al. 2007). Kemp's ridleys in the Gulf of Mexico have a mean age at maturation of 12 yr (range 9.9–16.7 yr) at around 60 cm SCL (Snover et al. 2007b), similar to olive ridleys from the Atlantic Ocean. Thus, it appears that despite ecological differences, such as a more benthic and coastal foraging in Kemp's ridley (Snover et al. 2007b), both species mature at similar ages.

ASM was also estimated using the von Bertalanffy growth model and from the rapprochement LAG; the former gave a range from 10 to 16 yr old (mean ~14 yr), while the second method gave between 13 and 21 yr old (mean ~16.6 yr). The von Bertalanffy growth model estimation was based on the minimum size of a nesting female (60.0 cm SCL) and the second approach was based on SCL back-calculated from the rapprochement LAG (56.1–68.6 cm SCL). However, as nesting females may mature before the first recorded nesting (Caillouet et al. 2011), individuals could mature at smaller sizes and earlier ages than our estimation. Because the model results showed smaller sizes and older ages at sexual maturity than the rapprochement LAG method, this discrepancy may be due to the limited growth after sexual maturity of sea turtles, and consequently SSM and ASM seem not to be correlated. After deposition of the rapprochement LAG, olive ridley sea turtle adult stage duration ranged from 1 to 7 yr, during which time they exhibited growth rates between 0 and 2.47 cm yr⁻¹ (mean ± SD: 0.69 ± 0.57 cm yr⁻¹). Thus, some individuals seem to have no growth after maturation, while others grew almost 2.5 cm. Therefore, SSM

and ASM from rapprochement LAG seem to be more reliable because there are large variations in female sizes, characteristic of sea turtle populations (Broderrick et al. 2003, Bjørndal et al. 2013). Moreover, for the sub-sample of 17 females confirmed as mature by formed eggs or tagging, the SSM estimates (60.8–68.5 cm SCL) fall within the range size of nesting females found at Sergipe coast (60.0–77.0 cm SCL), although these SSMs, corresponding with ASM estimates (15–21 yr), are greater than those yielded by the growth model.

Growth model and growth rate

Schnute and von Bertalanffy fits generated similar curves for Atlantic olive ridleys, with slower growth for turtles greater than 60 cm SCL (Fig. 6). At around this size, the turtles mature and presumably most resources consumed are directed toward reproduction instead of somatic growth (Bernardo 1993, Bjørndal et al. 2003). Similar growth patterns for larger olive ridley turtles in the Pacific were described by Zug et al. (2006) (Fig. 5). Colman et al. (2014) analyzed stomach contents from adult olive ridleys stranded dead along the Sergipe coast and found that of 30 turtles analyzed, 14 had empty stomachs and the remaining 16 had fed mostly on crustaceans (crabs and shrimps) and demersal fish. Even with benthic items holding higher caloric content than oceanic items, this high energy intake would be allocated to the energetic costs of reproduction, corresponding with observed low somatic growth rates for the adults sampled (Fig. 8).

Although little is known about the juvenile stage for olive ridleys, it is thought that in the Pacific Ocean, most juveniles inhabit the center of the Subtropical Gyre, characterized by warmer vertically stratified water and a deeper thermocline (Polovina et al. 2004). During this stage, the most common prey are pyrosomes and salps (Polovina et al. 2004), and it is likely that juveniles are feeding constantly and allocating energy to grow in size in order to minimize predation risks (Snover et al. 2007a). Zug et al. (2006) showed linear growth for olive ridley juveniles and consequently high growth rate (Fig. 5). The present study lacks juvenile samples, although it is clear in Fig. 8 that growth rates from inner LAGs are greater than LAGs related to the mean age-at-maturation (~16 yr old).

This growth scenario, with linear growth for juveniles and gradual growth for adults, is exhibited by all major ectothermic animal groups, which present

slow growth and late maturity, similar to all sea turtle species. In addition, most ectotherms grow more slowly in cold, but reach a larger adult size than at high temperatures (Kozłowski et al. 2004), as might be the case for the olive ridley, which reaches a maximum of 75 cm SCL, smaller than other temperate sea turtle species (Reichert 1993). This temperature effect is called the 'temperature-size rule', with large size in the cold attained by a prolonged growth period, which compensates for slow growth (Atkinson 1996). Moreover, this temperature effect differs from the effect of limited resources (growth retardation accompanied by smaller adult size; Kozłowski et al. 2004).

Implications for conservation

Estimated ages-at-maturation and growth rates are key parameters to support science-informed conservation actions of a given population. These estimates allow prediction of population resilience, but if the estimated is biased, it can lead to negative impacts (Avens et al. 2009). We estimated a mean age at maturation of 16 yr for the olive ridley sea turtle, greater than estimates for the north-central Pacific population (~13 yr old) (Zug et al. 2006). This means that at Sergipe state in northeastern Brazil, the olive ridley sea turtle would require at least 16 yr to recover from a negative impact. The estimated age-at-maturation is congruent with the step increase in the number of nests in the area, suggesting the effectiveness of protection of rookeries. TAMAR-ICMBio started protecting the nesting population in the area in 1982, and 16 yr later, in 1998, the number of nests started increasing (Silva et al. 2007). The nest monitoring effort has increased over the years, but, before protection, hunting of nesting female olive ridleys for meat and nest opening for egg consumption were common practices, which are nowadays prohibited (Castilhos et al. 2011). Thus, we are confident that the upward trend in the number of nests is a real increase in the population size.

Although the olive ridley sea turtle is the most abundant sea turtle species in the world (Plotkin 2007), this species is listed as Vulnerable by the IUCN Red List (IUCN 2015), with an inferred decreasing trend, and listed as Endangered in the Brazilian Red List (MMA 2014). Before 1982, in the present study area, this species was threatened by human consumption, while currently, olive ridleys are threatened throughout their annual and life cycles: in oceanic waters, mostly juveniles are inci-

dentally captured in pelagic longline fisheries, while in neritic waters, mostly adults are incidentally captured by shrimp trawlers (Sales et al. 2008, Silva et al. 2010). Moreover, olive ridleys washed ashore in this area are in the size range of adults, often with formed eggs in females (Castilhos & Tiwari 2006). In addition to potential effects on the population, caused by fisheries bycatch, the lack of planning for coastal development causes additional negative impacts, including moving sandy beaches (sand extraction and landfills), photopollution, vehicle traffic, human presence on the beaches, harbors, anchorages and jetties, occupation of the fringe by hotels and houses, and exploitation of oil and gas very close to beaches (Castilhos et al. 2011).

Our results have elucidated key aspects of olive ridley demography, such as age-at-maturation and growth rates, which are key parameters to PVA, to model prediction of extinction risk for this little-known, threatened species. Additional studies focused on the elusive juvenile stages, as well as studies integrating the role of individual threats to each life stage, would be important for accurate PVA analysis. Because the juvenile stages take place in oceanic waters, future studies benefiting from the study of individuals incidentally captured by pelagic longline fisheries, together with telemetry and stable isotope analysis of tissues from adults washed ashore, will further improve our understanding of habitat use and support effective conservation.

Acknowledgements. We acknowledge the TAMAR/ICMBio and FMA staffs for the humeri samples, with special thanks to Ederson Luiz Fonseca, Fabio Lira, Mari Weber, Jociery Vergara Parente, Bruno Almeida and veterinarians for their support. Bone sampling was possible due to the support of PRMEA (Regional Monitoring Program of Strandings and Abnormalities), a measure of environmental impact assessment required by federal environmental licensing for oil and gas exploration, conducted by IBAMA, Instituto Brasileiro do Meio Ambiente e dos Recursos Naturais Renováveis. The skeletochronology method was carried out with logistics provided by the Laboratório de Ecologia da Megafauna Marinha (Instituto de Oceanografia—FURG), with special thanks to Eduardo R. Secchi and Silvina Botta. R.P. received financial support from the Coordenação de Aperfeiçoamento de Pessoal de Nível Superior (CAPES). L.B. is a research fellow of the Brazilian CNPq, National Council for Scientific and Technological Development (Proc. No. 308697/2012-0). This research is part of the PhD thesis written by R.P. under the guidance of L.B.

LITERATURE CITED

- Atkinson D (1996) Ectotherm life history responses to developmental temperatures. In: Johnston IA, Bennett AF (eds) *Animals and temperature: phenotypic and evolutionary adaptation*. Cambridge University Press, Cambridge, p 183–204
- Avens L, Goshe LR (2007) Comparative skeletochronological analysis of Kemp's ridley (*Lepidochelys kempii*) and loggerhead (*Caretta caretta*) humeri and scleral ossicles. *Mar Biol* 152:1309–1317
- Avens L, Snover ML (2013) Age and age estimation in sea turtles. In: Wyneken J, Lohmann KJ, Musick JA (eds) *The biology of sea turtles*, Vol 3. CRC Press, Boca Raton, FL, p 97–133
- Avens L, Taylor JC, Goshe LR, Jones TT, Hastings M (2009) Use of skeletochronological analysis to estimate the age of leatherback sea turtles *Dermochelys coriacea* in the western North Atlantic. *Endang Species Res* 8:165–177
- Avens L, Goshe LR, Coggins L, Snover ML, Pajuelo M, Bjørndal KA, Bolten AB (2015) Age and size at maturation and adult stage duration for loggerhead sea turtles in the western North Atlantic. *Mar Biol* 162:1749–1767
- Beissinger SR, Westphal MI (1998) On the use of demographic models of population viability in endangered species management. *J Wildl Manag* 62:821–841
- Bernardo J (1993) Determinants of maturation in animals. *Trends Ecol Evol* 8:166–173
- Bernardo J, Plotkin PT (2007) An evolutionary perspective in the *arribada* phenomenon and reproductive behavioral polymorphism of olive ridley sea turtle (*Lepidochelys olivacea*). In: Plotkin PT (ed) *Biology and conservation of ridley sea turtles*. Johns Hopkins University Press, Baltimore, MD, p 59–87
- Bjørndal KA, Bolten AB, Dellinger T, Delgado C, Martins HR (2003) Compensatory growth in oceanic loggerhead sea turtles: response to a stochastic environment. *Ecology* 84:1237–1249
- Bjørndal KA, Parsons J, Mustin W, Bolten AA (2013) Threshold to maturity in a long-lived reptile: interactions of age, size, and growth. *Mar Biol* 160:607–616
- Bolten AB (1999) Techniques for measuring sea turtles. In: Eckert KL, Bjørndal KA, Abreu-Grobois FA, Donnelly M (eds) *Research and management techniques for the conservation of sea turtles*. Publ No. 4. IUCN/SSC Marine Turtle Specialist Group, Washington, DC, p 1–5
- Bolten AB (2003) Active swimmers-passive drifters: the oceanic stage of loggerheads in the Atlantic system. In: Bolten AB, Witherington BE (eds) *Loggerhead sea turtles*. Smithsonian Institution, Washington, DC, p 63–78
- Bowen BW, Clarck AM, Abreu-Grobois FA, Chaves A, Reichart RJ (1998) Global phylogeography of the ridley sea turtles (*Lepidochelys* spp.) as inferred from mitochondrial DNA sequences. *Genetica* 101:179–189
- Boyce MS (1992) Population viability analysis. *Annu Rev Ecol Syst* 23:481–506
- Broderick AC, Glen F, Godley BJ, Hays GC (2003) Variation in reproductive output of marine turtles. *J Exp Mar Biol Ecol* 288:95–109
- Brook BW, O'Grady JJ, Chapman AP, Burgman MA, Akçakaya HR, Frankham R (2000) Predictive accuracy of population viability analysis in conservation biology. *Nature* 404:385–387
- Caillouet CW Jr, Shaver DJ, Landry AM, Owens DW, Pritchard PCH (2011) Kemp's ridley sea turtle (*Lepidochelys kempii*) age at first nesting. *Chelonian Conserv Biol* 10:288–293
- Castanet J, Smirina E (1990) Introduction to the skeletochronological method in amphibians and reptiles. *Ann*

- Sci Nat Zool 13 ser 11:191–196
- Castanet J, Francillon-Vieillot H, Meunier FJ, De Ricqlès A (1993) Bone and individual aging. In: Hall BBK (ed) Bone: bone growth, Vol 7. CRC Press, Boca Raton, FL, p 245–283
- Castilhos JC, Tiwari M (2006) Preliminary data and observations from an increasing olive ridley population in Sergipe, Brazil. *Mar Turtle Newsl* 113:6–7
- Castilhos JC, Coelho AC, Argolo JF, Santos EAP, Marcovaldi AM, Santos ASS, Lopez M (2011) Avaliação do estado de conservação da tartaruga marinha *Lepidochelys olivacea* (Eschscholtz 1829) no Brasil. *Biodiversidade Brasileira* 1:28–36
- Coles WC, Musick JA, Williamson LA (2001) Skeletochronology validation from an adult loggerhead. *Copeia* 2001:240–242
- Colman LP, Sampaio CLS, Weber MI, Castilhos JC (2014) Diet of olive ridley sea turtles, *Lepidochelys olivacea*, in the waters of Sergipe, Brazil. *Chelonian Conserv Biol* 13: 266–271
- Ellison AM (2004) Bayesian inference in ecology. *Ecol Lett* 7: 509–520
- Francillon-Vieillot H, Arntzen JW, Géraudie J (1990) Age, growth, and longevity of sympatric *Triturus cristatus*, *T. marmoratus* and their hybrids (Amphibia, Urodela): a skeletochronological comparison. *J Herpetol* 24:13–22
- Francis RICC (1990) Back-calculation of fish length: a critical review. *J Fish Biol* 36:883–902
- Gelman A, Carlin JB, Stern HS, Rubin DB (2003) Bayesian data analysis, 2nd edn. Chapman & Hall, London
- Gilks WR, Thomas A, Spiegelhalter DJ (1994) A language and program for complex Bayesian modeling. *Statistician* 43:169–177
- Goshe LR, Avens L, Bybee J, Hohn AA (2009) An evaluation of histological techniques used in skeletochronological age estimation of sea turtle. *Chelonian Conserv Biol* 8: 217–222
- Goshe LR, Avens L, Scharf FS, Southwood AL (2010) Estimation of age at maturation and growth of Atlantic green turtles (*Chelonia mydas*) using skeletochronology. *Mar Biol* 157:1725–1740
- Guarino FM, Di Giá I, Sindaco R (2008) Age structure in a declining population of *Rana temporaria* from northern Italy. *Acta Zool Hung* 54:99–112
- IUCN (2015) The IUCN Red List of Threatened Species, version 2015.1. www.iucnredlist.org/details/11534/0 (accessed 3 June 2015)
- Klinger RC, Musick JA (1992) Annular growth layers in juvenile loggerhead turtles (*Caretta caretta*). *Bull Mar Sci* 51:224–230
- Kozłowski J (1992) Optimal allocation of resources to growth and reproduction: implications for age and size at maturity. *Trends Ecol Evol* 7:15–19
- Kozłowski J, Czarnoleski M, Danko M (2004) Can optimal resource allocation models explain why ectotherms grow larger in cold? *Integr Comp Biol* 44:480–493
- Metcalfe K, Agamboué PD, Augowet E, Boussamba F and others (2015) Going the extra mile: ground-based monitoring of olive ridley turtles reveals Gabon hosts the largest rookery in the Atlantic. *Biol Conserv* 190:14–22
- MMA (Ministério do Meio Ambiente) (2014) Répteis - *Lepidochelys olivacea* (Eschscholtz, 1829) - Tartaruga-oliva. In: Lista de espécies da fauna Brasileira ameaçadas de extinção. www.icmbio.gov.br/portal/biodiversidade/fauna-brasileira/lista-de-especies/6630-especie-6630 (accessed on 3 June 2015)
- Musick JA, Limpus CJ (1996) Habitat utilization and migration in juvenile sea turtles. In: Lutz PL, Musick JA (eds) The biology of sea turtles. CRC Press, New York, NY, p 137–163
- Pal A, Swain MM, Rath S (2009) Long bone histology and skeletochronology in a tropical Indian lizard, *Sitana ponticeriana* (Sauria: Agamidae). *Curr Herpetol* 28:13–18
- Patnaik BK, Behera HN (1981) Age determination in the tropical agamid garden lizard, *Calotes versicolor* (Daudin), based in bone histology. *Exp Gerontol* 16: 295–307
- Petitet R, Secchi ER, Avens L, Kinas PG (2012) Age and growth of loggerhead sea turtles in southern Brazil. *Mar Ecol Prog Ser* 456:255–268
- Plot V, Thoisy B, Georges JY (2015) Dispersal and dive patterns during the post-nesting migration of olive ridley turtles from French Guiana. *Endang Species Res* 26: 221–234
- Plotkin PT (2007) Introduction. In: Plotkin PT (ed) Biology and conservation of ridley sea turtles. Johns Hopkins University Press, Baltimore, MD, p 3–5
- Plotkin PT (2010) Nomadic behaviour of the highly migratory olive ridley sea turtle *Lepidochelys olivacea* in the eastern tropical Pacific Ocean. *Endang Species Res* 13: 33–40
- Polovina JJ, Balazs GH, Howell EA, Parker DM, Sekil MP, Dutton PH (2004) Forage and migration habitat of loggerhead (*Caretta caretta*) and olive ridley (*Lepidochelys olivacea*) sea turtles in the central north Pacific Ocean. *Fish Oceanogr* 13:36–51
- Pritchard PCH (2007) *Arribadas* I have known. In: Plotkin PT (ed) Biology and conservation of ridley sea turtles. Johns Hopkins University Press, Baltimore, MD, p 7–21
- R Core Team (2014) R: a language and environment for statistical computing. R Foundation for Statistical Computing, Vienna. www.R-project.org
- Rees AF, Al-Kiyumi A, Broderick AC, Papathanasopoulou N, Godley BJ (2012) Conservation related insights into the behaviour of the olive ridley sea turtle *Lepidochelys olivacea* nesting in Oman. *Mar Ecol Prog Ser* 450: 195–205
- Reichert HA (1993) Synopsis of biological data on the olive ridley sea turtle *Lepidochelys olivacea* (Eschscholtz, 1829) in the western Atlantic. NOAA Tech Memo NMFS-SEFSC-336
- Sales G, Giffoni BB, Barata PCR (2008) Incidental catch of sea turtles by the Brazilian pelagic longline fishery. *J Mar Biol Assoc UK* 88:853–864
- Schnute J (1981) A versatile growth model with statistically stable parameters. *Can J Fish Aquat Sci* 38:1128–1140
- Scholz S, Orlik M, Gonwouo LN, Kupfer A (2010) Demography and life history of a viviparous Central African caecilian amphibian. *J Zool* 280:17–24
- Silva ACCD, Castilhos JC, Lopez GG, Barata PCR (2007) Nesting biology and conservation of the olive ridley sea turtle (*Lepidochelys olivacea*) in Brazil, 1991/1992 to 2002/2003. *J Mar Biol Assoc UK* 87:1047–1056
- Silva ACCD, Castilhos JC, Santos EAP, Brondízio LS, Bugoni L (2010) Efforts to reduce sea turtle bycatch in the shrimp fishery in northeastern Brazil through a co-management process. *Ocean Coast Manag* 53:570–576
- Silva ACCD, Santos EAP, Oliveira FLC, Weber MI, Batista JAF, Serafini TZ, Castilhos JC (2011) Satellite-tracking reveals multiple foraging strategies and threats for olive

- ridley turtles in Brazil. *Mar Ecol Prog Ser* 443:237–247
- ✱ Skare O, Bolviken E, Holden L (2003) Improved sampling-importance resampling and reduced bias importance sampling. *Scand J Stat* 30:719–737
- Snover ML (2002) Growth and ontogeny of sea turtle using skeletochronology: methods, validation and application to conservation. PhD dissertation, Duke University, Durham, NC
- Snover ML, Hohn AA (2004) Validation and interpretation of annual skeletal marks in loggerhead (*Caretta caretta*) and Kemp's ridley (*Lepidochelys kempii*) sea turtles. *Fish Bull* 102:682–692
- ✱ Snover ML, Avens L, Hohn AA (2007a) Back-calculating length from skeletal growth marks in loggerhead sea turtles *Caretta caretta*. *Endang Species Res* 3:95–104
- Snover ML, Hohn AA, Crowder LB, Heppell SS (2007b) Age and growth in Kemp's ridley sea turtles: evidence from mark-recapture and skeletochronology. In: Plotkin PT (ed) *Biology and conservation of ridley sea turtles*. Johns Hopkins University Press, Baltimore, MD, p 89–105
- ✱ Snover ML, Hohn AA, Crowder LB, Macko SA (2010) Combining stable isotopes and skeletal growth marks to detect habitat shifts in juvenile loggerhead sea turtles *Caretta caretta*. *Endang Species Res* 13:25–31
- ✱ Snover ML, Hohn AA, Goshe LR, Balazs GH (2011) Validation of annual skeletal marks in green sea turtles *Chelonia mydas* using tetracycline labeling. *Aquat Biol* 12:197–204
- ✱ Snover ML, Balazs GH, Murakawa SKK, Hargrove SK, Rice MR, Seitz WA (2013) Age and growth rates of Hawaiian hawksbill turtles (*Eretmochelys imbricata*) using skeletochronology. *Mar Biol* 160:37–46
- ✱ Spiegelhalter DJ, Best NJ, Carlin BP, van der Linde A (2002) Bayesian measure of model complexity and fit. *J R Stat Soc B* 64:583–639
- TEWG (Turtle Expert Working Group) (2009) An assessment of the loggerhead turtle population in the western north Atlantic Ocean. NOAA Tech Memo NMFS-SEFSC-575
- ✱ von Bertalanffy L (1957) Quantitative laws in metabolism and growth. *Q Rev Biol* 32:217–231
- Wallace BP, Heppell SS, Lewison RL, Kelez S, Crowder LB (2008) Impacts of fisheries bycatch on loggerhead turtles worldwide inferred from reproductive value analyses. *J Appl Ecol* 45:1076–1085
- ✱ Whiting SD, Long JL, Coyne M (2007a) Migration routes and foraging behaviour of olive ridley turtles *Lepidochelys olivacea* in northern Australia. *Endang Species Res* 3:1–9
- ✱ Whiting S, Long J, Hadden K, Lauder A, Koch A (2007b) Insights into size, seasonality and biology of a nesting population of the olive ridley turtle in northern Australia. *Wildl Res* 34:200–210
- Zug GR, Parham J (1996) Age and growth in leatherback turtles, *Dermochelys coriacea* (Testudines: Dermochelyidae): a skeletochronological analysis. *Chelonian Conserv Biol* 2:244–249
- ✱ Zug GR, Rand S (1987) Estimation of age in nesting female *Iguana iguana*: testing skeletochronology in a tropical lizard. *Amphibia-Reptilia* 8:237–250
- ✱ Zug GR, Wynn AH, Ruckdeschel C (1986) Age determination of loggerhead sea turtles, *Caretta caretta*, by incremental growth marks in the skeleton. *Smithson Contrib Zool* 427:1–34
- ✱ Zug GR, Kalb HJ, Luzar SJ (1997) Age and growth in wild Kemp's ridley sea turtles *Lepidochelys kempii* from skeletochronological data. *Biol Conserv* 80:261–268
- ✱ Zug GR, Chaloupka M, Balazs GH (2006) Age and growth in olive ridley sea turtles (*Lepidochelys olivacea*) from the north-central Pacific: a skeletochronological analysis. *Mar Ecol* 27:263–270

Editorial responsibility: Susanne Schüller,
Oldendorf/Luhe, Germany

Submitted: July 17, 2015; Accepted: October 27, 2015
Proofs received from author(s): December 2, 2015

The following supplements accompany the article

Age and growth of olive ridley sea turtles (*Lepidochelys olivacea*) in the main Brazilian nesting ground

Roberta Petitot^{1,2,*}, Larisa Avens³, Jaqueline C. Castilhos⁴, Paul G. Kinas⁵, Leandro Bugoni¹

*Corresponding author: rpetitet@hotmail.com

Marine Ecology Progress Series 541: 205–218 (2015)

**SUPPLEMENT 1. MATERIALS AND METHODS
STATISTICAL ANALYSIS**

All analyses were performed with R software (R Core Team 2014), and JAGS program (<http://mcmc-jags.sourceforge.net> [accessed 4 February 2015]) to specify models and perform the Bayesian analysis (Gilks et al. 1994). The R-code on all applications can be obtained as following:

1.1 Correction factor for lost LAGs (lines of arrested growth) in resorbed area in humerus bone of olive ridley sea turtles. The following R-codes are the two model applied to the relationship between LAG number:HSD (humerus section diameter from Zug et al. (2006):

Power Function in JAGS

```
rm(list=ls())
```

Data entry

```
data1 <- read.table("LAGNxLAGD2.txt", header=T) #HSD:LAG number data
```

```
x <- data1$N
```

```
y <- data1$diam
```

Carrying the data list for JAGs

```
data1_lo <- list (L=length(y),x= log(x), y=log(y))
```

The model

```
sink("lostlags1.txt")
cat("model {
  for (i in 1:L){
    mu[i] <- b0 + b1*x[i]
    y[i] ~ dnorm(mu[i],tau)
  }
  b0 ~ dnorm(0.22,100)
  b1 ~ dnorm(0.0,1.0E-6)
  tau ~ dunif(0,10)
  sigma <- pow(tau,-0.5)
} ")
sink()
```

Set the parameter to get the posteriors

```
params <- c("b0", "b1", "sigma")
```

Initialize the chains (3)

```
outset1 <- list(list(b0=mean(y) ,b1=0, tau=1),
               list(b0=mean(y)+10 ,b1=0, tau=2),
               list(b0=mean(y)-10 ,b1=0, tau=2))
```

Load the 'rjags' library

```
library(rjags)
```

Let the model ready to generate the sample

```
lostlags1 <- jags.model("lostlags1.txt",data = data1_lo,
                      outset1,n.chains=3,n.adapt=1000)
```

MCMC in JAGS

```
lostlags.post <- coda.samples(lostlags1,params,n.iter=30000,thin=15)
```

Plot analysis

```
plot(lostlags.post)
```

Plot analysis for each selected posterior

```
plot(lostlags.post[,1],trace=F,density=T,main="Posterior",xlab="b0")
plot(lostlags.post[,2],trace=F,density=T,main="Posterior",xlab="b1")
plot(lostlags.post[,3],trace=F,density=T,main="Posterior",xlab="sigma")
```

Statistic summary of marginal posteriors

```
summary(lostlags.post)
```

Generate headquarters with posterior sample of combined chains

```
post.samp <- as.matrix(lostlags.post)
hist(post.samp[,1])
hist(post.samp[,2])
hist(post.samp[,3])
c(media=mean(post.samp[,1]), dp=sd(post.samp[,1]))
c(media=mean(post.samp[,2]), dp=sd(post.samp[,2]))
c(media=mean(post.samp[,3]), dp=sd(post.samp[,3]))
quantile(post.samp[,1],c(.025,.25,.50,.75,.975))
quantile(post.samp[,2],c(.025,.25,.50,.75,.975))
quantile(post.samp[,3],c(.025,.25,.50,.75,.975))
```

Diagnostic

```
plot(lostlags.post[,1],trace=T,density=F)
plot(lostlags.post[,2],trace=T,density=F)
plot(lostlags.post[,3],trace=T,density=F)
cumuplot(lostlags.post,probs=c(0.025,.5,.975))
autocorr.plot(lostlags.post)
gelman.diag(lostlags.post)
gelman.plot(lostlags.post)
```

DIC (Deviance Information Criteria) analysis

```
DIC.1 <- dic.samples(lostlags1,type="pD",n.iter=10000,thin=5)
DIC.1
```

Predicted x

```
b0.post <- post.samp[,1]
b1.post <- post.samp[,2]
sigma.post <- post.samp[,3]

y.hat <- 22.23451 #this number is an example of a humerus diameter#
y.hat2 <- log(y.hat)
x.pred <- exp(y.hat2-b0.post)/b1.post

# Predictive odds #
table(x.pred)/length(x.pred)

# And in histogram #
barplot(table(round(x.pred))/length(x.pred))
round(mean(x.pred))
```

1.2 Schnute's growth model R-code applied to age-at-size data of olive ridley:

```
# Run the file containing all functions which will be used later #
source ("SGMfunctions.r")
# Entry the data #
lo_cres <- read.table("modelo_schnute_lo_crc1_power.txt",header=T) #
Age:straight # carapace length (SCL) data #
age <- lo_cres[,1]
size <- lo_cres[,2]
yg <- as.numeric(tapply(log(size), age, mean))
ng <- as.numeric(tapply (size,age, length))
xg <- as.numeric(names(table(age)))
plot(xg,exp(yg))

# Preliminary non-linear model fit #
# Choose Additive (35) or Multiplicative (36) error structure #
# mst = c("Additive") #
mst = c("Multiplic")

# Define the parameters in SGM #
x1 <- min(xg)          # tau1
x2 <- max(xg)          # tau2
y1 <- mean(size[age==x1])
y2 <- mean(size[age==x2])
c(x1=x1,y1=y1,x2=x2,y2=y2)

# initial parameters vector ('a', 'b', 'y1', 'y2') #
p.in <- c(1/2,1,y1,y2)

# MLEs and Hessian approximation to the covariance matrix #
x <- as.numeric(age)
y <- size
if(mst=="Multiplic")
```

```

{ out1.schn <- nlm(dmq.schn.38,p.in,hessian=TRUE)
}
out1.teta <- out1.schn$estimate
out1.mtx.cov <- out1.schn$minimum/(length(y)-
length(out1.teta))*solve(out1.schn$hessian)
S2e <- out1.schn$minimum/(length(y)-length(out1.teta))

```

Graphic representation of data and fitted curve

```

xfit <- seq(x1,x2,0.25)
yfit1.schn <- y.hat.schn.15(out1.teta,xfit,x1,x2)
plot(x,y,xlim=range(xfit))
lines(xfit,yfit1.schn)

```

Bayesian Inference and Model fit

Bayesian fit of SGM using SIR algorithm

SAMPLING: Defining sample size for first stage of SIR

```

is.ssize1 <- 50000
df.sir <- 8 # degrees of freedom for multivariate student importance
function

```

Prior sample for sigma

**# Precision is sampled from a gamma density with expected value =
1/(S2e) #**

and coefficient of variation 'cv'

```

cv <- 0.5 # coefficient of variation for precision parameter
alfa <- 1/(cv*cv)
beta <- alfa*S2e
sigma2 <- 1/rgamma(is.ssize1,alfa,beta)

```

prior sample for vector (a, b, y1, y2)

```

prior.mtx.cov <- solve(out1.schn$hessian)
is.sample1 <- matrix(rep(0,4*is.ssize1),ncol=4)
for(i in 1: is.ssize1)
{ mtx.cov <- sigma2[i]*prior.mtx.cov

```

```

    is.sample1[i,] <- fsam(1,out1.teta,mtx.cov,df.sir)
}

# Calculating the weights of the sampled points #
# Calculating importance densities g(.) #
n <- length(y)
g.w <- rep(0,is.ssize1)
for(i in 1:is.ssize1)
{
  mtx.cov <- sigma2[i]*prior.mtx.cov
  dv <- det(mtx.cov)
  mtx.inv <- solve(mtx.cov)
  g.w[i] <- log(fdens(is.sample1[i,],out1.teta,mtx.inv,dv,df.sir)) +
  dgamma(1/sigma2[i],alfa,beta,log=T)
}

# Calculating posterior f(.) = L(data|teta)*p(teta) #
loglike <- rep(0,is.ssize1)
if(mst=="Multiplic")
{
  for(i in 1:is.ssize1) loglike[i] <- (-
  1)*negloglike.38(c(is.sample1[i,],sigma2[i],n))
}

# Calculating weights w(.) #
is.w <- loglike-g.w
n.NA <- sum(is.na(is.w))
n.NA

# Eliminating points that result in NA #
is.sample1 <- is.sample1[!is.na(is.w),]
is.w <- is.w[!is.na(is.w)]
is.w <- exp(is.w - max(is.w))

# SIR diagnostics #
max(is.w)/sum(is.w) # should be smaller than 0.05 #

```

```

# ERU
is.w[is.w == 0] <- 1E-16
k <- sum(is.w)
-sum(is.w*(log(is.w)-log(k)))/(k*log(is.ssize1)) # should exceed 0.90 #

# RESAMPLING (2nd stage in SIR) #
# Set 2nd stage sample size (approximately 10% of first stage sample
size #
is.ssize2 <- 4000
is.line <- sample(1:dim(is.sample1)[1], is.ssize2, replace=T, prob=is.w)
is.theta <- is.sample1[is.line,] # posterior sample for (a, b, y1, y2)
is.sigma <- sqrt(sigma2[is.line])

# Posterior Deviance -2log(p(y | teta, sigma)) #
dev <- numeric()
if(mst=="Multiplic")
{ for(i in 1:is.ssize2)
  { s2 <- is.sigma[i]*is.sigma[i]
    dev[i] <- 2*negloglike.38(c(is.theta[i,],s2,n))
  }
}

# Posterior summary #
par.names = c("a","b","y1","y2","sigma","deviance")
post.summary <-
bayes.post.summary(cbind(is.theta[,1:4],is.sigma,dev),par.names,r=3)
post.summary

# DIC #
post.mean <- as.numeric(as.vector(post.summary[,5]))
if(mst=="Multiplic")
{ dev.bar <- 2*negloglike.38(c(post.mean[1:4],post.mean[5]^2,n))
#dev(post.mean)
}

```

```

pD <- mean(dev) - dev.bar
pV <- var(dev)/2
DIC <- mean(dev) + pD
c(DIC=DIC, pD=pD, pV=pV )

```

GRAPHICS

FIGURE 1: marginal posterior distributions

```

par(mfrow=c(3,2))
for(i in 1:4) plot(density(is.theta[,i]),main=i,xlab=par.names[i])
plot(density(is.sigma),main=5,xlab=par.names[5])
plot(density(dev),main=6,xlab=par.names[6])
par(mfrow=c(1,1))

```

FIGURE 2: posterior growth curve

1: average SGM with posterior probability intervals (without sigma)

```

id <- seq(x1,x2,by=0.5)
c.id <- matrix(rep(0,5*length(id)),ncol=5)
pred <- as.numeric()
for(i in 1:length(id))
{ for(j in 1:is.ssize2)
  { pred[j] <- y.hat.schn.15(is.theta[j,],id[i],x1,x2)
  }
  c.id[i,] <- as.numeric(quantile(pred,c(.025,0.10,.5,0.90,.975),na.rm=T))
}

```

FIGURE 3: average size per age

```

plot(x,y,xlim=c(0,28),ylim=c(0,80),xlab="Estimated Age (yr)",
      ylab="Mean size (cm SCL)")
lines(id,c.id[,3],lwd=2,lty="solid") # mediana
lines(id,c.id[,1],lty="dashed")     #linf 95%
lines(id,c.id[,5],lty="dashed")     #lsup 95%
lines(id,c.id[,2],lty="dotted")     #linf 80%
lines(id,c.id[,4],lty="dotted")     #lsup 80%
dados_BC <- read.table("BC.txt",header=T)

```

```
points(dados_BC$id,dados_BC$L, pch=3)
points(dados_zug$age,dados_zug$size, pch=3)
```

FIGURE 4: predictions of individual size per age (including sigma)

```
c.ind <- matrix(rep(0,5*length(id)),ncol=5)
n.post <- dim(is.theta)[1]
for(i in 1:length(id))
{ for(j in 1:is.ssize2)
  { pred[j] <- y.hat.schn.15(is.theta[j,],id[i],x1,x2)
    yy <- exp(rnorm(n.post,log(pred[j]),is.sigma[i]))
  }
  c.ind[i,] <- as.numeric(quantile(yy,c(.10,0.25,.5,0.75,.90),na.rm=T))
}

plot(x,y,xlim=range(id),xlab="Age (yr)",ylab="Individual size (cm SCL)",
main="Schnute Growth Model",
ylim= c(min(c.ind[,1][!is.na(c.ind[,1]))-1, max(c.ind[,5][!is.na(c.ind[,5]))+1))
lines(id,c.ind[,3],lwd=2,lty="solid") # mediana
lines(id,c.ind[,1],lty="dashed") #linf 80%
lines(id,c.ind[,5],lty="dashed") #lsup 80%
lines(id,c.ind[,2],lty="dotted") #linf 50%
lines(id,c.ind[,4],lty="dotted") #lsup 50%
```

Probability for model to fit some cases

case 1: $0 < a$ and $0 < b < 1$

```
case1 <- sum(is.w[is.sample1[,1] > 0 & is.sample1[,2] > 0 & is.sample1[,2] <
1])/k
```

case 2: $0 < a$ and $1 \leq b$

```
case2 <- sum(is.w[is.sample1[,1] > 0 & is.sample1[,2] >= 1])/k
```

case 3: $-b \cdot \log(y_2/y_1)/(x_2-x_1) < a \leq 0$ and $1 < b$

```
lim.a <- -is.sample1[,2]*log(is.sample1[,4]/is.sample1[,3])/(x2-x1)
```

```
case3 <- sum(is.w[is.sample1[,1] > lim.a & is.sample1[,1] <= 0 &
is.sample1[,2] > 1])/k
```

```
# case 4:  $-b \cdot \log(y_2/y_1)/(x_2-x_1) < a \leq 0$  and  $0 \leq b \leq 1$  #
```

```
case4 <- sum(is.w[is.sample1[,1] > lim.a & is.sample1[,1] <= 0 &
is.sample1[,2] <= 1 & is.sample1[,2] >= 0])/k
```

```
# case 5:  $a \leq -b \cdot \log(y_2/y_1)/(x_2-x_1)$  and  $0 \leq b$  #
```

```
case5 <- sum(is.w[is.sample1[,1] <= lim.a & is.sample1[,2] >= 0])/k
```

```
# case 6:  $a < 0$  and  $b < 0$  #
```

```
case6 <- sum(is.w[is.sample1[,1] < 0 & is.sample1[,2] < 0])/k
```

```
# case 7:  $0 \leq a \leq -b \cdot \log(y_2/y_1)/(x_2-x_1)$  and  $b < 0$  #
```

```
case7 <- sum(is.w[is.sample1[,1] > 0 & is.sample1[,1] <= lim.a &
is.sample1[,2] < 0])/k
```

```
# case 8:  $-b \cdot \log(y_2/y_1)/(x_2-x_1) < a$  and  $b \leq 0$  #
```

```
case8 <- sum(is.w[is.sample1[,1] > lim.a & is.sample1[,2] <= 0])/k
```

```
round(c(p.M1=case1,
```

```
p.M2=case2,p.M3=case3,p.M4=case4,p.M5=case5,p.M6=case6,p.M7=case7,
p.M8=case8),4)
```

```
# GRAPHICS: Posterior distributed in Fig. 1 #
```

```
minimos <- c(min(is.theta[,1]),min(is.theta[,2]))
```

```
maximos <- c(max(is.theta[,1]),max(is.theta[,2]))
```

```
y1.post <- mean(is.theta[,3],na.rm=T)
```

```
y2.post <- mean(is.theta[,4],na.rm=T)
```

```
# Option: dispersion #
```

```
plot( is.theta[,1],is.theta[,2],xlim=c(minimos[1],maximos[1]),xlab="a", ylab="b",
      ylim= c(minimos[2],maximos[2]),main="SGM: regions (Fig.1)")
```

```
# Option: contours #
```

```

# sca.contour(is.theta[,1],is.theta[,2],n.classes=16) #
abline(h=0)
abline(v=0)
abline(0,-(x2-x1)/log(y2.post/y1.post))
segments(-log(y2.post/y1.post)/(x2-x1),1, maximos[1]+1,1)

# Calculating probabilities for RESAMPLED posterior #
# case 1: 0 < a and 0 < b < 1 #
case1 <- sum(is.theta[,1] > 0 & is.theta[,2] > 0 & is.theta[,2] < 1)/is.ssize2

# case 2: 0 < a and 1 <= b #
case2 <- sum(is.theta[,1] > 0 & is.theta[,2] >= 1)/is.ssize2

# case 3: -b*log(y2/y1)/(x2-x1) < a <= 0 and 1 < b #
lim.a <- -is.theta[,2]*log(is.theta[,4]/is.theta[,3])/(x2-x1)
case3 <- sum(is.theta[,1] > lim.a & is.theta[,1] <= 0 & is.theta[,2] > 1)/is.ssize2

# case 4: -b*log(y2/y1)/(x2-x1) < a <= 0 and 0 <= b <= 1 #
case4 <- sum(is.theta[,1] > lim.a & is.theta[,1] <= 0 & is.theta[,2] <= 1 &
is.theta[,2] >= 0)/is.ssize2

# case 5: a <= -b*log(y2/y1)/(x2-x1) and 0 <= b #
case5 <- sum(is.theta[,1] <= lim.a & is.theta[,2] >= 0)/is.ssize2

# case 6: a < 0 and b < 0 #
case6 <- sum(is.theta[,1] < 0 & is.theta[,2] < 0)/is.ssize2

# case 7: 0 <= a <= -b*log(y2/y1)/(x2-x1) and b < 0 #
case7 <- sum(is.theta[,1] > 0 & is.theta[,1] <= lim.a & is.theta[,2] < 0)/is.ssize2

# case 8: -b*log(y2/y1)/(x2-x1) < a and b <= 0 #
case8 <- sum(is.theta[,1] > lim.a & is.theta[,2] <= 0)/is.ssize2

```

```
round(c(p.M1=case1,
p.M2=case2,p.M3=case3,p.M4=case4,p.M5=case5,p.M6=case6,p.M7=case7,
p.M8=case8),4)
```

```
# Calculating tau.zero, tau.star, y.star and y.inf #
```

```
# Expressions (24) (25) (26) and (27) [Schnute, 1981] #
```

```
linhas <- 1:is.ssize2
```

```
# number of excluded lines (a = 0 and b = 0) #
```

```
is.ssize2 - sum(is.theta[,1]!=0 & is.theta[,2]!=0)
```

```
linesel <- linhas[is.theta[,1]!=0 & is.theta[,2]!=0]
```

```
new.is <- is.theta[linesel,]
```

```
gg <- (exp(x2*new.is[,1])*(new.is[,4]^new.is[,2]) -
```

```
exp(x1*new.is[,1])*(new.is[,3]^new.is[,2]))/((new.is[,4]^new.is[,2]) -
(new.is[,3]^new.is[,2]))
```

```
y.gg<- (exp(x2*new.is[,1])*(new.is[,4]^new.is[,2]) -
```

```
exp(x1*new.is[,1])*(new.is[,3]^new.is[,2]))/(exp(x2*new.is[,1]) -
exp(x1*new.is[,1]))
```

```
# Removing points outside possible range #
```

```
tau.zero <- x1 + x2 - log(gg)/new.is[,1]
```

```
tau.star <- x1 + x2 - log(new.is[,2]*gg)/new.is[,1]
```

```
y.star <- ((1-new.is[,2])*y.gg)^(1/new.is[,2])
```

```
y.inf <- (y.gg)^(1/new.is[,2])
```

```
# Posterior summary #
```

```
par.trans = c("tau.zero", "tau.star", "y.star", "y.inf")
```

```
bayes.post.summary(cbind(tau.zero,tau.star,y.star,y.inf),par.trans,r=3)
```

```
# Effective sample size #
```

```
c(n.tau.zero=is.ssize2-sum(is.na(tau.zero)),n.tau.star=is.ssize2-
sum(is.na(tau.star)),
```

```
n.y.star=is.ssize2-sum(is.na(y.star)),n.y.inf=is.ssize2-sum(is.na(y.inf)))
```

```

# Function to find MLE of the parameters for Schnute's model by "nlm()"
#
# This function will assume that ages ='x', sizes='y', tau1='x1, tau2='x2' #
# source ("SGMfunctions.r") #
dmq.schn.37 <- function(p)
  sum((y -(p[3]^p[2] + (p[4]^p[2]-p[3]^p[2])*(1-exp(-p[1]*(x-x1)))/(1-exp(-p[1]*(x2-
x1))))^(1/p[2]))^2)
dmq.schn.38 <- function(p)
  sum((log(y) - log((p[3]^p[2] + (p[4]^p[2]-p[3]^p[2])*(1-exp(-p[1]*(x-x1)))/(1-
exp(-p[1]*(x2-x1))))^(1/p[2])))^2)
dmq.schn.38.pos <- function(p)
  sum((log(y) - log((p[3]^(exp(p[2])) + (p[4]^exp(p[2])-p[3]^exp(p[2]))*(1-exp(-
exp(p[1]*(x-x1)))/(1-exp(-exp(p[1]*(x2-x1))))^(1/exp(p[2]))))^2)
dmq.vbgm.38 <- function(p)
  sum((log(y) - log(p[2] + (p[3]- p[2])*(1-exp(-exp(p[1]*(x-x1)))/(1-exp(-
exp(p[1]*(x2-x1))))))^2)

# Function to calculate the predictive values y.hat by equation 15 from
Schnute (1981) #
y.hat.schn.15 <- function(p,x,x1,x2)
  (p[3]^p[2] + (p[4]^p[2]-p[3]^p[2])*(1-exp(-p[1]*(x-x1)))/(1-exp(-p[1]*(x2-
x1))))^(1/p[2])
y.hat.vbgm.15 <- function(p,x,x1,x2)
  (p[2] + (p[3]- p[2])*(1-exp(-exp(p[1]*(x-x1)))/(1-exp(-exp(p[1]*(x2-x1))))))

# Functions by HUMBER AGRELLI ANDRADE (HAA) #
# Function for a multidimensional student sample #
# This function is used to generate the first sample, it is the first
important
# function #
# A sample of size "n" would be obtained from a student with an average
"m"
# covariance matrix "E" and degrees of freedom "gl" #

```

The function output is a vector or matrix (depending on the number of parameters)

of length or number of lines (depending on the case) equal to n

```
fsam <-function(n,m,E,gl){  
  teta<-rep(NA,length(m))  
  cv<-t(chol(E))  
  for(i in 1:n) teta<-rbind(teta,c(m+cv%*%rt(length(m),gl)))  
  teta<-teta[-c(1),]  
  teta}
```

```
fdens<-function(x,m=m0,iv=iv0,dv=dv0,gll=gl0)  
  {res<-t(x-m)%*%iv%*%(x-m)  
  res1<-gamma(gll/2)*gll^(length(x)/2)*pi^(length(x)/2)  
  res1<-gamma((gll+length(x))/2)/res1  
  res<-res1*1/sqrt(dv)*(1+1/gll*res)^(-(gll+length(x))/2)  
  res}
```

End of the HAA's functions

Function to calculate $-\log(L(\text{data}|\text{teta}))$

```
negloglike.38 <- function(param){  
  dmq.schn.38(param[1:4])/(2*param[5]) + param[6]*log(param[5])/2  
}
```

Calculating of $-\log(L(\text{param}))$ for the data

```
negloglike.37 <- function(param){  
  dmq.schn.37(param[1:4])/(2*param[5]) + param[6]*log(param[5])/2  
  # calculo da  $-\log(L(\text{param}))$  para os dados  
}
```

```
negloglike.38vbgm <- function(param){  
  dmq.vbgm.38(param[1:3])/(2*param[4]) + param[5]*log(param[4])/2  
  # calculo da  $-\log(L(\text{param}))$  para os dados  
}
```

Bayes-posterior summary

```
bayes.post.summary <- function(mc.matrix,parnames,r=4)
```

```

{ nr.col <- dim(mc.matrix)[2]
  stats.sum <- matrix(rep(0,nr.col*5),ncol=5)
  for(i in 1:nr.col)
  { stats.sum[i,1:3] <- quantile(mc.matrix[,i],c(.025,.5,.975),na.rm=T)
    stats.sum[i,4] <- mean(mc.matrix[,i],na.rm=T)
    stats.sum[i,5] <- sd(mc.matrix[,i],na.rm=T)
  }
  stats <- as.data.frame(cbind(parnames,round(stats.sum,r)))
  names(stats) <- c("param", "2.5%", "median", "97.5%", "mean", "sdev")
  stats}

sca.contour <- function(var1,var2, n.classes = 30,g.pc = 0.1,
                        q.line=c(0.01,0.25,0.5,0.80))

```

This function creates a contour plot from scatterplots

x = var1 and y = var2

n.classes and g.pc control smoothness and window width

q.line gives percentage of maximum high for contour lines

```

{ x.axis <- var1
  y.axis <- var2

```

Creating classes

```

x.lim <- c(min(x.axis),max(x.axis))
y.lim <- c(min(y.axis),max(y.axis))
dif.x <- x.lim[2]-x.lim[1]
dif.y <- y.lim[2]-y.lim[1]
c.x <- seq(x.lim[1]-g.pc*dif.x,x.lim[2]+g.pc*dif.x, length.out = n.classes)
c.y <- seq(y.lim[1]-g.pc*dif.y,y.lim[2]+g.pc*dif.y, length.out = n.classes)

```

Calculating matrix of frequencies

```

mp.x <- rep(0,n.classes-1)
mp.y <- mp.x
for(i in 2:n.classes)
{ mp.x[i-1] <- mean(c.x[c(i-1,i)])
  mp.y[i-1] <- mean(c.y[c(i-1,i)])

```

```
}  
p1.axis <- cut(x.axis,breaks<-c.x,right=F)  
p2.axis <- cut(y.axis,breaks<-c.y,right=F)  
f.axis <- matrix(as.numeric(table(p1.axis,p2.axis)),ncol= n.classes-1 )  
f.axis <- f.axis/max(f.axis)  
  
# Making the contourplot #  
plot(mp.x,mp.y,xlab="a", ylab="b",main="SGM (Regions)",type="n")  
contour(mp.x,mp.y,f.axis,levels=q.line,lwd=2.0,add=T)  
}
```

1.3 Von Bertalanffy growth model (VBGM) R-code applied to age-at-size data of olive ridley:

Entry the data

```
data2 <- read.table("crc_lo_von3.txt", header=T) # Age:SCL data #
```

```
age <- data2$id
```

```
size <- data2$L
```

```
maxage <- max(age)
```

```
ma <- mean(size[age==maxage])
```

```
mo <- mean(size[age==0])
```

Carrying the data list for JAGs

```
data2_lo <- list(M=length(age),age=age,size=size)
```

Set the parameter to get the posteriors

```
# VBGM parameterized for L0 (in place of t0)
```

```
parameters <- c("linf","L0","k","sigma")
```

Initialize the chains (3)

```
outset2 <- list(list(loglinf=log(max(comp)),logL0=1.4,logk=log(0.04),sigma=1),
```

```
list(loglinf=log(max(comp))+0.2,logL0=1.3,logk=log(0.02),sigma=1.5),
```

```
list(loglinf=log(max(comp))-0.2,logL0=1.2,logk=log(0.06),sigma=0.8))
```

The model

```
sink("vb_L0_PGK2.txt")
```

```
cat("model {
```

```
  logL0 ~ dnorm(1.3,0.25)I(0.5,2.5)
```

```
  loglinf ~ dnorm(4.5,0.5)I(4,5)
```

```
  logk ~ dnorm(0,0.005)I(-10,10)
```

```
  sigma ~ dunif(0,5)
```

```
  k <- exp(logk)
```

```
  linf <- exp(loglinf)
```

```
  L0 <- exp(logL0)
```

```
  tau <- 1/(sigma*sigma)
```

```

for(i in 1:M){
  expkt[i] <- exp(-k*idade[i])
  expmu[i] <- linf - (linf-L0)*expkt[i]
  mu[i] <- log(expmu[i])
  comp[i] ~ dlnorm(mu[i],tau)
}
} ")
sink()
library(R2jags)
n.cad <- 3
salto <- 3
comp.cad <- 12000
n.aq <- 3000
vbgm <- jags(data2_lo,outset2,parameters,"vb_L0_PGK2.txt",n.chains=n.cad,
             n.thin=salto,n.iter=comp.cad,n.burnin=n.aq)
print(vbgm,dig=3)

```

Marginal posterior densities for each parameter

```

output <- vbgm$BUGSoutput
Linf.post <- output$sims.matrix[, "linf"]
k.post <- output$sims.matrix[, "k"]
L0.post <- output$sims.matrix[, "L0"]
sigma.post <- output$sims.matrix[, "sigma"]

```

```

hist(Linf.post,nclass=150,main="Linf")
hist(k.post,nclass=150,main="k")
hist(L0.post,nclass=150,main="L0")
hist(sigma.post,nclass=150,main="sigma")

```

Joint posterior distribution

```

plot(k.post, Linf.post)

```

Plots

1: Size predictive for VBGM with credibility interval

```

id <- seq(0,max(age),by=1)
c.ind <- matrix(rep(0,5*length(id)),ncol=5)
n.post <- length(Linf.post)
for(i in 1:length(id))
{ pred <- log(Linf.post - (Linf.post-L0.post)*exp(-k.post*id[i]))
  yy <- exp(rnorm(n.post,pred,sigma.post))
  c.ind[i,] <- as.numeric(quantile(yy,c(0.10,0.25,.5,0.75,0.90)))
}
plot(data2$id,data2$L,xlim=c(0,28),ylim=c(0,80),
      xlab="Estimated Age (yr)", ylab="Mean size (cm SCL)")
lines(id,c.ind[,3],lwd=2,lty="solid") # mediana
lines(id,c.ind[,1],lty="dashed")    #linf 95%
lines(id,c.ind[,5],lty="dashed")    #lsup 95%
lines(id,c.ind[,2],lty="dotted")    #linf 80%
lines(id,c.ind[,4],lty="dotted")    #lsup 80%

# Insert values for the species you are working on #
abline(h=60.0) # size data of a mature olive ridley sea turtle #
y0 <- 60.0
x.pred <- log((y0-Linf.post)/-(Linf.post-L0.post))/-k.post
table(round(x.pred))/length(x.pred)
barplot(table(round(x.pred))/length(x.pred),xlim=c(0,10),ylim=c(0,0.6),
        xlab="Estimated age (yr)",ylab="Frequency")
round(mean(x.pred,na.rm=T))
quantile(x.pred,c(0.025,0.5,0.975),na.rm=T)

```

1.4 Back-calculate model r-code applied to humerus section diameter (HSD) and size data

Entry the data

```
data3 <- read.table("bph_lo_crc.txt", header=T) # HSD:SCL data #  
lop <- 4.03 # Mean value of SCL of olive ridley hatchlings #  
dop <- 2.20 # Mean value of humerus diameter from olive ridley  
hatchlings #
```

Carrying the data list for JAGs

```
data3_lo <- list(n=length(data3$l), x=log((data3$d)-dop),  
               y=log((data3$l)-lop))
```

The model

```
sink("bph1.txt")  
cat("model {  
  for (i in 1:n){  
    mu[i] <- B + c*x[i]  
    y[i] ~ dnorm(mu[i],tau)  
  }  
  B ~ dnorm(4.0,1.0E-6)|(1,8)  
  c ~ dnorm(0.0,1.0E-6)  
  tau <- 1/(sigma*sigma)  
  #tau ~ dgamma(0.01,0.01)  
  sigma ~ dunif(0,10)  
  b <- exp(B)  
  }")  
sink()
```

Defining the estimated parameters

```
parameters2 <- c("B", "b", "c", "sigma")
```

```
y <- log((data3$l)-lop)  
x <- log((data3$d)-dop)  
plot(x,y)
```

```

outset3 <- list(list(B=mean(y) ,c=0, sigma=1),
               list(B=mean(y)+1 ,c=0, sigma=2),
               list(B=mean(y)-1,c=0, sigma=3))
library(rjags)
bph_fit <- jags.model("bph1.txt", data = data3,
                    outset3, n.chains=3, n.adapt=100000)
bph_fit.post <- coda.samples(bph_fit,parameters2,n.iter=400000,thin=200)

```

Output analysis

```
plot(bph_fit.post)
```

Or from selected posterior

```

plot(bph_fit.post[,1],trace=F,density=T,main="Posterior",xlab="B")
plot(bph_fit.post[,2],trace=F,density=T,main="Posterior",xlab="b")
plot(bph_fit.post[,3],trace=F,density=T,main="Posterior",xlab="c")
plot(bph_fit.post[,4],trace=F,density=T,main="Posterior",xlab="sigma")
B <- numeric(bph_fit.post[,2])

```

Statistical summary of marginal posteriors

```
summary(bph_fit.post)
```

Creating matrixes with posterior sample of combined chains

```

post.samp2 <- as.matrix(bph_fit.post)
hist(post.samp2[,1])
hist(post.samp2[post.samp2[,2]<40,2])
hist(post.samp2[,3])
c(media=mean(post.samp2[,1]), dp=sd(post.samp2[,1]))
c(media=mean(post.samp2[,2]), dp=sd(post.samp2[,2]))
c(media=mean(post.samp2[,3]), dp=sd(post.samp2[,3]))
quantile(post.samp2[,1],c(.025,.25,.50,.75,.975))
quantile(post.samp2[,2],c(.025,.25,.50,.75,.975))
quantile(post.samp2[,3],c(.025,.25,.50,.75,.975))

```

Diagnostics

```

plot(bph_fit.post[,1],trace=T,density=F)
plot(bph_fit.post[,2],trace=T,density=F)
plot(bph_fit.post[,3],trace=T,density=F)
plot(bph_fit.post[,4],trace=T,density=F)
cumuplot(bph_fit.post,probs=c(0.025,.5,.975))
autocorr.plot(bph_fit.post)
gelman.diag(bph_fit.post)
gelman.plot(bph_fit.post)

```

DIC analysis

```

DIC.1 <- dic.samples(bph_fit,type="pD",n.iter=10000,thin=5)
DIC.1

```

Predicted x

```

B.post_lo <- post.samp2[,1]
b.post_lo <- post.samp2[,2]
c.post_lo <- post.samp2[,3]
sigma.post_lo <- post.samp2[,4]

```

Estimated SCL from humerus diameter

```

data4 <- read.table("tc_lo_crc.txt", header=T) # HSD:SCL data#
attach(data4)
outset4 <- list (L=length(l1),l1=l1, d1=d1, d.hat=d.hat)
crc.est <- function(l1,d1,d.hat)
{ x <- log(d1-dop)
  y.pred <- B.post_lo + c.post_lo*x
  x.hat <- log(d.hat-dop)
  y.hat <- B.post_lo + c.post_lo*x.hat
  l.hat <- exp(y.hat)+lop
  list(L=length(l1), l.hat=l.hat)
}
object <- numeric()
other.obj <- numeric()
for(i in 1:68) {

```

```

    exit <- crc.est(l1[i],d1[i],d.hat[i])
    other.obj[i] <- mean(exit$l.hat)
  }
other.obj
as.data.frame(other.obj)

# Estimated SCL from each LAG #
data5 <- read.table("tc_lo_1.txt", header=T) # LAG diameter:SCL data #
attach(data5)
outset5 <- list (L=length(l1),l1=l1, d1=d1, d.hat.1=d.hat.1)
scl.est_1 <- function(l1,d1,d.hat.1)
{ x <- d1-dop
  y.pred <- b0.post_lo + b1.post_lo*x
  taxa <- l1/(y.pred+lop)
  x.hat <- d.hat.1-dop
  y.hat <- b0.post_lo + b1.post_lo*x.hat
  l.hat2 <- y.hat+lop
  l.hat.1 <- l.hat2*taxa
  list(L=length(l1), l.hat.1=l.hat.1, taxa=taxa)
}
other.obj2 <- numeric()
object2 <- numeric()
for(i in 1:68) {
  exit2 <- scl.est(l1[i],d1[i],d.hat.1[i])
  other.obj2[i] <- mean(exit2$l.hat.1)
  object2[i] <- mean(exit2$taxa)
}
other.obj2
as.data.frame(other.obj2)

# Growth rate calculated from the difference between estimated SCL
from each # LAG #
# Plot of growth rate from each LAG #
data_gr <- read.table("idxtc.txt", header=T) # Age:growth rate data #

```

```
nro.linhas <- as.numeric(tapply(data_gr$tc,data_gr$id,length))
x <- as.factor(data_gr$id)
plot(data_gr$tc~x, ylim=c(0,6)
      ,xlab="Estimated age (yr)", ylab="Growth rate (cm/yr)", outline=FALSE)
```

LITERATURE CITED

- Gilks WR, Thomas A, Spiegelhalter DJ (1994) A language and program for complex Bayesian modeling. *Statistician* 43:169–177
- R Core Team (2014) R: A language and environment for statistical computing. R Foundation for Statistical Computing, Vienna, www.R-project.org
- Schnute J (1981) A versatile growth model with statistically stable parameters. *Can J Fish Aquat Sci* 38:1128–1140
- Zug GR, Chaloupka M, Balazs GH (2006) Age and growth in olive ridley sea turtles (*Lepidochelys olivacea*) from the north-central Pacific: A skeletochronological analysis. *Mar Ecol* 27:263–270

APÊNDICE II

**High habitat use plasticity by female olive ridley sea turtles
(*Lepidochelys olivacea*) revealed by stable isotope analysis in multiple
tissues**

Roberta Petitet, Leandro Bugoni

SUBMETIDO PARA O PERIÓDICO *MARINE BIOLOGY*

High habitat use plasticity by female olive ridley sea turtles (*Lepidochelys olivacea*) revealed by stable isotope analysis in multiple tissues

Roberta Petitet^{1,2*}, Leandro Bugoni¹

¹ Laboratório de Aves Aquáticas e Tartarugas Marinhas, Instituto de Ciências Biológicas, Universidade Federal do Rio Grande (FURG), Campus Carreiros, Avenida Itália s/n, CP 474, 96203-900, Rio Grande, RS, Brazil

² Programa de Pós-Graduação em Oceanografia Biológica, Instituto de Oceanografia, Universidade Federal do Rio Grande (FURG), Campus Carreiros, Avenida Itália s/n, CP 474, 96203-900 Rio Grande, RS, Brazil

Corresponding author, Email: rpetitet@hotmail.com

Abstract The marine habitat use of olive ridley sea turtles (*Lepidochelys olivacea*) from northeastern Brazil was analyzed via stable isotope analysis (SIA). Blood (red blood cells and serum), epidermis and scute samples from 46 females were collected for SIA of carbon ($\delta^{13}\text{C}$) and nitrogen ($\delta^{15}\text{N}$) in order to infer the habitats used at distinct time windows, the dietary contributions of pelagic and neritic sources, and the trophic level of the turtles. Differences in the average residence time of $\delta^{13}\text{C}$ and $\delta^{15}\text{N}$ among samples indicated a shift from oceanic feeding grounds to neritic habitats before nesting. However, two individuals seemed to have used neritic feeding habitats for longer timespans before the nesting period. Stable isotope mixing models (SIMMs) demonstrated high individual variability, suggesting the

variable use of non-breeding grounds. Moreover, serum indicated that olive ridleys might feed during the nesting season, most likely opportunistically on discards from trawl fisheries. Therefore, the habitats used by olive ridley sea turtles from Brazil are vast, encompassing both oceanic and neritic habitats, where they encounter pelagic longline and trawl fisheries, respectively. The high individual variability in the population results in turtles experiencing distinct and variable threats during their annual cycle.

Introduction

Understanding the ecology, demography and evolutionary biology of migratory species depends on identifying the connections among the habitats they use during their entire life cycle (Rubenstein and Hobson 2004). Especially for threatened migratory species, knowledge regarding habitat connectivity is essential, as threats faced in non-breeding areas or along the migratory route may affect their demography. This knowledge can allow the formation of inferences regarding how populations respond to climate change, incidental capture and habitat loss and degradation (Hobson and Norris 2008).

The habitat use of sea turtles has been studied based on genetics, tracking-device technologies, mark-recapture methods and stable isotope analysis (SIA) (Morreale et al. 2007; Ceriani et al. 2014). Stable isotopes of light elements such as carbon ($\delta^{13}\text{C}$) and nitrogen ($\delta^{15}\text{N}$) are used to study migratory connectivity (Ceriani et al. 2014). Because distinct isotopic landscapes occur in nature, it is possible to infer the movement patterns of individuals that travel between them (Rubenstein and Hobson 2004). Each

habitat has a pattern of $\delta^{13}\text{C}$ and $\delta^{15}\text{N}$ values at the base of the food web that is mirrored upward through the food web to top predators (Post 2002). $\delta^{13}\text{C}$ values change at the scale of c. 1‰ between a consumer and its food source, while $\delta^{15}\text{N}$ values increase by c. 3–5‰ at each trophic level; such values are called the trophic discrimination factor (TDF) (Peterson and Fry 1987). Therefore, due to its lower variability, $\delta^{13}\text{C}$ is used to infer habitats used previously, during tissue synthesis, near the coast $\delta^{13}\text{C}$ values are higher than in oceanic waters (Post, 2002). While $\delta^{15}\text{N}$ values is used as a proxy for trophic level position due to its higher level of increase across the food web (Post 2002). Stable isotope mixing models (SIMMs) involving both isotopes are used to study the contributions of different food sources to the diet (Hopkins-III and Kurle 2016).

Thus, by sampling tissues with distinct half-lives from the same individuals, SIA allows the understanding of resource utilization at multiple temporal scales (Martínez del Rio et al. 2009). Isotopic signatures are maintained at the time of tissue synthesis either permanently, in metabolically inert tissues such as feathers, hair and nails, or temporarily, in metabolically active tissues such as blood, skin and bone. Because each tissue has a specific average residence time of $\delta^{13}\text{C}$ and $\delta^{15}\text{N}$, i.e., the time required for integrating dietary input, that varies from days to months or even years, each tissue reflects past time periods. Therefore, habitats, diet contribution and trophic levels at different time periods before sampling can be inferred (DeNiro and Epstein 1978, 1981; Hobson 1999).

All sea turtle species are listed on the IUCN Red List (IUCN 2015) except *Natator depressus*, for which there are insufficient data for status

assessment. These reptiles utilize distinct foraging and reproduction areas that often occur far from each other. The olive ridley sea turtle (*Lepidochelys olivacea*) is the most abundant sea turtle worldwide (Reichert 1993) and is highly migratory, with post-hatchling and juvenile stages occurring in oceanic waters and then mature individuals recruit to coastal environments for nesting (Reichert 1993). After nesting, turtles migrate back to their feeding grounds. However, there may be individual variability in residence time at the nesting beaches before and between nesting periods. There are reports of females mating during migration to the neritic zone, which may reduce their residence time in the neritic habitat previous to egg laying (Kopitsky et al. 1999).

The migratory connectivity of loggerhead sea turtles (*Caretta caretta*) has been extensively studied using SIA in Japan, the North Atlantic and the Mediterranean (Hatase et al. 2002; Revelles et al. 2007; Vander Zanden et al. 2016). However, habitat use of olive ridley sea turtles has previously been studied only via satellite telemetry of adults and juveniles (Polovina et al. 2004; Whiting et al. 2007; Plotkin 2010; Silva et al. 2011; Chambault et al. 2016). On the coast of French Guiana, after nesting, olive ridleys remain over the continental shelf in areas with high availability of food resources due to the eddies formed by the North Brazil retroflexion, an area characterized by low turbulence and high micronekton biomass (Chambault et al. 2016). In the Pacific Ocean off the coast of Costa Rica, olive ridley adults migrate long distances but without fidelity to any feeding ground (Plotkin 2010), while juveniles exhibited a habitat use of oceanic waters at 10–20°N at a temperature range of 23–28°C (Polovina et al. 2004). In Australia, this species also migrates long distances and uses several habitats such as

coastal areas, the continental shelf and the continental slope, after reproduction (Whiting et al. 2007). In Brazil, Silva et al. (2011) demonstrated a variable pattern in post-nesting migration for this species: after nesting, some individuals migrate back to oceanic feeding grounds, while others migrate to neritic feeding grounds.

Olive ridley sea turtles are known to be opportunistic, carnivorous and generalist feeders during their entire life cycle (Reichert 1993). Colman et al. (2014) demonstrated the predominance of fish in the diet of adult olive ridleys at Pirambu Beach, northeastern Brazil, whereas along the Pacific coast of Mexico, crustaceans and fish were the predominant food items (Montenegro-Silva et al. 1986). For juveniles, salps and pyrosomes were the most important foods in oceanic waters of the Pacific Ocean (Polovina et al. 2004).

Olive ridley sea turtles utilize several different types of habitats, including oceanic and neritic waters, where they face distinct threats (Silva et al. 2011). In oceanic waters of the Atlantic Ocean, juvenile and adult olive ridley sea turtles are incidentally captured by pelagic longline fisheries targeting tuna, swordfish and sharks (Sales et al. 2008). In neritic waters adjacent to nesting beaches as well as in distant feeding grounds, olive ridleys are drowned in shrimp trawl nets (Silva et al. 2010; Di Benedetto et al. 2015). In the study area (Fig. 1), the number of adult olive ridleys found stranded dead has increased in recent years (Castilhos et al. 2011), which may affect the persistence of the local population. On the other hand, this mortality could be natural due to an increase in the population at study area (Castilhos et al. 2011).

The present study aims to infer the habitats used by nesting female

olive ridley sea turtles during the non-breeding period in the western Atlantic Ocean. Presumably, SIA of older tissues will reflect contributions to the diet from oceanic or neritic waters, and recent tissues will reflect contributions to the diet only for neritic waters. Red blood cells (RBCs), serum, epidermis and scutes have different average residence time of $\delta^{13}\text{C}$ and $\delta^{15}\text{N}$ (see review in Table 1), and each tissue may indicate whether a particular olive ridley turtle inhabited oceanic or neritic habitats during the inter-nesting period or only immediately before nesting and where they may remain during the non-breeding period. Habitat use was inferred based on $\delta^{13}\text{C}$ and $\delta^{15}\text{N}$ values from tissues with different half-life, representing different time windows before nesting. In addition, SIMM was used to determine the diet contribution of potential sources and habitats at these different time scales.

Methods

Study site

Sampling was conducted at Pirambu Beach, on the central coast of Sergipe State, northeastern Brazil (Fig. 1). Pirambu is a high-energy beach with a narrow continental shelf that is located in the tropical zone and has warm temperatures and a dry summer (Silva et al. 2007). In 1982, TAMAR-ICMBio (the Brazilian Sea Turtle Conservation Program) established a research station in this area to monitor the nesting activity of the following four sea turtle species: olive ridley, loggerhead (*Caretta caretta*), green (*Chelonia mydas*) and hawksbill (*Eretmochelys imbricata*) (Marcovaldi and Marcovaldi 1999). In Sergipe, olive ridleys nest mainly at Pirambu Beach, which shows higher numbers of olive ridley nests compared to nests of other sea turtle

species and to adjacent beaches (Silva et al. 2007). Olive ridleys are known to perform arribadas, in which thousands of females emerge simultaneously to lay their eggs (Pritchard 2007), but in the study area, only solitary nesters occur, with two clutches per female during each nesting season (Silva et al. 2007). The nesting season occurs between September and March, with small numbers of turtles nesting year-round (Silva et al. 2007). The number of nests has increased since 1998, 16 years after the beginning of TAMAR-ICMBio activities (Silva et al. 2007).

Sampling methods

During the reproductive season, TAMAR-ICMBio performs standard night patrols covering 12 km of beach at Pirambu, looking for female sea turtles and their nests. In November 2014, in partnership with TAMAR-ICMBio, serum, RBC, epidermal and carapace samples of female olive ridley sea turtles were collected for SIA. Sampling began as soon as the turtle initiated egg laying, as nesting desertion due to disturbance does not occur in this population once egg laying starts. The curved carapace length (CCL) of each turtle was measured from the nuchal notch to the tip of the longest posterior marginal scute using flexible tape measures (± 0.1 cm) (Bolten 1999), and sampling was only performed using females with a healthy appearance, i.e., no tumors. Blood samples (3 ml) were collected with a 25 \times 0.7 mm needle and syringe via the lateral cervical sinus and were transferred to non-heparinized containers. At the end of monitoring, whole blood was separated into serum and RBC by centrifugation (5000 rotations per minute (RPM) over 10 minutes), and the samples were then frozen. Epidermis samples were

collected from the right shoulder, between the neck and the front flipper, using a sterile scalpel. Carapace samples were collected from the first left scute in two places, one from the outer edge and another from the inner edge, representing the youngest and oldest tissues, respectively (Reich et al. 2007).

During the same period of turtle sampling, potential prey items based on the dietary study of Colman et al. (2014) were collected in the same area. Prey items were obtained from the bycatch of shrimp fisheries in the study area and from the stomach contents of four olive ridley sea turtles that were found stranded dead at Pirambu Beach and necropsied. Prey items that were classified as neritic include muscle tissue from the spider crab (*Libinia ferreirae*), box crab (*Calappa sulcata*), brachyuran crab (*Hepatus pudibundus*), clock crab (*Persephona lichtensteini*), purse crab (*Persephona punctata*), blue crab (*Callinectes* sp.), two species of shrimps from the Caridae family and seven species of fish from Sciaenidae family. For oceanic prey, we used isotopic values from jellyfish (*Veleva veleva*) that were stranded and collected from Trindade Island, Brazil. This island is located at the eastern end of the sea mountain chain Vitória-Trindade, 1160 km from mainland Brazil, and samples collected here are assumed to represent isotopic values of oceanic prey. This jellyfish feeds mostly on zooplankton (Mianzan and Girola 1990; Purcell et al. 2015 and references therein) while the pelagic salps eaten by Pacific Ocean olive ridley turtles (Montenegro-Silva et al. 1986) are filter-feeder relying mostly on phytoplankton (Hereu et al. 2010), and large jellyfish feed on higher trophic levels (Fleming et al. 2015). Thus, *V. veleva* seems to be at intermediate trophic levels among other gelatinous organisms, and thus represents well oceanic pelagic prey

potentially ingested by olive ridleys.

Tissue samples were rinsed with distilled water, and in all tissues except blood, the lipids were then extracted to remove the influence of the ^{13}C -depleted values of lipids (Post et al. 2007). The lipids were extracted using a Soxhlet apparatus with a 2:1 solvent mixture of chloroform and methanol (Medeiros et al. 2015); one cycle of 4 h was used for scute samples, and 2 cycles of 10 h were used for prey muscle and sea turtle epidermis. The samples were then dried at 60°C in an oven for 24–48 h to remove the residual solvent, while serum and RBCs were lyophilized for 8 h, and then all tissues were ground into powder. Serum was the only tissue in our study that had C:N ratios >3.5, indicating that its high lipid content may alter $\delta^{13}\text{C}$ values (Post et al. 2007). Therefore, 10 serum samples were lipid-extracted as described above for other tissues and were then prepared for SIA. This procedure aimed to provide an equation for normalization between lipid-extracted and non-extracted serum samples. The lipid-extracted and non-extracted samples were then compared using a Bayesian paired t-test to determine whether there was a difference in the ^{13}C values (see Results).

SIA

For each of the samples from potential prey items and turtles, approximately 0.7 mg was loaded into a sterilized tin capsule and then analyzed using a continuous-flow isotope-ratio mass spectrometer (CF-IRMS, Thermo Finnigan Delta Plus XP, Bremen, Germany) coupled to an elemental analyzer (Costech ECS 4010, Milan, Italy) at the Stable Isotope Laboratory of Washington State University, School of Biological Sciences, Pullman, Washington, USA. Stable

isotope ratios are expressed in δ notation as parts per thousand (‰) deviation from the international standards Pee Dee Belemnite limestone (carbon) and atmospheric air (nitrogen) as in equation 1:

$$\delta X(\text{‰}) = \left[\left(\frac{R_{\text{sample}}}{R_{\text{standard}}} \right) - 1 \right] \quad (1)$$

where R_{sample} and R_{standard} are the corresponding ratios of heavy to light isotopes ($^{13}\text{C}/^{12}\text{C}$ and $^{15}\text{N}/^{14}\text{N}$) in the sample and standard, respectively.

Statistical analysis

A Bayesian paired t-test (Kruschke 2015) was used to test for significant differences between lipid-extracted and non-extracted serum samples and between outer and inner scute samples. A Bayesian variance test (ANOVA) was also applied to compare $\delta^{13}\text{C}$ and $\delta^{15}\text{N}$ values among all tissues analyzed.

Linear regressions were conducted for the $\delta^{13}\text{C}$ and $\delta^{15}\text{N}$ values among all tissues collected to provide a tissue-to-tissue conversion (Vander Zanden et al. 2014). These conversions are useful because scute and epidermis samples can be easily collected with minimum stress to turtles without affecting the nesting behavior, health or physiological status of the individuals (Bjorndal and Bolten 2010; Vander Zanden et al. 2014). Moreover, blood samples require immediate centrifugation and freezing, which can present logistical challenges for sampling in remote places where electricity is not available (Vander Zanden et al. 2014). Pearson's correlation test was applied to the linear regressions fitted among tissues.

SIMM in IsotopeR (Hopkins-III and Ferguson 2012) was used to estimate the relative contributions of different sources to the diets of female

olive ridley sea turtles. Sampling occurred in November, as some olive ridley females recruit to coastal zones around September to reproduce, the assumption was that serum reflected the recent diet and therefore that serum may reflect the contribution of the neritic habitat to the diet (Silva et al. 2007; Reich et al. 2008). The TDF used for SIMM in the present study was from early juvenile loggerhead sea turtles (Reich et al. 2008) (Table 1) due to the similar diets and habitats of loggerhead and olive ridley sea turtles. Reich et al. (2008) determined the average of residence time of $\delta^{13}\text{C}$ and $\delta^{15}\text{N}$ and TDF of the epidermis, scutes, RBC and serum based on diets with different protein/lipid proportions. For the analysis of the contributions of potential prey items to the diet assimilation in different olive ridley tissues, the items were grouped into crustaceans (crab and shrimp species), demersal fish (all fishes from Sciaenidae family) and jellyfish, with the first two groups representing neritic prey (higher $\delta^{13}\text{C}$ values) and the last group representing oceanic prey (lower $\delta^{13}\text{C}$ values) (Post 2002; Bugoni et al. 2010).

All statistical inferences were performed within a Bayesian statistical framework (Ellison 2004). In Bayesian analysis, estimates of unknown parameters are given as probability distributions denoted 'posteriors' (Gelman et al. 2003). We used vague priors for all unknown model parameters. Samples for the posterior distributions were drawn by Markov Chain Monte Carlo (MCMC) simulation methods (Gelman et al. 2003). In contrast to conventional hypothesis tests and p-values, the Bayesian paired t-test provides direct probability statements about the values of interest and the highest (posterior) density intervals (HDIs) covering the 95% most likely values. The odds ratios are obtained by dividing the probability that the

difference is greater than or equal to zero by the probability that it is lower than zero, indicating the relative plausibility of both hypotheses. For example, an odds ratio above 20 indicates strong evidence in favor of a positive difference, while an odds-ratio below 1/20 indicates strong evidence to the contrary (Kruschke 2015). In addition, for Bayesian ANOVA analysis, Bayes Factor (BF) values indicate how many times in the simulation a given difference is likely to occur under the alternative or the null hypothesis (Rouder et al. 2012).

All analyses were performed using R software (R Core Team 2014) and the JAGS program (<http://mcmc-jags.sourceforge.net> [accessed 4 February 2015]) to specify models and perform the Bayesian analysis (Gilks et al. 1994). The package used for the paired t-test was BayesianFirstAid, BayesFactor was used for the ANOVA analysis, and IsotopeR was used for SIMMs (Hopkins-III et al. 2012).

Results

The 46 adult female olive ridley sea turtles sampled ranged in size from 64.0 to 76.0 cm CCC (mean \pm SD = 71.4 \pm 3.10 cm). Sampling occurred during nesting, thus turtles that finished laying eggs and returned to the ocean precluded sampling of all tissues for a few individuals. After lipids were extracted, all serum samples had C:N ratios <3.5. Moreover, the Bayesian paired *t*-test provided strong evidence that the lipid-extracted and non-extracted serum samples differed in both $\delta^{13}\text{C}$ and $\delta^{15}\text{N}$ values. The mean paired difference of $\delta^{13}\text{C}$ values was -1.6‰, with a credibility interval (CrI) of -1.9 to -1.2‰ and an odds ratio of 0.001. The mean paired difference of $\delta^{15}\text{N}$

values was -0.26‰ , with a CrI of -0.40 to -0.11‰ and an odds ratio of 0.002 . Thus, all other serum $\delta^{13}\text{C}$ values were corrected by a linear regression generated using these values (Fig. 2), while the original $\delta^{15}\text{N}$ values were used without mathematical normalization. Despite a minor difference between the lipid-extracted and non-extracted $\delta^{15}\text{N}$ values, this difference was within the range of standard deviation/accuracy of the equipment used (for $\delta^{13}\text{C}$ SD ± 0.06 ; for $\delta^{15}\text{N}$ SD ± 0.26). The scute samples provided weak evidence of a difference between the outer and inner samples (mean paired difference = -0.03‰ , CrI = $-0.12 - 0.07\text{‰}$, odds ratio = 0.31 for $\delta^{13}\text{C}$ values; mean paired difference = 0.06‰ , CrI = $-0.07 - 0.19\text{‰}$, odds ratio = 0.83 for $\delta^{15}\text{N}$ values).

$\delta^{13}\text{C}$ values showed the following order: RBC < serum < inner scute < outer scute < epidermal tissue (Table 2; Figs. 3 and 4), which corroborates the results from the MCMC simulation ANOVA. For $\delta^{13}\text{C}$, the Bayes factor (BF) was the highest (5.33) and had a posterior probability of 88% , indicating that tissues differed from each other in 88% of the simulation values (Table 3). For $\delta^{15}\text{N}$ values, the order was inner scute < outer scute < RBC < epidermis < serum tissue (Table 2; Figs. 3 and 4), which was corroborated by the MCMC simulation ANOVA (Table 3; Fig. 4). For $\delta^{15}\text{N}$, ANOVA also showed the highest BF of 5.71 and a posterior probability of 95% (Table 3).

Because there was little evidence of differences between the inner and outer scute samples, only the inner scute values were used for linear regressions and SIMM analysis. All linear regressions of the $\delta^{15}\text{N}$ values resulted in high correlation, while between the $\delta^{13}\text{C}$ values was lower than $\delta^{15}\text{N}$ values (Figs. 5 and 6). For $\delta^{13}\text{C}$ values, the epidermis had the lowest r ($r = 0.42$ to 0.55) compared to the other tissues (Figs. 5). $\delta^{15}\text{N}$ values did not

differ between the various tissues despite epidermal tissue having the lowest Pearson's correlation coefficient ($r = 0.81$ to 0.90) among all the tissues (Figs. 6).

The SIMM with values from RBC and epidermal samples demonstrated that the greatest contribution was from jellyfish, followed by demersal fish, with a negligible contribution of crustaceans (Table 4; Fig. 7). Scute and serum samples showed that the greatest contribution was from demersal fish, followed by jellyfish, with a negligible contribution from crustaceans (Table 4; Fig. 7). Although most individuals exhibited this pattern, some individuals showed different dietary compositions (Fig. 7). Two individuals had the highest $\delta^{13}\text{C}$ values (-16.81 to -14.86‰) and the lowest $\delta^{15}\text{N}$ values in all tissues (4.89 to 10.21‰).

Discussion

Methodological considerations

Serum samples demonstrated moderate lipid contents, and most samples had C:N ratios >3.5 after proper extraction using chloroform:methanol, allowing for the mathematical normalization of $\delta^{13}\text{C}$. However, lipid extraction also increased the $\delta^{15}\text{N}$ contents. Logan et al. (2008) and Hussey et al. (2012) showed an increase in $\delta^{15}\text{N}$ values in the muscle of some marine fish species and in the muscle of two elasmobranch species, respectively, when samples were submitted to lipid extraction with the same solvent used in the present study. Nevertheless, the average increase in $\delta^{15}\text{N}$ values is within the range of accuracy of the equipment ($\sim 0.26\text{‰}$) and is much lower than biologically meaningful differences under most circumstances, such as in changes

between trophic levels, for which such values are expected to vary 3–5‰ (Peterson and Fry 1987). However, several studies did not find any alteration in $\delta^{15}\text{N}$ values after lipid extraction using a chloroform:methanol solution (e.g., Arrington et al. 2006; Medeiros et al. 2015). Therefore, because some samples showed increases of up to 0.50‰ and because the differences between the groups being compared are small, lipid extraction should be undertaken carefully, e.g., by using the same procedure for all samples. Furthermore, because the results of lipid extraction studies vary, this topic deserves further investigation.

We provided tissue-to-tissue equations for the conversion of $\delta^{13}\text{C}$ and $\delta^{15}\text{N}$ values, which could allow comparisons between studies measuring stable isotopes in different tissues. $\delta^{13}\text{C}$ values also showed lower correlations than for the $\delta^{15}\text{N}$ values between tissues, suggesting that olive ridley sea turtles may commute between habitats or switch diets frequently, due tissues with different half-lives representing different habitats or diets. Alternatively, different metabolic routing used for tissue synthesis may result in the distinct assimilation of isotopes depending on the protein composition of each tissue (Martínez del Rio et al. 2009).

Habitat use

To the best of our knowledge, this is the first study using SIA for olive ridley sea turtles. It also appears to be the first study attempting to infer habitat use during non-breeding periods by using intrinsic markers in several tissues. The stable isotope values of $\delta^{13}\text{C}$ and $\delta^{15}\text{N}$ in various tissues indicated patterns of habitat use similar to those demonstrated by satellite telemetry of a few

individuals of the same population (Silva et al. 2011).

This species undergoes long migrations during adulthood; thus, tissues may show different isotopic values, especially in terms of $\delta^{13}\text{C}$, as turtles move between habitats with distinct isotopic signatures (Post 2002). Adult olive ridleys nesting in northeastern Brazil may migrate to post-nesting feeding grounds in oceanic waters in the central Atlantic or to neritic waters over the continental shelf. A third individual strategy may be to spend some time in neritic feeding grounds and then to migrate to the open ocean (Silva et al. 2011). Reis et al. (2010) reported 23 olive ridley sea turtles stranded dead on the Rio de Janeiro coast between August 2005 and November 2009. One specimen had been previously tagged when nesting at Pirambu Beach, our study site, which confirms that some individuals may remain in neritic waters over the continental shelf during the non-nesting period. In contrast, Sales et al. (2008) showed that adult olive ridleys intensively use oceanic waters between 5°N and 5°S and along the continental shelf of northeastern Brazil in the western Atlantic Ocean. In the eastern tropical Pacific Ocean, adults displayed no fidelity to specific feeding habitats and were classified as nomadic (Plotkin 2010). This pattern differs from loggerhead sea turtles, which have strong fidelity to non-breeding areas (Hall et al. 2015; Vander Zanden et al. 2016). Overall, the diet of olive ridleys is poorly known and has been limited to studies of adults, which maintain foraging consistency, relying on the same areas and prey (Vander Zanden et al. 2013). The few dietary studies of this species have all reported similar prey items: demersal fishes, crustaceans and jellyfishes (Montenegro-Silva et al. 1986; Colman et al. 2014; Di Benedetto et al. 2015). However, these studies are biased toward stranded

turtles, which may not be representative of oceanic turtles. In the tropical Pacific oceanic waters where olive ridleys were sampled offshore, it was demonstrated that adults and juveniles have similar diets, based mostly on jellyfish and ctenophores, and share the same habitat (Kopitsky et al. 2001).

$\delta^{15}\text{N}$ values showed high correlations among the different tissues (Fig. 6). Although $\delta^{15}\text{N}$ values may be a good proxy for trophic level, interpretation is difficult if the baseline values of each habitat are unknown. Moreover, in highly migratory species such as olive ridley sea turtles, it is more difficult to interpret these values (Martínez del Rio et al. 2009). McMahon et al. (2013) showed limited differences in copepod zooplankton $\delta^{15}\text{N}$ values between neritic and oceanic waters around northeastern Brazil. Thus, the baselines of the trophic webs in these habitats are most likely similar; alternatively, the scale of sampling in that study was too coarse and thus lacked the resolution to detect such differences. Although our sampling included several tissues with different half-life, the interpretation of changes in habitats based on $\delta^{15}\text{N}$ is challenging. In addition, some factors may influence both $\delta^{13}\text{C}$ and $\delta^{15}\text{N}$ values, such as metabolic processing, macronutrient routing, biochemical composition, and differential fractionation during assimilation (Martínez del Rio et al. 2009; Vander Zanden et al. 2014), which influence tissue average residence time (Reich et al. 2008).

Each tissue reflects the olive ridley diet at different times due to different average residence time of $\delta^{13}\text{C}$ and $\delta^{15}\text{N}$, but this time in adult sea turtles are unknown, as shown in Table 1. RBCs, epidermis and scutes of tortoises and juvenile sea turtles reflect the foraging grounds used at least 4–7 months prior to sampling (Brace and Altland 1955; Hamann et al. 2003;

Reich et al. 2010; Seminoff et al. 2007; Ceriani et al. 2014). Moreover, in reptiles, RBCs can persist for up to 11 months because they are nucleated, long-lived cells (Frische et al. 2001). In juvenile loggerhead sea turtles, RBCs had an average residence time of 40 days for $\delta^{13}\text{C}$ (Reich et al. 2008), based on an experiment submitting turtles to two different diets to detect how long turtles last to assimilate the second diet. However, the two diets used in Reich et al. (2008) had similar $\delta^{13}\text{C}$ values, and thus the average residence time of $\delta^{13}\text{C}$ may be higher. The lowest $\delta^{13}\text{C}$ value in RBCs presented here most likely represents the period during which olive ridleys were in oceanic waters (Post 2002). Nonetheless, two individuals had higher $\delta^{13}\text{C}$ values for RBCs than the others, suggesting that they were most likely in neritic feeding grounds before nesting. In addition to RBCs, serum, scute and epidermal tissues also exhibited high $\delta^{13}\text{C}$ values for these two individuals. Although the majority of olive ridley adults migrate to oceanic waters after the nesting season, a small proportion of individuals forage in coastal waters (Reis et al. 2010; Santos et al. 2016), and the two individuals with higher $\delta^{13}\text{C}$ values may represent specimens from neritic non-breeding areas. The $\delta^{15}\text{N}$ values in these two specimens also differed markedly from the others, being the lowest values from all samples and tissues. Although there are reports of olive ridley sea turtles on the Rio de Janeiro coast in southeastern Brazil, local upwelling occurs at this location, and upwellings are areas characterized by low $\delta^{15}\text{N}$ values at the food web baseline (Holmes et al. 2002). Thus, these two individuals with low $\delta^{15}\text{N}$ values were most likely present in feeding grounds on the Rio de Janeiro coast or other coastal areas along the Brazilian shelf that had prey with similar isotopic values before migrating to breed on the

Sergipe coast (Di Benedetto et al. 2015). Alternatively, they could be individuals specialized in low trophic levels (thus low $\delta^{15}\text{N}$ values), such as crustaceans, food items which could be part of the diet of the species (Colman et al. 2014, Appendix III).

Migration is a crucial component of the sea turtle life cycle and life history; these reptiles migrate in search of food resources, mates, nesting beaches or more optimal temperatures. Because these components are characteristics of each species, individual variability is expected in species with wide distributions (Morreale et al. 2007). Individual variability has been reported in numerous populations of vertebrates and invertebrates. In such situations, individuals use a small subset of the resource base of the population (Bolnick et al. 2003). Consequently, generalist populations may be formed by specialized individuals (Bolnick et al. 2003). In our study, SIMM analysis showed large individual variability for all tissues, which may indicate that turtles can migrate to breed from both neritic and oceanic habitats or that they commute between neritic and oceanic habitats during the period before nesting or during inter-nesting, resulting in considerable variation among tissues. An alternative non-exclusive explanation is that turtles originate from distinct non-breeding areas with different isotopic values. This scenario is consistent with the low correlations among the $\delta^{13}\text{C}$ values of the tissues sampled. Moreover, the RBCs, epidermis, scute and serum showed a gradual increase in $\delta^{13}\text{C}$ values, suggesting a habitat shift from oceanic to neritic habitats for reproduction in female turtles. Because RBCs reflect less recent periods than other tissues, jellyfish contributed 81%, while demersal fish contributed 19%. The contribution of demersal fish increased from the

epidermis to scutes and serum in SIMMs, with the latter having the fastest average residence time of $\delta^{13}\text{C}$ and $\delta^{15}\text{N}$. Because serum reflects the most recent time period, it showed the greatest contribution of demersal fish, corresponding to the bulk of the population inhabiting neritic habitat during the nesting season. Therefore, SIMMs showed a marked switch in habitat use for feeding in olive ridley sea turtles immediately before and during reproduction. However, individual variability was again represented by some individuals still having oceanic isotopic signatures (~5% of the sample). The narrow shelf break near the nesting beaches may facilitate displacement to offshore waters immediately before nesting or during the inter-nesting period.

Female olive ridley turtles nest from 1 to 3 times each season, with ~22 days between clutches (Matos et al. 2011). Because our sampling occurred in November, it is unknown whether the samples corresponded to the first or second clutches. If they were first clutches, the sampled turtle was most likely in neritic waters for some time during courtship, mating, ovulation and oviductal egg development (Rostal 2007). Therefore, although sea turtles rarely invest in feeding during the nesting season, they are opportunistic and may therefore make use of discards from shrimp trawl fisheries (Carvalho 2007; Romero et al. 2008) or the presence of other prey in the vicinity of nesting beaches between the two laying events. Serum samples showed the highest contribution of demersal fish (95%) and the lowest contribution of jellyfish (5%). This suggests that the sampled olive ridleys were most likely feeding during breeding. Colman et al. (2014) demonstrated the great importance of neritic items such as shrimps, crabs and demersal fishes, which are typically discarded by shrimp trawl fisheries, for olive ridley adults found

stranded dead at Pirambu Beach (Di Benedetto et al. 2015). In addition, based on satellite tracking, Silva et al. (2011) demonstrated active movements during the inter-nesting period and suggested that reproductive females in Sergipe forage during nesting. Measurements of turtle body mass in successive nesting attempts for some turtles in the area also confirm that they are feeding between laying events (Castilhos and Tiwari 2006). However, based on the quantification of the hormones ghrelin (a hunger-stimulating peptide) and leptin (an appetite-suppressing protein), hawksbill sea turtles (*Eretmochelys imbricata*) seem not to feed during breeding (Goldberg et al. 2013). Hawksbill turtles also feed opportunistically (Witzell 1983), similar to olive ridley sea turtles (Colman et al. 2014). Vitellogenesis in sea turtles occurs approximately 4–6 months before migration for nesting (Rostal et al. 1998), and turtles then undergo several steps in preparation for nesting. Therefore, if there is no easily available prey, turtles most likely do not eat for a long time. Because reproduction requires high levels of energy consumption, fasting turtles can mobilize their own tissues as energy sources, which may be an alternative explanation for the high $\delta^{15}\text{N}$ values found in serum.

Implications for conservation

Here, based on stable isotopes from several tissues, we have demonstrated that olive ridley sea turtle populations nesting in northeastern Brazil use a wide range of habitats, such as oceanic and neritic waters south and north of the nesting grounds, confirming previous studies that used other methods and that were based on small numbers of individuals (Reis et al. 2010; Silva et al.

2011). Stable isotope analysis in multiple tissues demonstrated that although the bulk of the population uses oceanic habitats during the non-breeding season, there is high individual variability. Thus, threats imposed by shrimp trawl fisheries adjacent to nesting areas (Silva et al. 2010) are in fact year-round problems for the portion of the population that remains over the continental shelf year-round, as trawling targeting shrimp and finfish occurs all along the Brazilian coast (Isaac et al. 2006). Furthermore, most individuals face the threat of incidental capture both in shrimp trawl nets during breeding and in pelagic longline fisheries in oceanic waters during the non-breeding period (Sales et al. 2008; Silva et al. 2011). Mitigating incidental capture by both fishery types is essential, as turtles using both oceanic and neritic foraging strategies are important for maintaining the population as well as for preserving the ecological plasticity of the population.

This species matures at approximately 16 years of age (Petitet et al. 2015), and although it is the most abundant sea turtle species globally (Reichert 1993), the number of adults found stranded dead on the Sergipe coast has increased (Castilhos et al. 2011). Shrimp trawling is prohibited during part of the nesting season, but turtles nesting before the closed period or after its end are not protected. In addition, the enforcement of legislation related to fisheries is difficult in Brazil, and turtles spend some time in neritic feeding grounds nearby before migrating to non-breeding areas (Silva et al. 2011).

The SIA of serum showed that turtles most likely forage just before and during the breeding season and therefore that olive ridley sea turtles spend time in neritic waters before, during and after nesting. Stable isotope studies

together with previous analyses based on satellite telemetry and stomach contents contribute to a better understanding of feeding behavior, migration and habitat use during a larger proportion of the life cycle of olive ridleys, including the poorly known non-breeding period. Conservation plans for this species in Brazil benefit greatly from such information. Bycatch mitigation measures for longline and trawl fisheries should continue to be the focus for conservation.

Acknowledgements We acknowledge the TAMAR/ICMBio staff for help with sampling; special thanks to Maria Angela Marcovaldi, Jaqueline Castilhos Roberto Garcia, Adriano Henrique, Buiú, Ederson Luiz Fonseca, Fabio Lira, Mari Weber, and veterinarians for their support. Authors are also grateful to A.S. Martins, E.R. Secchi, P.G. Kinas, M. Haimovici, S. Botta, and two anonymous reviewers for careful revisions of the MS. R.P. received financial support from the Coordenação de Aperfeiçoamento de Pessoal de Nível Superior (CAPES). L.B. is a research fellow of the Brazilian CNPq, National Council for Scientific and Technological Development (Proc. No. 310550/2015-7). This research is part of the PhD thesis written by R.P. under the guidance of L.B. and was authorized under the license number 36852-2 (SISBIO - *Sistema de Autorização e Informação em Biodiversidade*).

Compliance with Ethical Standards

Funding: R. Petitet received financial support from the 'Coordenação de Aperfeiçoamento de Pessoal de Nível Superior – CAPES' (Ministry of Education). L. Bugoni received a Research Fellowship from CNPq (PQ

310550/2015-7). This research is part of the PhD thesis written by R.P. under the guidance of L.B. and was authorized under the license number 36852-2 (SISBIO - *Sistema de Autorização e Informação em Biodiversidade*).

Conflict of interest: The authors declare that they have no conflict of interest.

Ethical approval: This article does not contain any studies with human participants. All applicable international, national, and institutional guidelines for the care of animals found stranded alive were followed. We did not conduct experiments with animals.

References

- Arrington DA, Davidson BK, Winemiller KO, Layman CA (2006) Influence of life history and seasonal hydrology on lipid storage in three neotropical fish species. *J Fish Biol* 68:1347–1361
- Bernardo J, Plotkin PT (2007) An evolutionary perspective in the *arribada* phenomenon and reproductive behavioral polymorphism of olive ridley sea turtle (*Lepidochelys olivacea*). In: Plotkin PT (ed) *Biology and conservation of ridley sea turtles*. Johns Hopkins University Press, Baltimore, MD, p 59–87
- Bjorndal KA, Bolten AB (2010) Hawksbill sea turtles in seagrass pastures: success in a peripheral habitat. *Mar Biol* 157:135–145
- Bolnick DI, Svanbäck R, Fordyce JA, Yang LH, Davis JM, Hulsey CD, Forister ML (2003) The ecology of individuals: incidence and implications of individual specialization. *Am Nat* 161:1–28

- Bolten AB (1999) Techniques for measuring sea turtles. In: Eckert KL, Bjorndal KA, Abreu-Grobois FA, Donnelly M (eds) Research and management techniques for the conservation of sea turtles. IUCN/SSC Marine Turtle Specialist Group, Publication No. 4, Washington, DC, p 1–5
- Brace KC, Altland PD (1955) Red cell survival in the turtle. *Am Physiol Soc* 183:91–94
- Bugoni L, McGill RAR, Furness RW (2010) The importance of pelagic longline fishery discards for a seabird community determined through stable isotope analysis. *J Exp Mar Biol Ecol* 391:190–200
- Carvalho FL (2007) Composição e distribuição dos carangueijos (Crustacea, Brachyura) presentes na fauna acompanhante da pesca do camarão no sul e sudeste da Bahia. BS Thesis, Universidade Estadual de Santa Cruz, Ilhéus, Brazil
- Castilhos JC, Tiwari M (2006) Preliminary Data from an Increasing Olive Ridley Population in Sergipe, Brazil. *Marine Turtle Newsletter* 113:8
- Castilhos JC, Coelho AC, Argolo JF, Santos EAP, Marcovaldi AM, Santos ASS, Lopez M (2011) Avaliação do estado de conservação da tartaruga marinha *Lepidochelys olivacea* (Eschscholtz, 1829) no Brasil. *Biodiv Bras* 1:28–36
- Ceriani SA, Roth JD, Ehrhart LM, Quintana-Ascencio PF, Weishampel JF (2014) Developing a common currency for stable isotope analyses of nesting marine turtles. *Mar Biol* 161:2257–2268
- Chambault P, Thoisy B, Heerah K, Conchon A, Barrioz S, Reis V, Berzins R, Kelle L, Picard B, Roquet F, Le Maho Y, Chevallier D (2016) The

- influence of oceanographic features on the foraging behavior of the olive ridley sea turtle *Lepidochelys olivacea* along the Guiana coast. *Prog Oceanogr* 142:58–71
- Colman LP, Sampaio CLS, Weber MI, Castilhos JC (2014) Diet of olive ridley sea turtles, *Lepidochelys olivacea*, in the waters of Sergipe, Brazil. *Chelonian Conserv Biol* 13:266–271
- DeNiro MJ, Epstein S (1978) Influence of diet on the distribution of carbon isotopes in animals. *Geochim Cosmochim Acta* 42:495–506
- DeNiro MJ, Epstein S (1981) Influence of diet on the distribution of nitrogen isotopes in animals. *Geochim Cosmochim Acta* 45:341–351
- Di Benedetto APM, Moura JF, Siciliano S (2015) Feeding habits of the sea turtles *Caretta caretta* and *Lepidochelys olivacea* in south-eastern Brazil. *Mar Biodiv Rec* 8:1–5
- Ellison AM (2004) Bayesian inference in ecology. *Ecol Lett* 7: 509–520
- Fleming NEC, Harrod C, Newton J, Houghton JDR (2015) Not all jellyfish are equal: isotopic evidence for inter and intraspecific variation in jellyfish trophic ecology. *PeerJ* 3:e1110
- Frische S, Bruno S, Fago A, Weber RE, Mozzarelli A (2001) Oxygen binding by single red blood cells from the red-eared turtle *Trachemys scripta*. *J Appl Physiol* 90:1679–1684
- Gelman A, Carlin JB, Stern HS, Rubin DB (2003) Bayesian data analysis, 2nd edn. Chapman & Hall, London
- Gilks WR, Thomas A, Spiegelhalter DJ (1994) A language and program for complex Bayesian modeling. *Statistician* 43:169–177

- Goldberg DW, Leitão SAT, Godfrey MH, Lopez GG, Santos AJB, Neves FA, Souza EPG, Moura AS, Bastos JC, Bastos VLFC (2013) Ghrelin and leptin modulate the feeding behaviour of the hawksbill turtle *Eretmochelys imbricata* during nesting season. *Conserv Physiol* 1:doi:10.1093/conphys/cot016
- Hall AG, Avens L, McNeill JB, Wallace B, Goshe LR (2015) Inferring long-term foraging trends of individual juvenile loggerhead sea turtles using stable isotopes. *Mar Ecol Prog Ser* 537: 265–276
- Hamann M, Limpus CJ, Owens DW (2003) Reproductive cycles of males and females. In: Lutz PL, Musick JA, Wyneken J (eds) *The biology of sea turtles*, vol. II. CRC Press, Boca Raton, pp 135–162
- Hatase H, Takai N, Matsuzawa Y, Sakamoto W, Omuta K, Goto K, Arai N, Fujiwara T (2002) Size-related differences in feeding habitat use of adult female loggerhead *Caretta caretta* around Japan determined by stable isotope analyses and satellite telemetry. *Mar Ecol Prog Ser* 233:273–281
- Hereu CM, Lavaniego BE, Goerick R (2010) Grazing impact of salp (Tunicata, Thaliacea) assemblages in the eastern tropical North Pacific. *J Plankton Res* 32:785–804
- Hobson KA (1999) Tracing origins and migration of wildlife using stable isotopes: a review. *Oecologia* 120:314–326
- Hobson KA, Norris DR (2008) Animal migration: a context for using new techniques and approaches. In: Hobson KA, Wassenaar LI (eds) *Tracking animal migration with stable isotope*. Environment Canada, Saskatoon, Saskatchewan, pp 1–19

- Holmes E, Lavik G, Fischer G, Segl M, Ruhland G, Wefer G (2002) Seasonal variability of $\delta^{15}\text{N}$ in sinking particles in the Benguela upwelling region. *Deep-Sea Res* 49:377–394
- Hopkins-III JB, Ferguson JM (2012) Estimating the diets of animals using stable isotopes and a comprehensive Bayesian mixing model. *PLoS ONE* 7:e28478
- Hopkins-III JB, Kurle CM (2016) Measuring the realized niches of animals using stable isotopes: from rats to bears. *Methods Ecol Evol* 7:210–221
- Hussey NE, Olin JA, Kinney MJ, McMeans BC, Fisk AT (2012) Lipid extraction effects on stable isotope values ($\delta^{13}\text{C}$ and $\delta^{15}\text{N}$) of elasmobranch muscle tissue. *J Exp Mar Biol Ecol* 434–435:7–15
- Isaac VJ, Martins AS, Haimovici M, Andriguetto JM (eds) (2006) *A pesca marinha e estuarina do Brasil no Século XXI: recursos, tecnologias, aspectos socioeconômicos e institucionais*. Belém, Universidade Federal do Pará, Brazil.
- IUCN (2015) Red list of threatened species. Version 2015-4. <www.iucnredlist.org>. Accessed on 02 May 2016
- Kopitsky K, Pitman RL, Plotkin PT (1999) Investigations on at-sea mating and reproductive status of olive ridleys, *Lepidochelys olivacea*, captured in the eastern tropical Pacific. In: *Proceedings of the 19th Annual Symposium on Sea Turtle Biology and Conservation*. NOAA, pp 291
- Kopitsky K, Pitman RL, Dutton PH (2001) Aspects of olive ridley feeding ecology in the eastern tropical Pacific. In: *Proceedings of the 21th Annual Symposium on Sea Turtle Biology and Conservation*. NOAA, pp 217

- Kruschke (2015) Doing Bayesian Data Analysis (2nd Ed). Elsevier, 759p.
- Logan JM, Jardine TD, Miller TJ, Bunn SE, Cunjak RA, Lutcavage ME (2008) Lipid corrections in carbon and nitrogen stable isotope analyses: comparison of chemical extraction and modelling methods. *J Anim Ecol* 77:838–846
- Marcovaldi MA, Marcovaldi GGD (1999) Marine turtles of Brazil: the history and structure of Projeto TAMAR-IBAMA. *Biol Conserv* 91:35–41
- Martínez del Rio C, Wolf N, Carleton SA, Gannes LZ (2009) Isotopic ecology ten years after a call for more laboratory experiments. *Biol Rev* 84:91–111
- Matos L, Silva ACCD, Castilhos JC, Weber MI, Soares LS, Vicente L (2011) Strong site fidelity and longer internesting interval for solitary nesting olive ridley sea turtles in Brazil. *Mar Biol* 159:1011–1019
- McMahon KW, Hamady LL, Thorrold SR (2013) A review of ecogeochemistry approaches to estimating movements of marine animals. *Limnol Oceanogr* 58:697–714
- Medeiros L, Monteiro DS, Petitet R, Bugoni L (2015) Effects of lipid extraction on the isotopic values of sea turtle bone collagen. *Aquat Biol* 23:191–199
- Mianzan HW, Girola CV (1990) The pleustonic coelenterates *Physalia physalis* (Linne, 1758), *Velella velella* (Linne, 1758) and *Porpita umbella* Muller, 1776 in southwestern Atlantic waters. *Invest Mar CICIMAR* 5:97–98
- Montenegro-Silva BC, Gonzalez NGB, Guerrero AM (1986). Estudio del contenido estomacal de la tortuga marina *Lepidochelys olivacea*, em la

costa de Oaxaca, México. An Inst Cienc Mar Limnol Univ Nac Auton Mex 13:121–132

Morreale SJ, Plotkin PT, Shaver DJ, Kalb HJ (2007) Adult migration and habitat utilization: ridley turtles in their elements. In Plotkin PT (ed) Biology and conservation of ridley sea turtles, The Johns Hopkins University Press, Baltimore, MD, pp 213–229

Peterson BJ, Fry B (1987) Stable isotopes in ecosystem studies. Ann Rev Ecol System 18:298–320

Petit R, Avens L, Castilhos JC, Kinas PG, Bugoni L (2015) Age and growth of olive ridley sea turtles *Lepidochelys olivacea* in the main Brazilian nesting ground. Mar Ecol Prog Ser 541:205–218

Plotkin PT (2010) Nomadic behaviour of the highly migratory olive ridley sea turtle *Lepidochelys olivacea* in the eastern tropical Pacific Ocean. Endang Species Res 13:33–40

Polovina JJ, Balazs GH, Howell EA, Parker DM, Seki MP, Dutton PH (2004) Forage and migration habitat of loggerhead (*Caretta caretta*) and olive ridley (*Lepidochelys olivacea*) sea turtles in the central north Pacific Ocean. Fish Oceanogr 13:36–51

Post DM (2002) Using stable isotopes to estimate trophic position: models, methods, and assumptions. Ecology 83:703–718

Post DM, Layman CA, Arrington DA, Takimoto G, Quattrochi J, Montaña CG (2007) Getting to the fat of the matter: models, methods and assumptions for dealing with lipids in stable isotope analyses. Oecologia 152:179–189

- Pritchard PCH (2007) *Arribadas* I have known. In: Plotkin PT (ed) *Biology and conservation of ridley sea turtles*. The Johns Hopkins University Press, Baltimore, MA, p 7–21
- Purcell JE, Milisenda G, Rizzo A, Carrion SA, Zampardi S, Airoidi S, Zagami G, Guglielmo L, Boero F, Doyle TK, Piraino S (2015) Digestion and predation rates of zooplankton by the pleustonic hydrozoan *Velevella velevella* and widespread blooms in 2013 and 2014. *J Plankton Res* 37:1056–1067
- R Core Team (2014) *R: A language and environment for statistical computing*. R Foundation for Statistical Computing, Vienna, www.R-project.org
- Reich KJ, Bjorndal KA, Bolten AB (2007) The ‘lost years’ of green turtles: using stable isotopes to study cryptic lifestages. *Biol Lett* 3:712–714
- Reich KJ, Bjorndal KA, Martínez del Rio C (2008) Effects of growth and tissue type on the kinetics of ^{13}C and ^{15}N incorporation in a rapidly growing ectotherm. *Oecologia* 155:651–663
- Reich KJ, Bjorndal KA, Frick MG, Witherington BE, Johnson C, Bolten AB (2010) Polymodal foraging in adult female loggerheads (*Caretta caretta*). *Mar Biol* 157:113–121
- Reichert HA (1993) Synopsis of biological data on the olive ridley sea turtle *Lepidochelys olivacea* (Eschscholtz, 1882) in the western Atlantic. NOAA Tech Memo NMFS- SEFSC-336
- Reis EC, Moura JF, Lima LM, Rennó B, Siciliano S (2010) Evidence of migratory movements of olive ridley turtles (*Lepidochelys olivacea*) along the Brazilian coast. *Braz J Oceanogr* 58:255–259
- Revelles M, Cardona L, Aguilar A, Borrell A, Fernández G, San Félix M (2007)

- Stable C and N isotope concentration in several tissues of the loggerhead sea turtle *Caretta caretta* from the western Mediterranean and dietary implications. *Sci Mar* 71:87–93
- Romero RM, Moraes LE, Santos MN, Rocha GRA, Cetra M (2008) Biology of *Isopisthus parvipinnis*: an abundant sciaenid species captured bycatch during sea-bob shrimp fishery in Brazil. *Neotrop Ichthyol* 6:67–74
- Rostal DC (2007) Reproductive physiology of the ridley sea turtle. In: Plotkin PT (ed) *Biology and conservation of ridley sea turtles*. Johns Hopkins University Press, Baltimore, MD, p 151–165
- Rostal DC, Owens DW, Grumbles JS, Mackenzie DS, Amoss MS (1998) Seasonal reproductive cycle of the Kemp's ridley sea turtle (*Lepidochelys kempii*). *Gen Comp Endocr* 109:232–243
- Rouder NJ, Morey RD, Speckman, PL, Province JM (2012) Default Bayes factors for ANOVA designs. *J Math Psychol* 56:356–374
- Rubenstein DR, Hobson KA (2004) From birds to butterflies: animal movement and stable isotopes. *Trends Ecol Evol* 19:256–263
- Sales G, Giffoni BB, Barata PCR (2008) Incidental catch of sea turtles by the Brazilian pelagic longline fishery. *J Mar Biol Assoc UK* 88:853–864
- Santos EAP, Silva ACCD, Sforza R, Oliveira FLC, Weber MI, Castilhos JC, Garcia RS, Marcovaldi MAAG, Ramos RMA, DiMatteo (2016) Where do olive ridley go after nesting along the Brazilian coast. In: *Proceedings of the 36th Annual Symposium on Sea Turtle Biology and Conservation*. NOAA

- Seminoff JA, Jones TT, Eguchi T, Jones DR, Dutton PH (2006) Stable isotope discrimination ($\delta^{13}\text{C}$ and $\delta^{15}\text{N}$) between soft tissues of the green sea turtle *Chelonia mydas* and its diet. *Mar Ecol Prog Ser* 308:271–278
- Seminoff JA, Bjorndal KA, Bolten AB (2007) Stable carbon and nitrogen isotope discrimination and turnover in pond sliders *Trachemys scripta*: insights for trophic study of freshwater turtles. *Copeia* 2007:534–542
- Seminoff JA, Jones TT, Eguchi T, Hastings M, Jones DR (2009) Stable carbon and nitrogen isotope discrimination in soft tissues of the leatherback turtle (*Dermochelys coriacea*): insights for trophic studies of marine turtles. *J Exp Mar Biol Ecol* 381:33–41
- Silva ACCD, Castilhos JC, Lopez GG, Barata PCR (2007) Nesting biology and conservation of the olive ridley sea turtle (*Lepidochelys olivacea*) in Brazil, 1991/1992 to 2002/2003. *J Mar Biol Assoc UK*, 87:1047–1056
- Silva ACCD, Castilhos JC, Santos EAP, Brondízio LS, Bugoni L (2010) Efforts to reduce sea turtle bycatch in the shrimp fishery in northeastern Brazil through a co-management process. *Ocean Coast Manage* 53:570–576
- Silva ACCD, Santos EAP, Oliveira FLC, Weber MI, Batista JAF, Serafini TZ, Castilhos JC (2011) Satellite-tracking reveals multiple foraging strategies and threats for olive ridley turtles in Brazil. *Mar Ecol Prog Ser* 443:237–247
- Vander Zanden HB, Bjorndal KA, Mustin W, Ponciano JM, Bolten AB (2012) Inherent variation in stable isotope values and discrimination factors in two life stages of green turtles. *Physiol Biochem Zool* 85:431–441

- Vander Zanden HB, Bjorndal KA, Bolten AB (2013) Temporal consistency and individual specialization in resource use by green turtles in successive life stages. *Oecologia* 173:767–777
- Vander Zanden HB, Tucker AD, Bolten AB, Reich KJ, Bjorndal KA (2014) Stable isotopic comparison between loggerhead sea turtle tissues. *Rapid Commun Mass Spectrom* 28:2059–2064
- Vander Zanden HB, Bolten AB, Tucker AD, Hart KM, Lamont MM, Fujisaki I, Reich KJ, Addison DS, Mansfield KL, Phillips KF, Pajuelo M, Bjorndal KA (2016) Biomarkers reveal sea turtles remained in oiled areas following the *Deepwater Horizon* oil spill. *Ecol Appl* 26:2145–2155
- Wallace BP, Heppell SS, Lewison RL, Kelez S, Crowder LB (2008) Impacts of fisheries bycatch on loggerhead turtles worldwide inferred from reproductive value analyses. *J Appl Ecol* 45:1076–1085
- Whiting SD, Coyne LM (2007) Migration routes and foraging behaviour of olive ridley turtles *Lepidochelys olivacea* in northern Australia. *Endang Species Res* 3:1–9
- Witzell WN (1983) Synopsis of biological data on the hawksbill sea turtle *Eretmochelys imbricata* (Linnaeus 1766). FAO Fisheries Synopsis No.137

FIGURE LEGENDS

Fig. 1 Sampling location of olive ridley (*Lepidochelys olivacea*) nesting females at Pirambu Beach, Sergipe State, Brazil

Fig. 2 Linear regressions between pairs of $\delta^{13}\text{C}$ values (a) and between pairs of $\delta^{15}\text{N}$ values (b) of lipid-extracted and non-extracted serum samples. Equations inside the graphics indicate the relationship between samples with and without lipids. Ex: extracted lipids; non-ex: non-extracted lipids

Fig. 3 $\delta^{13}\text{C}$ and $\delta^{15}\text{N}$ values from red blood cells (RBCs), serum, epidermis (EPI), inner scute (InS) and outer scute (OuS) samples. The horizontal black line indicates the median value, the box indicates the quantiles of 25% and 75%, dashed lines indicate extreme values, and empty circles indicate outlier values

Fig. 4 Posterior probability of Markov Chain Monte Carlo (MCMC) simulation from ANOVA analysis of each tissue sampled. RBCs: red blood cells; OScute: outer scute; IScute: inner scute; EPI: epidermis

Fig. 5 Linear relationships among $\delta^{13}\text{C}$ values of tissues from olive ridley sea turtles (scute, epidermis, serum and red blood cells). The regression equation and the Bayesian First Aid Pearson's correlation coefficient (r) are provided inside each graph

Fig. 6 Linear relationships among $\delta^{15}\text{N}$ values of tissues from olive ridley sea turtles (scute, epidermis, serum and red blood cells). The regression equation and the Bayesian First Aid Person's correlation test (r) are provided inside each graph

Fig. 7 Estimated stable isotope values ($\delta^{13}\text{C}$, $\delta^{15}\text{N}$) (a, c, e and h) for red blood cells (RBCs), epidermis, scute and serum from olive ridley sea turtles

(*Lepidochelys olivacea*) and the proportional dietary contributions (expressed as marginal posterior distributions) of different potential sources: jellyfish (triangle), demersal fish (circle) and crustacean (square) (b, d, f and g). Gray lines indicate each individual sampled, and the line in the middle is the mean diet contribution (b, d, f and g)

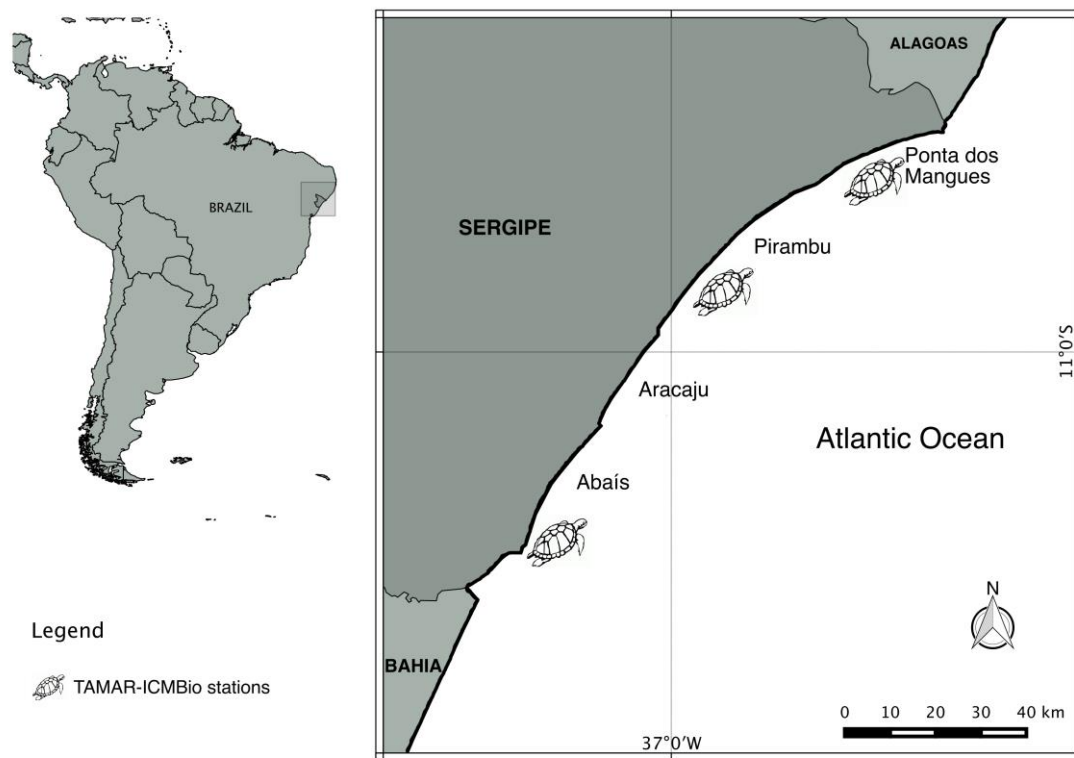


Figure 1

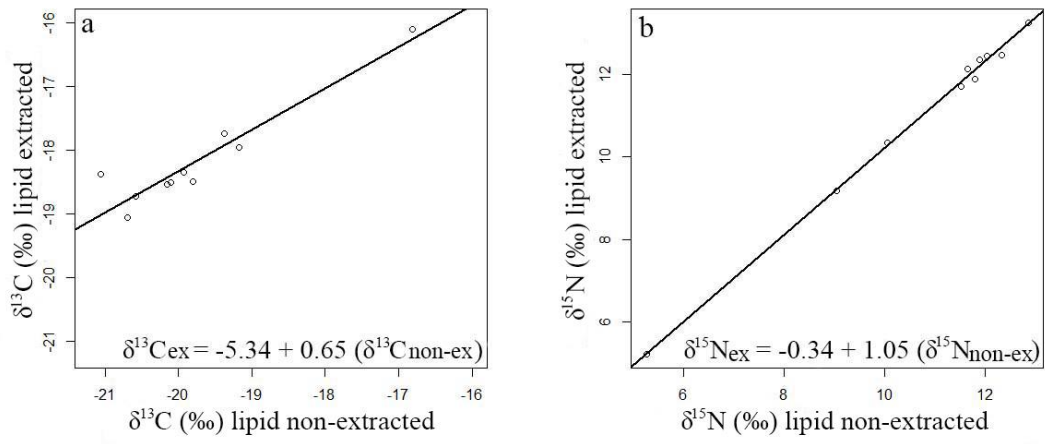


Figure 2

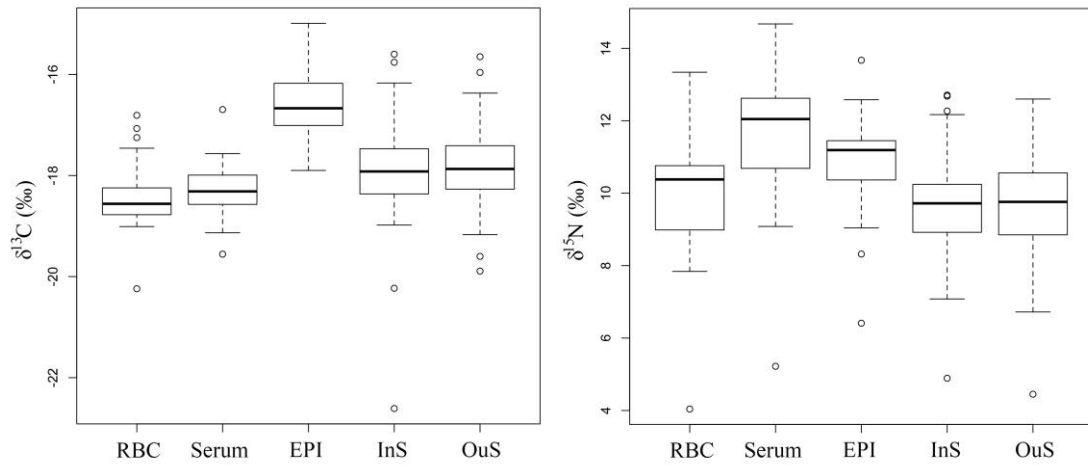


Figure 3

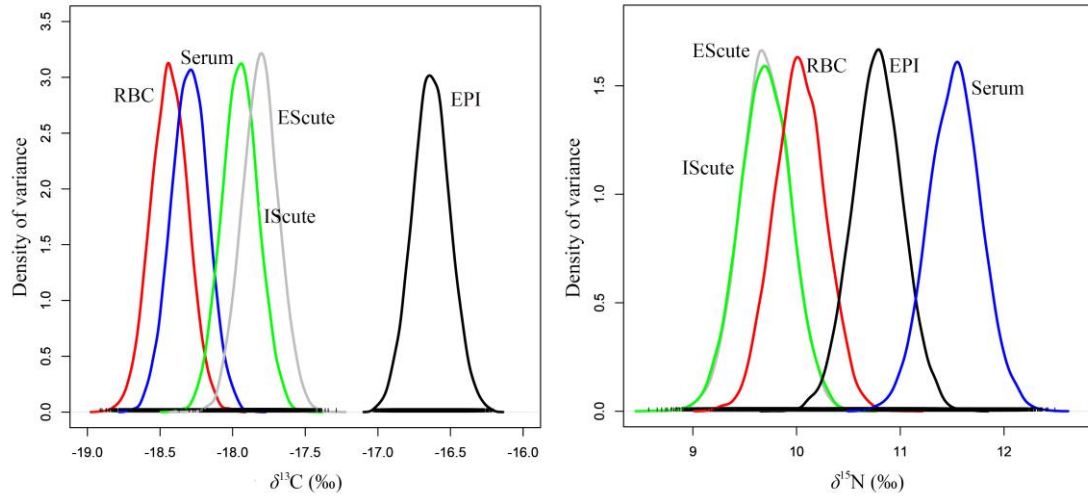


Figure 4

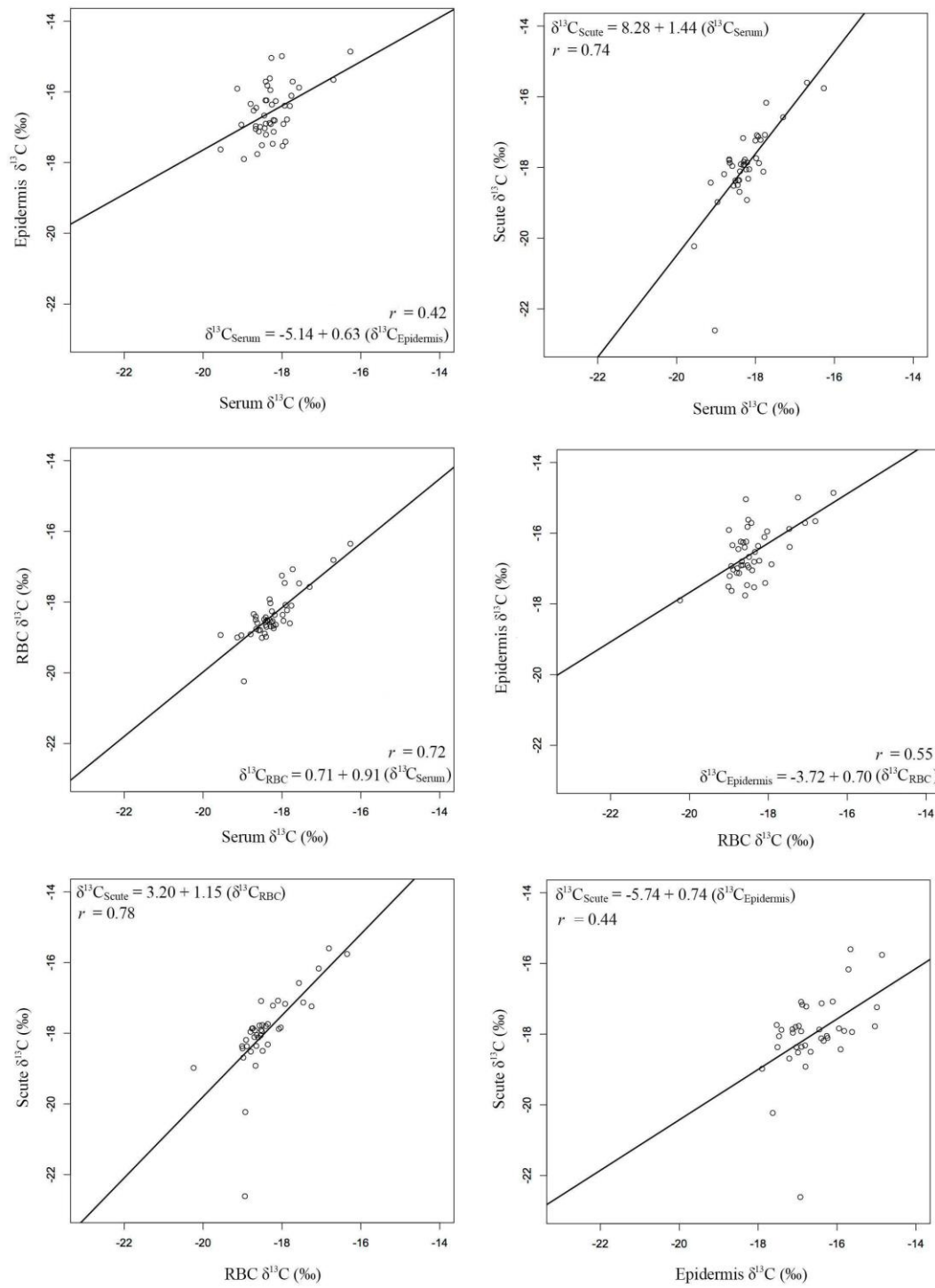


Figure 5

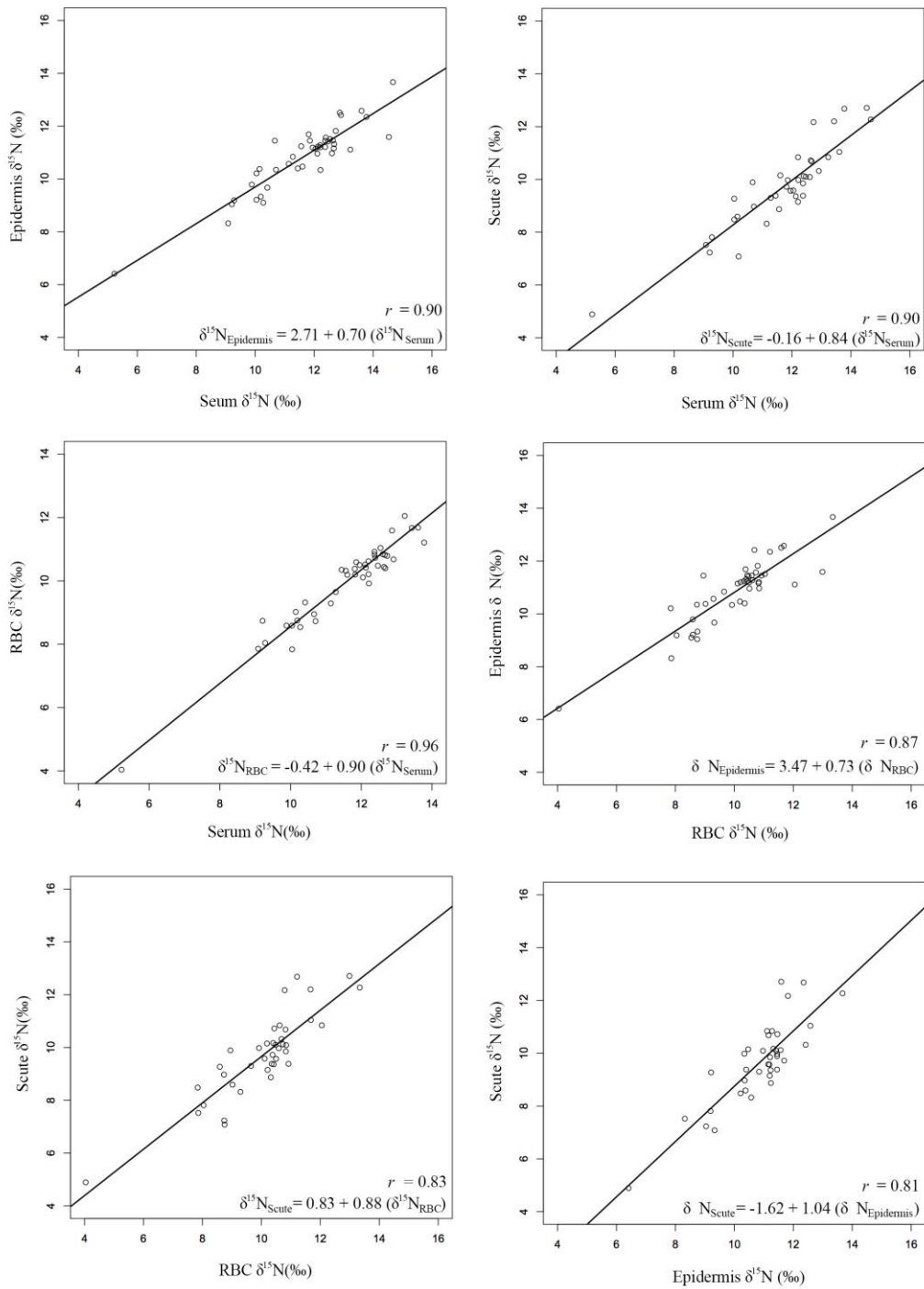


Figure 6

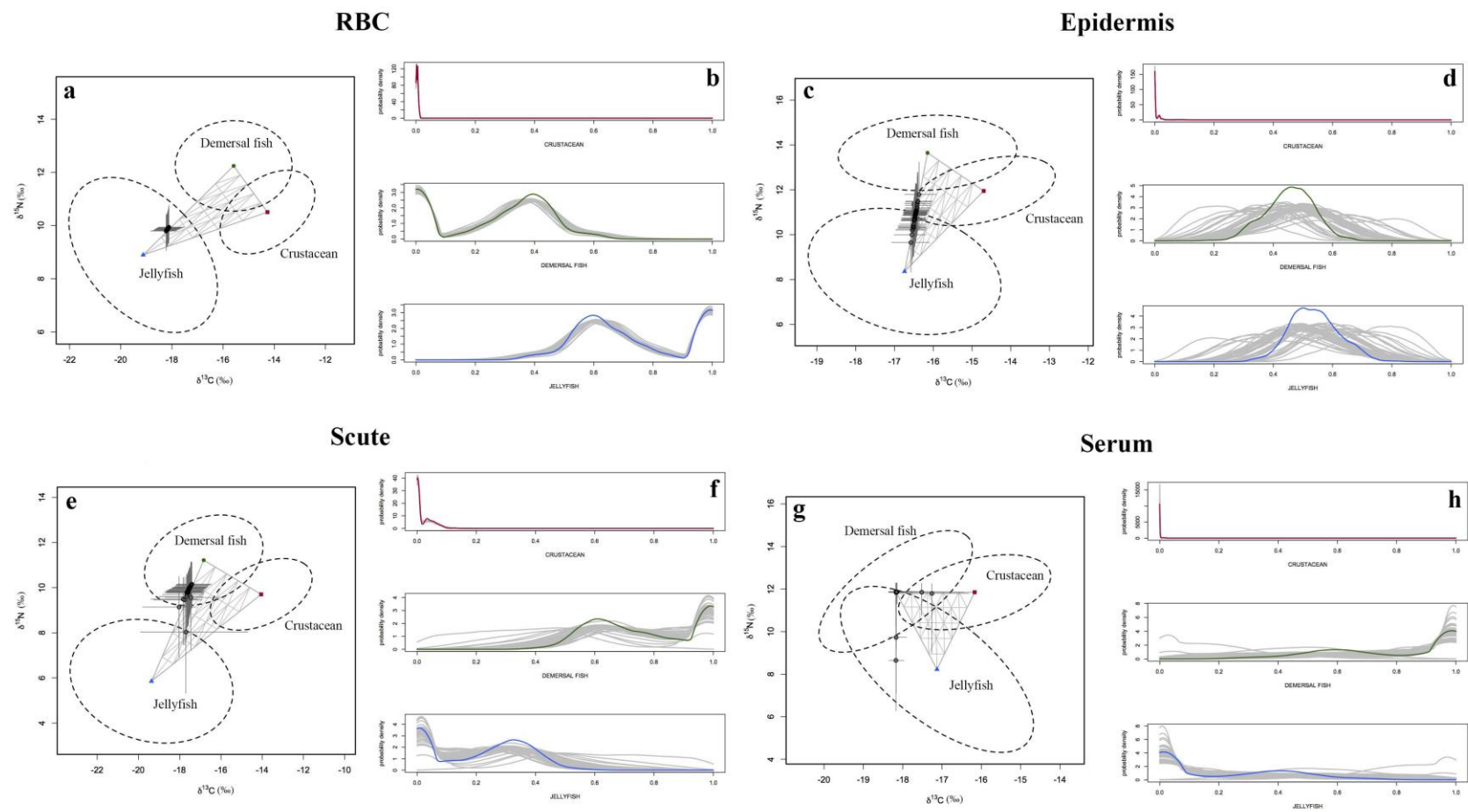


Figure 7

Table 1 Overview of residence time and discrimination factors of $\delta^{13}\text{C}$ and $\delta^{15}\text{N}$ from serum, red blood cells (RBC), epidermis and scute tissues from sea turtles

	<i>Caretta caretta</i> juvenile ^a <i>n</i> = 12		<i>Chelonia mydas</i> adult ^b <i>n</i> = 30	<i>Chelonia mydas</i> juvenile ^b <i>n</i> = 40	<i>Chelonia mydas</i> juvenile ^c <i>n</i> = 8	<i>Dermochelys coriacea</i> Juvenile ^d <i>n</i> = 7
Tissue	Residence time (days)	Discriminatio n factor (‰)	Discrimination factor (‰)	Discrimination factor (‰)	Discrimination factor (‰)	Discrimination factor (‰)
$\delta^{13}\text{C}$						
Serum/Plasma	39.9 ± 9.1	-0.38 ± 0.21	0.24 ± 0.61	1.16 ± 0.56	-0.12 ± 0.08	-0.58 ± 0.53
RBC	40.1 ± 3.4	1.53 ± 0.17	0.30 ± 0.58	0.51 ± 0.56	-1.11 ± 0.17	0.46 ± 0.35
Epidermis	46.1 ± 8.9	1.11 ± 0.17	1.62 ± 0.61	1.87 ± 0.56	0.17 ± 0.08	2.26 ± 0.61
Scute	50.9 ± 13.14	1.77 ± 0.58	--	--	--	--
$\delta^{15}\text{N}$						
Serum/Plasma	22.5 ± 5.1	1.50 ± 0.17	4.17 ± 0.41	4.06 ± 0.37	2.92 ± 0.08	2.86 ± 0.62
RBC	36.3 ± 3.4	0.16 ± 0.08	2.48 ± 0.35	2.36 ± 0.37	0.22 ± 0.08	1.49 ± 0.76
Epidermis	44.9 ± 3.1	1.60 ± 0.07	4.04 ± 0.44	4.77 ± 0.40	2.80 ± 0.31	1.85 ± 0.50
Scute	16.2 ± 2.3	-0.64 ± 0.09	--	--	--	--

^a Reich et al. (2008)

^b Vander Zanden et al. (2012)

^c Seminoff et al. (2006)

^d Seminoff et al. (2009)

Table 2 $\delta^{13}\text{C}$ and $\delta^{15}\text{N}$ stable isotope values (mean \pm standard deviation) from serum, red blood cells (RBCs), epidermis and scute tissues of olive ridley (*Lepidochelys olivacea*) females sampled at Pirambu, Sergipe State, Brazil. Values in parentheses are the range of $\delta^{13}\text{C}$ (‰) and $\delta^{15}\text{N}$ (‰); n is the number of individuals sampled

Tissue	n	$\delta^{13}\text{C}$ (‰)	$\delta^{15}\text{N}$ (‰)
Serum	46	-18.25 \pm 0.56 (-19.56 – -16.27)	11.68 \pm 1.65 (5.22 – 14.67)
RBCs	46	-18.39 \pm 0.66 (-20.24 – -16.35)	10.06 \pm 1.52 (4.04 – 13.34)
Epidermis	43	-16.56 \pm 0.74 (-17.90 – -14.86)	10.83 \pm 1.27 (6.41 – 13.67)
Inner scute	40	-17.95 \pm 1.14 (-22.61 – -15.60)	9.70 \pm 1.56 (4.89 – 12.71)
Outer scute	40	-17.81 \pm 0.85 (-19.89 – -15.65)	9.64 \pm 1.67 (4.45 – 12.60)

Table 3 Bayesian variance analyses for each order restriction with Bayes Factor (BF) values and posterior probability from Markov Chain Monte Carlo (MCMC) simulations of $\delta^{13}\text{C}$ and $\delta^{15}\text{N}$ values. Higher BF values and higher posterior probabilities are strong support for differences. RBCs: red blood cells; IScute: inner scute; OScute: outer scute; EPI: epidermis

Tissue/restriction	Bayes factor (BF)	Posterior probability (%)
$\delta^{13}\text{C}$ (‰)		
RBCs < Serum	4.77	79.5
RBCs < IScute	5.98	99.6
RBCs < OScute	5.99	99.9
RBCs < EPI	6.00	100.0
Serum < IScute	5.85	97.4
Serum < OScute	5.97	99.7
Serum < EPI	6.00	100
IScute < OScute	4.70	78.4
IScute < EPI	6.00	100.0
OScute < EPI	6.00	100.0
RBCs < Serum < IScute < OScute < EPI	5.33	88.0
$\delta^{15}\text{N}$ (‰)		
IScute < OScute	3.00	50.2
IScute < RBCs	4.98	83.2
IScute < EPI	5.99	99.9
IScute < Serum	6.00	100.0
OScute < RBCs	5.00	83.4
OScute < EPI	5.99	99.9
OScute < Serum	5.99	99.9
RBCs < EPI	5.90	98.5
RBCs < Serum	5.99	99.9
EPI < Serum	5.90	98.3
IScute < OScute < RBCs < EPI < Serum	5.71	95.0

Table 4 Dietary contributions of different sources for olive ridley females (*Lepidochelys olivacea*) from Pirambu, Sergipe State, Brazil. Crl: credibility interval; RBCs: red blood cells

Tissue	Jellyfish		Demersal fish		Crustacean	
	Mean (%)	Crl (%)	Mean (%)	Crl (%)	Mean (%)	Crl (%)
RBCs	81	37–100	19	14–62	0	0–1
Epidermis	54	39–70	45	29–60	0	0–7
Scute	20	0–47	79	49–100	2	0–8
Serum	4	0–40	95	60–100	0	0–1

The following Electronic Supplementary Material accompany the article

High habitat use plasticity by female olive ridley sea turtles (*Lepidochelys olivacea*) revealed by stable isotope analysis in multiple tissues

Roberta Petitet, Leandro Bugoni

Table S1 Mean \pm SD of $\delta^{15}\text{N}$ and $\delta^{13}\text{C}$ values of each potential prey species/family of *Lepidochelys olivacea*. SD: standard deviation; *n*: number of individuals

Family/species	$\delta^{15}\text{N}$ (‰)	$\delta^{13}\text{C}$ (‰)
Crustacean (n = 8)	10.35 \pm 0.31	-15.81 \pm 0.37
<i>Libinia ferreire</i> (n = 1)	10.39	-15.51
<i>Calapa sulcata</i> (n = 1)	10.34	-15.49
Cariidae (n = 1)	10.78	-15.85
Cariidae (n = 1)	9.73	-16.38
<i>Hematus pundibundus</i> (n = 1)	10.25	-15.63
<i>Callinectes</i> spp. (n = 1)	10.29	-16.24
<i>Persephona lichtensteinii</i> (n = 1)	10.64	-15.36
<i>Persephona punctata</i> (n = 1)	10.34	-15.98
Demersal fish (n = 7)	12.08 \pm 0.34	-16.87 \pm 0.63
<i>Nebris microps</i> (n = 1)	11.78	-16.76
<i>Menticirrhus</i> spp. (n = 1)	12.54	-16.1
<i>Larimus breviceps</i> (n = 1)	11.68	-17.19
Unidentified Sciaenidae (n = 1)	12.5	-17.84
<i>Cynoscion</i> spp. (n = 1)	11.87	-16.19
<i>Stellifer</i> spp. (n = 1)	12.21	-16.68
<i>Isopisthus parvipinnis</i> (n = 1)	12.01	-17.36
Jellyfish (<i>Velella velella</i>, n = 3)	6.44 \pm 0.88	-16.69 \pm 0.47

APÊNDICE III

**Individual specialization and temporal consistency in resource use by
olive ridley sea turtles (*Lepidochelys olivacea*) inferred by stable isotope
analysis in humerus growth layers**

Roberta Petitet, Jaqueline C. Castilhos, Leandro Bugoni

FORMATADO PARA O PERIÓDICO *MARINE BIOLOGY*

Individual specialization and temporal consistency in resource use by olive ridley sea turtles (*Lepidochelys olivacea*) inferred by stable isotope analysis in humerus growth layers

Roberta Petitet^{1,2*}, Jaqueline C. Castilhos³, Leandro Bugoni¹

¹ Laboratório de Aves Aquáticas e Tartarugas Marinhas, Instituto de Ciências Biológicas, Universidade Federal do Rio Grande (FURG), Campus Carreiros, Avenida Itália s/n, CP 474, 96203–900, Rio Grande, RS, Brazil

² Programa de Pós-Graduação em Oceanografia Biológica, Instituto de Oceanografia, Universidade Federal do Rio Grande (FURG), Campus Carreiros, Avenida Itália s/n, CP 474, 96203–900, Rio Grande, RS, Brazil

³ Fundação Centro Brasileiro de Proteção e Pesquisa das Tartarugas Marinhas, Reserva Biológica de Santa Isabel s/n, Centro, 49190–000, Pirambu, SE, Brazil

* Corresponding author Email: rpetitet@hotmail.com

Abstract

Bone collagen in lines of arrested growth in humeri of adult olive ridley sea turtles (*Lepidochelys olivacea*) were used for stable isotope analysis of carbon and nitrogen, aiming to detect habitat use and diet shift through years. Adult olive ridleys from northeastern Brazil has an ontogenetic shift around 17 years old, which corresponds to the age at sexual maturity, when individuals recruit from oceanic waters to coastal waters to breed. After this period, however, some individuals seem to inhabit continental shelf waters, instead of returning to offshore areas. Younger individuals (14 to 18 years old) and older

individuals (19 to 23 years old) had similar degree of individual specialization. However, older individuals had less variable carbon and nitrogen values through time than younger individuals, suggesting consistent use of the same feeding grounds. Thus, adults were classified as a generalist population with specialist individuals. Nevertheless, the high individual variability and consequently vast habitats used, make olive ridley susceptible to fisheries bycatch in neritic habitats, where shrimp trawl fishery operates, as well as in oceanic habitats, where pelagic longline fishery occurs. Therefore, results indicate the need for actions in both coastal and offshore areas for the effective conservation and a decrease in adult mortality.

Introduction

High individual variation in resource use may lead to individual specialization, that is, individuals using a small subset of resources used by the population (Bolnick et al. 2003). This phenomenon is widespread and it has been demonstrated in invertebrate and vertebrata taxa (Bolnick et al. 2003). Thus, “Individual specialist” is defined as the individual whose the niche is substantial narrowest than the population niche (Bolnick *et al.*, 2003), while “individual specialization” designates both the predominance of specialist individuals in the population as well as the level at which the diet of individuals is restricted relative to their population (Bolnick *et al.*, 2003).

Olive ridley sea turtle (*Lepidochelys olivacea*) is the most abundant sea turtle species worldwide (Reichert 1993). However, this species is listed as vulnerable at the global red list (IUCN 2015). In addition, it is the most oceanic among sea turtle species, which coupled with limited funding to research of

the species in comparison with others, make it one of the least studied sea turtle species. Olive ridley sea turtles spend all juvenile stage in oceanic waters (Reichert 1993) and in the western Atlantic Ocean mature about 16 years old (Petitet et al. 2015), while in eastern Pacific Ocean mature about 13 years old (Zug et al. 2006). Then, this species recruits to coastal waters for nesting. Adults can be either oceanic or neritic during the non-nesting period (Plotkin 2010), or use both habitats in variable proportions. For the population nesting in northeastern Brazil, 3 post-nesting migration patterns were described: moving to oceanic waters; moving to neritic waters northward, along the Brazilian coast (Silva et al. 2011); and moving southward, e.g. to Rio de Janeiro coast (Di Benedetto et al. 2015). Therefore, this species has high individual variation in habitat use and diet.

Individual specialization is evaluated by total niche width (TNW), that is, the variance in the type or size of all captured prey by the population, which can be partitioned into two components: within-individual component (WIC), i.e. the average variance of resources found within individuals' diet, and between-individual component (BIC), defined as the variance among individuals (Bolnick et al. 2003). Therefore, individual variation is large when BIC encompass a large proportion of TNW and the WIC/TNW ratio is small (Bolnick et al. 2003). However, WIC/TNW ratio measures the degree of individual specialization, with values near 0 indicating specialist individuals, while values near 1 indicate generalist individuals (Bolnick et al. 2002).

Besides individual specialization, temporal consistency can be evaluated by WIC values trough time (Vander Zanden et al. 2013). As WIC measures the variance within each individual, a specimen sampled several

times in different moments, with high WIC value, did not have temporal consistency through time (Vander Zanden et al. 2013). Carbon and nitrogen stable isotopes values, $\delta^{13}\text{C}$ and $\delta^{15}\text{N}$, respectively, have been used to infer diet and habitat used by animals (Fry 2007). Biological materials that retain the isotopic signature during synthesis and are inert or have long turnover periods are an alternative to the recapture and resampling of individuals, an option frequently unfeasible. Thus, stable isotopes may be used to measure temporal consistency and individual specialization through time in sea turtles scutes (Vander Zanden et al. 2010, 2013; Pajuelo et al. 2016), baleen of whales (Schell et al. 1989), whiskers of otters and seals (Newsome et al. 2009) and teeth of fur seals (Albernaz et al. 2017). However, stable isotope in sea turtle humeri only there are two studies with loggerhead sea turtle and they analyzed only nitrogen isotope (Avens et al. 2013; Ramirez et al. 2015).

$\delta^{13}\text{C}$ and $\delta^{15}\text{N}$ are mainly used to infer habitat or trophic level, respectively, because the former increase by about c. 1‰ between the food and its consumer, while the latter increase in a scale of c. 3–5 ‰ each trophic level (Peterson and Fry 1987; Post 2002). Thus, the variances of these stable isotopes between and within individual have been used to characterize populations: specialist population, generalist population with generalist individuals, and generalist population with specialist individuals (Bearhop et al. 2004; Fig. 1a–c in Vander Zanden et al. 2013). Specialist populations occupy a narrow isotopic niche with a low TNW and individuals have temporal consistency through time and consequently low WIC; generalist populations with high TNW may be composed by generalist individuals that have low temporal consistency and high isotopic variance between individuals and

consequently high WIC; and finally, specialist individuals from a generalist population have high temporal consistency and low isotopic variance through time and consequently low WIC (Vander Zanden et al. 2013).

Based on stable isotope analysis (SIA) from scutes, the population of adult male and female loggerheads (*Caretta caretta*) from North Atlantic Ocean was classified as a generalist population with specialist individuals (Vander Zanden et al. 2010; Pajuelo et al. 2016). Adult green sea turtles (*Chelonia mydas*) from a nesting beach in Costa Rica also demonstrated a generalist population with specialist individuals, based on SIA in scutes (Vander Zanden et al. 2013). Therefore, we hypothesize that adult olive ridleys from northeastern Brazil most likely fits in the generalist population, with younger individuals more generalists and low temporal consistency, and older individuals as specialists with high temporal consistency (as in Fig. 1c from Vander Zanden et al. 2013).

Olive ridley sea turtles are commonly found stranded dead in their nesting beaches in northeastern Brazil, and mostly are adult females, with fully formed eggs (Castilhos et al. 2011). Olive ridley sea turtles interact strongly with shrimp trawl fisheries, which is the main threat for this species in neritic waters of the Sergipe state (Silva et al. 2011). Moreover, longline fishery is the threat at oceanic waters, where large numbers of adults and juveniles are incidentally captured (Carranza et al. 2006; Sales et al. 2008). Despite the high mortality of adult females in fisheries and a non-negligible impact on the population, the number of olive ridley nests in northeastern Brazil increased in recent years (Castilhos et al. 2011). Thus, the identification of individual specialization, intrapopulational variability in habitat uses and

temporal consistency from this population may be useful to infer individual differences in susceptibility to capture in fisheries, in distinct areas and along the life cycle.

Thus, the present study aims to identify habitat use and diet shifts from stable isotope analysis in lines of arrested growth (LAG) of olive ridley sea turtle humeri. Sequential samples from an individual generate a trajectory by year, allowing the evaluation of the degree of individual specialization (WIC/TNW ratio) and temporal consistency (WIC). In addition, it was built a stable isotope mixing model to evaluate contribution of oceanic and neritic dietary sources, and infer habitat use of the population and individually, in order to complement the individual specialization and temporal consistency analysis.

Material and methods

Sample collection

Humeri of olive ridley sea turtles were obtained from a previous study at the southern coast of Alagoas and coast of Sergipe states, in northeast Brazil, between 2009 and 2011 as in Petitet et al. (2015). There are 173 km of beach, between 10°31'S and 11°25'S, which is monitored by TAMAR-ICMBio (the Brazilian Sea Turtle Conservation Programme) in partnership with the *Fundação Mamíferos Aquáticos* (FMA). Pirambu is the main nesting area; a high-energy beach with a narrow continental shelf (~20 km) located in the tropical zone and has warm temperatures and a dry summer (Silva et al. 2007). The coast of Sergipe state is the main Brazilian reproduction area for

solitary olive ridley sea turtles, where there are 7000 nests per year with increased number over the years (Silva et al. 2007).

All turtles sampled had curved carapace length (CCL) recorded, measured from the nuchal notch to the posterior end of the posterior marginal. Only turtles with apparently good health, i.e. no tumors, were sampled. Humeri samples ($n = 68$) were processed for a previous skeletochronological study (Petitet et al. 2015). For the present study, a sub-set of 20 olive ridley humeri was analyzed. Before sampling bone sections for skeletochronological analysis it was taken a 1 mm thick section for SIA.

Based on Colman et al. (2014), potential neritic prey for olive ridley sea turtles were collected at the study area from shrimp trawling bycatch. Neritic prey consisted by crustaceans and demersal fishes. Isotopic values of a jellyfish (*Velilla velilla*) from Trindade Island, which is located 1160 km from mainland Brazil were chosen as the reference for oceanic prey.

Stable isotope analysis

Whole humerus sections and prey muscle were lipid extracted using a soxhlet apparatus with a 2:1 solvent mixture of chloroform and methanol during a cycle of 4 h for bone collagen and 2 cycles of 10 h for prey muscle (Medeiros et al. 2015; Post et al. 2007). Then, samples were dried at 60°C in an oven for 24–48 h to remove the residual solvent. Prey muscles were ground into powder and 0.7 mg was loaded in tin capsules for further analysis. For humerus sections, it was used a microscope stereoscope to identify the LAGs in the untreated humerus sections with the stained humerus section as a guide (Avens et al. 2013). When a LAG was identified, the largest amount of

sample over the LAG circumference was manually collected with a low power micro motor with a 0.2 mm thick drill. Before the next LAG sampling the humerus section and the drill were rinsed with distilled water and dried in an oven at 60°C for 30 minutes. Each sample was loaded into sterilized silver capsules, and further acidified by 10% HCl using the “drop-by-drop” technique (Jacob et al. 2005) until no gas bubbles were produced (Medeiros et al. 2015), and dried in oven at 60°C.

All samples were analyzed by a continuous-flow isotope-ratio mass spectrometer (CF-IRMS, Thermo Finnigan Delta Plus XP, Bremen, Germany) coupled to an elemental analyzer (Costech ECS 4010, Milan, Italy) at the Stable Isotope Laboratory at Washington State University, School of Biological Sciences, Pullman, Washington, USA. Stable isotope ratios were expressed in δ notation as parts per thousand (‰) deviation from the international standards Vienna Pee Dee Belemnite limestone (carbon) and atmospheric air (nitrogen), as in equation 1:

$$\delta X(\text{‰}) = \left[\left(\frac{R_{\text{sample}}}{R_{\text{standard}}} \right) - 1 \right] \times 1000 \quad (1)$$

where R_{sample} and R_{standard} are the corresponding ratios of heavy to light isotopes ($^{13}\text{C}/^{12}\text{C}$ and $^{15}\text{N}/^{14}\text{N}$) in the sample and standard, respectively.

Statistical analysis

Stable isotope mixing models (SIMMs) were used to estimate prey source contribution for a bone collagen tissue analyzed based in the $\delta^{13}\text{C}$ and $\delta^{15}\text{N}$ values. The sample was divided in two groups, one group with an age at sampling ranging between 14 and 18 years old (younger individuals) and another group with an age range between 19 and 23 years old (older

individuals), and the SIMM was applied separately to each group. Moreover, it was included all LAGs sampled for each individual as replicates to analyze intra-individual variation. The trophic discrimination factor (TDF) for sea turtle bone collagen is not known. However, as a broad value averaged from different trophic webs, it is acceptable that $\delta^{13}\text{C}$ values increase at the scale of c. 1‰ between a consumer and its food source, while $\delta^{15}\text{N}$ values increase by c. 3–5‰ at each trophic level (Peterson & Fry 1987; Post 2002). Therefore, it was used a TDF of 1‰ for carbon and 3‰ for nitrogen. Neritic prey (crustaceans and demersal fish species) and oceanic prey (jellyfish species) were used in mixing models. SIMMs were not intended to infer the diet of olive ridley, but rather assess the different contributions of oceanic vs. neritic food sources, and thus complement inferences on the use of these two large marine habitat by the species.

Each LAG in sea turtles represent 1 year, and although in olive ridley it had not been validated, the closest Kemp's ridley sea turtle (*Lepidochelys kempii*), had been validated (Snover and Hohn 2004). Temporal consistency and degree of specialization were measured by the within-individual component (WIC), between-individual component (BIC) and total niche width (TNW) (Bolnick et al. 2003). These indexes were calculated by the variance of $\delta^{13}\text{C}$ and $\delta^{15}\text{N}$ values from each individual LAGs, as in Vander Zanden et al. (2013). WIC was a measure for temporal consistency while WIC/TNW ratio was a measure for individual specialization (Bolnick et al. 2003). ANOVA framework was used to compare variation within and between individuals to calculate proxies for WIC and BIC values (Matich et al. 2011; Vander Zanden

et al. 2013). The mean sum of squares within-individuals (MSW) measures the variability within individuals, which was used as a proxy for WIC:

$$MSW = \frac{\sum_i \sum_j (x_{ij} - \bar{x}_i)^2}{(N-k)} \quad (2)$$

The mean sum of squares between individuals (MSB) measures the variability among individuals and was a proxy for BIC:

$$MSB = \frac{\sum_i \sum_j (\bar{x}_i - \bar{x})^2}{(k-1)} \quad (3)$$

Where i represents an individual, j represents a LAG, N is the number of LAGs sampled and k is the number of individuals sampled. The sum of MSW and MSB is the proxy to TNW. For these calculations, the sample was also divided in two groups as in SIMM analysis.

Statistical inferences were performed within a Bayesian statistical framework (Ellison 2004) for the SIMM. The package used for the SIMMs was IsotopeR (Hopkins-III and Ferguson 2012), while frequentist statistical inference was used for the WIC and WIC/TNW ratio calculations. All analyses were performed with R software (R Core Team 2014) and the JAGS program (<http://mcmc-jags.sourceforge.net> [accessed 4 February 2015]) to specify models and perform the Bayesian analysis (Gilks et al. 1994).

Results

The sub-set of 20 humeri sections from olive ridley sea turtles ranged in size from 58.0 to 77.0 cm of CCL, with an age ranging between 14 and 23 year old (Petitet et al. 2015). Up to 5 LAGs from each specimen were collected, resulting in 82 LAGs sampled. These LAGs represented backcalculated sizes between 50.6 and 77.0 cm CCL, and backcalculated age range between 12

and 23 year old (Petitet et al. 2015). Individuals were classified as adults based in the age at sexual maturity (ASM) of olive ridley from Brazil (Petitet et al., 2015). Thus, 6 out of 20 individuals sampled were mature females due the presence of eggs formed in their oviducts, and another 14 individuals are within the size range of mature olive ridley sea turtles in the area (Silva et al. 2007), despite sex and maturation had not been determined.

$\delta^{13}\text{C}$ values ranged from -11.94‰ to -20.96‰ (mean \pm SD = $-15.45 \pm 1.35\text{‰}$) and $\delta^{15}\text{N}$ values ranged from 7.34‰ to 14.21‰ ($10.73 \pm 1.47\text{‰}$). For younger individuals, $\delta^{13}\text{C}$ values had a greater range when compared with older individuals (Fig. 1a; Fig. 1 S). $\delta^{15}\text{N}$ values increased with age (Fig. 1b), but the range was similar for all ages (Fig. 1 S).

$\delta^{13}\text{C}$ values demonstrated segregation in two groups based in age (Fig. 1a). For younger individuals the greatest contribution was from jellyfish following crustacean and demersal fish with minor contributions (Table 1; Fig. 2). Older individuals also had the greatest contribution of jellyfish, but crustacean had higher contribution than younger individuals, and demersal fish also had limited contribution (Table 1; Fig. 2). The two groups demonstrated a clearer inter-individual variation (Fig. 2), but the credibility interval from older individuals is much larger than for younger individuals (Table 1).

WIC of carbon and nitrogen, as a proxy for temporal consistency, was smaller for older individuals than for younger individuals (Table 2). However, the WIC/TNW ratio of carbon and nitrogen as a proxy of individual specialization was similar for both age groups (Table 2).

Discussion

In the present study, ontogenetic shifts in diet and habitat use of olive ridley sea turtles in northeastern Brazil were elucidated. Each sample from each LAG was considered as an integration of information throughout that given year, thus reflecting the “averaged” dietary and habitat stable isotope values for that time interval. Therefore, analysis of sequential LAGs should detect potential shifts of $\delta^{13}\text{C}$ and $\delta^{15}\text{N}$ values on annual time frames (Avens et al. 2013). We found that there is an ontogenetic shift 16 and 17 years old, which coincides with the mean of ASM (16.6 years old) of this population (Petitet et al. 2015).

Younger individuals had more variable $\delta^{13}\text{C}$ values than older individuals, which suggest that older turtles have temporal consistency in habitats and feeding, while youngsters use a range of habitats and food items (Post 2002). This interpretation is also in line with WIC values for $\delta^{13}\text{C}$ of older individuals 3–4 times lower than younger individuals (WIC = 0.76 and 2.63, respectively), as WIC is a proxy for temporal consistency (Bolnick et al. 2002). Younger individuals could be in a phase when they learn where have to go for foraging and development, thus consequently visit more habitats than older individuals and may ingest any sort of food items they find (Snover et al. 2007). In other vertebrate groups, juveniles are also less selective on feeding than adults, because they have to grow to minimize predation risk (Snover et al. 2007). Moreover, a consistency in $\delta^{13}\text{C}$ values seems to establish from 17 years old onward, shortly after of ASM (Petitet et al. 2015). ASM is the time when olive ridley turtles migrate to coastal waters to mate and nest (Plotkin 2010). Therefore, recruitment to the breeding population seems accompanied

by changes in diet and habitat use, after spending the immature phase in oceanic waters. Moreover, although there is a high temporal consistency in older individuals, there is also a high degree of individual variation among them (Fig. 1 S)

Overall, $\delta^{15}\text{N}$ values increased with age, with small oscillations in each individual trajectory. As there is a high probability that younger individuals were at oceanic waters, pelagic prey such as jellyfish are supposedly commonly found by turtles in this habitat. On their turn, older individuals, most likely mature individuals, may forage in neritic areas, and eventually travel to areas offshore the continental shelf, which is narrow in northeastern Brazil. Colman et al. (2014) demonstrated that demersal fish and crustaceans had great importance in olive ridley diet at the study area, based mainly on adults stranded dead.

SIMM also demonstrated differences in habitats used by younger vs. older individuals. Younger individuals showed major contribution by jellyfish, most likely, as they were in oceanic waters in previous years. Moreover, some of these younger individuals were in the range size of mature adults (Silva et al. 2007), despite not all turtles have the same size at sexual maturity (SSM) (Avens et al. 2015; Petit et al. 2015). Although older individuals also had jellyfish as the main contributing source, crustacean contribution was greater than for younger individuals group. At northeastern Brazilian coast this species has three post-nesting migration patterns, travel vast distances to oceanic waters, or neritic waters south or northward from the nesting beach at Sergipe state (Silva et al. 2011). At nesting beaches in the eastern Pacific coast, the same three post-nesting migrations patterns were detected

(Morreale et al. 2007; Plotkin 2010). Therefore, the crustacean contribution may be from mature turtles that migrated to neritic foraging grounds after nesting and stayed there until the next nesting season. In addition, in the group of older individuals there were seven identified as mature females because there had fully formed eggs in their oviducts, and therefore the crustacean contribution may be from these mature females from neritic feeding grounds.

Post-nesting migration patterns generate high level of inter-individual variation, which was demonstrated by isotopic mixing models (see individual gray lines in Fig. 2), and corroborated by WIC/TNW ratio values for both $\delta^{13}\text{C}$ and $\delta^{15}\text{N}$ which both had lower values (Table 2; Bolnick et al. 2003). For both younger and older individuals the WIC/TNW ratios for $\delta^{13}\text{C}$ and $\delta^{15}\text{N}$ were more close to 0 than 1, suggesting a moderate level of individual specialization (Bolnick et al. 2002). Due to high variability in migration patterns of adult olive ridley among individuals (Silva et al. 2011), individuals seems to end up specializing, because they migrate to different habitats with different resources available. Moreover, migration to varied areas may relax intraspecific competition, increasing individual specialization due to low density (Araújo et al. 2011).

The level of individual specialization indicated by $\delta^{15}\text{N}$ values was higher than for $\delta^{13}\text{C}$. Although younger individuals had slightly higher level of individual specialization indicated by $\delta^{13}\text{C}$ than older individuals, the level of individual specialization indicated by $\delta^{15}\text{N}$ was identical for both groups (WIC/TNW = 0.09). Even after recruitment they may not change trophic level if the food web baseline is the same, as expected given homogeneous

isoscapes in northeastern Brazil (McMahon et al. 2013). Adult loggerhead and green sea turtles studied by Vander Zanden et al. (2013) and Pajuelo et al. (2016) also had similar levels of specialization for $\delta^{15}\text{N}$, but $\delta^{13}\text{C}$ seems indicate higher specialization than found for olive ridley sea turtles in the current study. Notwithstanding, adult loggerhead and green sea turtles use to forage mostly near the coast, while olive ridley has, in addition to foraging grounds near the coast, also forage in oceanic waters (Silva et al. 2011), two marine realms with contrasting $\delta^{13}\text{C}$ values (McMahon et al. 2013).

WIC values based on $\delta^{13}\text{C}$ and $\delta^{15}\text{N}$ as proxy for temporal consistency were higher for older than younger individuals, as expected. However, temporal consistency for $\delta^{15}\text{N}$ was higher than $\delta^{13}\text{C}$, most likely due to olive ridley recruiting to neritic waters from oceanic waters where they inhabited before maturation, which has more contrasting $\delta^{13}\text{C}$ than $\delta^{15}\text{N}$ values.

Conclusions

This study demonstrated that olive ridley sea turtles nesting in southwestern Atlantic Ocean are better classified as a generalist population with specialist individuals; the population is heterogeneous, composed by groups of individuals with distinct diets, using a range of habitats during the non-nesting period. However, because sampled LAGs integrates a full year of habitat use and feeding $\delta^{13}\text{C}$ and $\delta^{15}\text{N}$ values could also be a mixture of neritic and oceanic habitats. Olive ridley sea turtle could migrate between these habitats to reproduce or between neritic habitats with different isotopic values along the year (Silva et al. 2007).

Variable migration patterns of olive ridley sea turtles increase threats to this species, with shrimp trawl fisheries near nesting beaches, shrimp and finfish trawler all along the Brazilian continental shelf, and longline fisheries in oceanic waters (Sales et al 2008; Silva et al. 2010). Therefore, it is essential a better understanding about the year-round cycle of this species, aiming subsidizes conservation plans and decrease adult mortality.

Acknowledgements We acknowledge the TAMAR-ICMBio and Fundação Mamíferos Aquáticos – FMA staffs for humeri samples, with special thanks to Ederson Luiz Fonseca, Fabio Lira, Mari Weber, Jociery Vergara Parente, Bruno Almeida and veterinarians for their support. Bone sampling was possible due to the support of PRMEA (Regional Monitoring Program of Strandings and Abnormalities), a measure of environmental impact assessment required by federal environmental licensing for oil and gas exploration, conducted by IBAMA, Instituto Brasileiro do Meio Ambiente e dos Recursos Naturais Renováveis. Sampling of humeri for stable isotope analysis was carried out with logistics provided by the Laboratório de Ecologia da Megafauna Marinha (Instituto de Oceanografia – FURG), with special thanks to Eduardo R. Secchi and Silvina Botta. We are in debt with Hannah Vander Zanden for support on niche specialization and scripts for R analysis. Authors are also grateful to A.S. Martins, E.R. Secchi, P.G. Kinas, M. Haimovici and S. Botta, for careful revisions of the MS. R.P. received financial support from the Coordenação de Aperfeiçoamento de Pessoal de Nível Superior (CAPES). L.B. is a research fellow of the Brazilian CNPq, National Council for Scientific and Technological Development (Proc. No.

310550/2015–7). This research is part of the PhD thesis written by R.P. under the guidance of L.B.

References

- Albernaz TL, Secchi ER, Oliveira LR, Botta S (2017) Ontogenetic and gender-related variation in the isotopic niche within and between three species of fur seals (genus *Arctocephalus*). *Hydrobiologia* 787:1213–139.
- Araújo MS, Bolnick DI, Layman CA (2011) The ecological causes of individual specialisation. *Ecol Lett* 14:948–958
- Avens L, Goshe LR, Pajuelo M, Bjorndal KA, MacDonald BD, Lemons GE, Bolten AB, Seminoff JA (2013) Complementary skeletochronology and stable isotope analyses offer new insight into juvenile loggerhead sea turtle oceanic stage duration and growth dynamics. *Mar Ecol Prog Ser* 491: 235–251
- Avens L, Goshe LR, Coggins L, Snover ML, Pajuelo M, Bjorndal KA, Bolten AB (2015) Age and size at maturation and adult stage duration for loggerhead sea turtles in the western North Atlantic. *Mar Biol* 162:1749–1767
- Bearhop S, Adams CE, Waldron S, Fuller RA, Macleod H (2004) Determining trophic niche width: a novel approach using stable isotope analysis. *J Anim Ecol* 73:1007–1012
- Bolnick DI, Yang LH, Fordyce JA, Davis JM, Svanback R (2002) Measuring individual-level resource specialization. *Ecology* 83:2936–2941

- Bolnick DI, Svanback R, Fordyce JA, Yang LH, Davis JM, Hulseley CD, Forister ML (2003) The ecology of individuals: incidence and implications of individual specialization. *Am Nat* 161:1–28
- Bugoni L, McGill RAR, Furness RW (2010) The importance of pelagic longline fishery discards for a seabird community determined through stable isotope analysis. *J Exp Mar Biol Ecol* 391:190–200
- Castilhos JC, Coelho AC, Argolo JF, Santos EAP, Marcovaldi AM, Santos ASS, Lopez M (2011) Avaliação do estado de conservação da tartaruga marinha *Lepidochelys olivacea* (Eschscholtz, 1829) no Brasil. *Biodiv Bras* 1:28–36
- Colman LP, Sampaio CLS, Weber MI, Castilhos JC (2014) Diet of olive ridley sea turtles, *Lepidochelys olivacea*, in the waters of Sergipe, Brazil. *Chelonian Conserv Biol* 13:266–271
- Di Benedetto APM, Moura JF, Siciliano S (2015) Feeding habits of the sea turtles *Caretta caretta* and *Lepidochelys olivacea* in south-eastern Brazil. *Mar Biodiv Rec* 8:1–5
- Ellison AM (2004) Bayesian inference in ecology. *Ecol Lett* 7:509–520
- Fry B (2006) Stable isotope ecology. Springer, New York, NY
- Gilks WR, Thomas A, Spiegelhalter DJ (1994) A language and program for complex Bayesian modeling. *Statistician* 43:169–177
- Hopkins-III JB, Ferguson JM (2012) Estimating the diets of animals using stable isotopes and a comprehensive Bayesian mixing model. *PLoS ONE* 7:e28478
- IUCN (2015) Red list of threatened species. Version 2015–4. <www.iucnredlist.org>. Accessed on 02 May 2016

- Jacob U, Mintenbeck K, Brey T, Knust R, Beyer K (2005) Stable isotope food web studies: a case for standardized sample treatment. *Mar Ecol Prog Ser* 287:251–253
- Matich P, Heithaus MR, Layman CA (2011) Contrasting patterns of individual specialization and trophic coupling in two marine apex predators. *J Anim Ecol* 80:294–305
- McMahon KW, Hamady LL, Thorrold SR (2013) A review of ecogeochemistry approaches to estimating movements of marine animals. *Limnol Oceanogr* 58:697–714
- Medeiros L, Monteiro DS, Petitet R, Bugoni L (2015) Effects of lipid extraction on the isotopic values of sea turtle bone collagen. *Aquat Biol* 23:191–199
- Morreale SJ, Plotkin PT, Shaver DJ, Kalb HJ (2007) Adult migration and habitat utilization: ridley turtles in their element. In: Plotkin PT (ed) *Biology and conservation of ridley sea turtles*. Johns Hopkins University Press, Baltimore, MD, p 213–229
- Newsome SD, Tinker MT, Monson DH, Oftedal OT, Ralls K, Staedler MM, Fogel ML, Estes JA (2009) Using stable isotopes to investigate individual diet specialization in California sea otters (*Enhydra lutris nereis*). *Ecology* 90:961–974
- Pajuelo M, Bjorndal KA, Arendt MD, Foley AM, Schroeder BA, Witherington BE, Bolten AB (2016) Long-term resource use and foraging specialization in male loggerhead turtles. *Mar Biol* 163:235
- Peterson BJ, Fry B (1987) Stable isotopes in ecosystem studies. *Ann Rev Ecol System* 18:298–320

- Petit R, Avens L, Castilhos JC, Kinas PG, Bugoni L (2015) Age and growth of olive ridley sea turtles *Lepidochelys olivacea* in the main Brazilian nesting ground. *Mar Ecol Prog Ser* 541:205–218
- Plotkin PT (2010) Nomadic behaviour of the highly migratory olive ridley sea turtle *Lepidochelys olivacea* in the eastern tropical Pacific Ocean. *Endang Species Res* 13:33–40
- Post DM (2002) Using stable isotopes to estimate trophic position: models, methods, and assumptions. *Ecology* 83:703–718
- Post DM, Layman CA, Arrington DA, Takimoto G, Quattrochi J, Montaña CG (2007) Getting to the fat of the matter: models, methods and assumptions for dealing with lipids in stable isotope analyses. *Oecologia* 152:179–189
- R Core Team (2014) R: A language and environment for statistical computing. R Foundation for Statistical Computing, Vienna, www.R-project.org
- Ramirez MD, Avens L, Jeminoff JA, Goshe LR, Heppell SS (2015) Patterns of loggerhead turtle ontogenetic shifts revealed through isotopic analysis of annual skeletal growth increments. *Ecosphere*, 6:1–17
- Reichert HA (1993) Synopsis of biological data on the olive ridley sea turtle *Lepidochelys olivacea* (Eschscholtz, 1982) in the western Atlantic. NOAA Tech Memo NMFS–SEFSC–336
- Sales G, Giffoni BB, Barata PCR (2008) Incidental catch of sea turtles by the Brazilian pelagic longline fishery. *J Mar Biol Assoc UK* 88:853–864
- Schell DM, Saupe SM, Haubenstock N (1989) Bowhead whale (*Balaena mysticetus*) growth and feeding as estimated by $\delta^{13}\text{C}$ techniques. *Mar Biol* 103:433–443

- Silva ACCD, Castilhos JC, Lopez GG, Barata PCR (2007) Nesting biology and conservation of the olive ridley sea turtle (*Lepidochelys olivacea*) in Brazil, 1991/1992 to 2002/2003. *J Mar Biol Assoc UK* 87:1047–1056
- Silva ACCD, Castilhos JC, Santos EAP, Brondízio LS, Bugoni L (2010) Efforts to reduce sea turtle bycatch in the shrimp fishery in northeastern Brazil through a co-management process. *Ocean Coast Manage* 53:570–576
- Silva ACCD, Santos EAP, Oliveira FLC, Weber MI, Batista JAF, Serafini TZ, Castilhos JC (2011) Satellite-tracking reveals multiple foraging strategies and threats for olive ridley turtles in Brazil. *Mar Ecol Prog Ser* 443:237–247
- Snover ML, Hohn AA (2004) Validation and interpretation of annual skeletal marks in loggerhead (*Caretta caretta*) and Kemp's ridley (*Lepidochelys kempii*) sea turtles. *Fish Bull* 102:682–692
- Snover ML, Avens L, Hohn AA (2007) Back-calculating length from skeletal growth marks in loggerhead sea turtles *Caretta caretta*. *Endang Species Res* 3:95–104
- Vander Zanden HB, Bjorndal KA, Reich KJ, Bolten AB (2010) Individual specialists in a generalist population: results from a long-term stable isotope series. *Biol Lett* 6:711–714
- Vander Zanden HB, Bjorndal KA, Bolten AB (2013) Temporal consistency and individual specialization in resource use by green turtles in successive life stages. *Oecologia* 173:767–777

Table 1 Prey source contribution based in $\delta^{13}\text{C}$ and $\delta^{15}\text{N}$ values in bone collagen tissue of olive ridley sea turtles (*Lepidochelys olivacea*) stranded dead on northeastern Brazil, by groups separated in younger individuals (14–18 year old) and late adults (19–23 year old) individuals

Age interval (year)	N	Jellyfish		Demersal Fish		Crustacean	
		Mean (%)	CrI (%)	Mean (%)	CrI (%)	Mean (%)	CrI (%)
14–18	8	72	45–97	0.7	0–8	26	2–55
19–23	12	58	0–99	7	0–99	34	0–99

Table 2 Within–individual component (WIC), between–individual component (BIC) and total niche width (TNW) values calculated from ANOVA framework of carbon and nitrogen stable isotopes in lines of arrested growth in humeri of olive ridley sea turtles (*Lepidochelys olivacea*) from two different age groups in northeastern Brazil

Age interval (year)	N	$\delta^{13}\text{C}$				$\delta^{15}\text{N}$			
		WIC	BIC	TNW	WIC/TNW	WIC	BIC	TNW	WIC/TNW
14–18	8	2.63	5.58	8.21	0.32	0.86	8.92	9.78	0.09
19–23	12	0.76	0.96	1.72	0.44	0.35	3.35	3.70	0.09

FIGURE LEGENDS

Fig. 1 $\delta^{13}\text{C}$ (a) and $\delta^{15}\text{N}$ (b) values for each line of arrested growth (LAG) sampled from olive ridley sea turtles (*Lepidochelys olivacea*) humeri. Each trajectory represents an individual and each LAG represents an age from this individual

Fig. 2 (a) Stable isotope values ($\delta^{13}\text{C}$, $\delta^{15}\text{N}$, in ‰) in bone collagen tissue in lines of arrested growth (LAG) which is related to an age range of 12 and 18 year (group 1; black crosses) and an age range of 19 and 23 year (group 2; gray crosses) from individuals of olive ridley sea turtles (*Lepidochelys olivacea*). (b) proportional dietary contributions (expressed as marginal posterior distributions) of different potential sources: jellyfish (triangle), demersal fish (circle) and crustacean (square) for group 1 and group 2. Gray lines indicate each LAG sampled, dashed line is the mean of diet contribution for each group and the solid line in the middle is the mean diet contribution for the whole sample

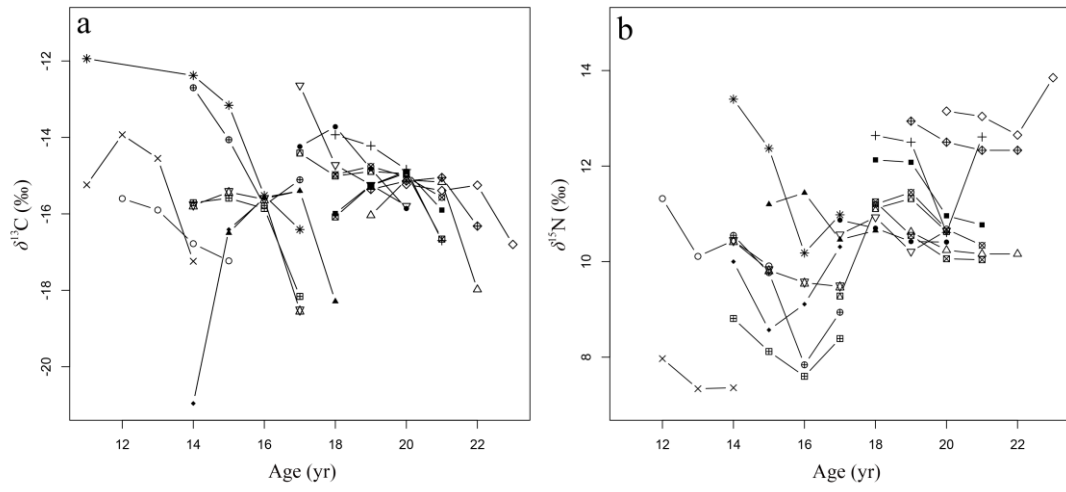


Figure 1

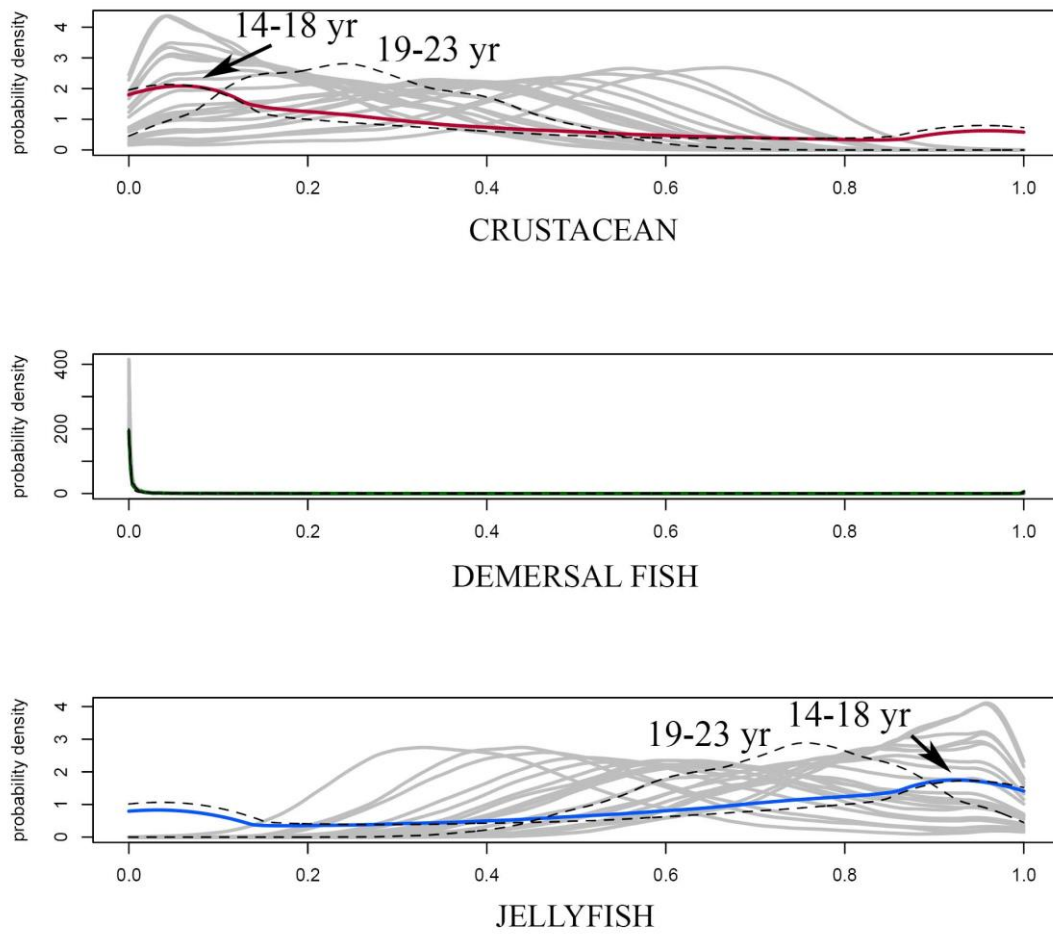


Figure 2

The following supplements accompany the article

Individual specialization and temporal consistency in resource use by olive ridley sea turtles (*Lepidochelys olivacea*) inferred by stable isotope analysis in humerus

Roberta Petitet^{1,2}, Jaqueline C. Castilhos³, Leandro Bugoni¹

¹ **Laboratório de Aves Aquáticas e Tartarugas Marinhas, Instituto de Ciências Biológicas, Universidade Federal do Rio Grande (FURG), Campus Carreiros, Avenida Itália s/n, CP 474, 96203–900, Rio Grande, RS, Brazil**

² **Programa de Pós-Graduação em Oceanografia Biológica, Instituto de Oceanografia, Universidade Federal do Rio Grande (FURG), Campus Carreiros, Avenida Itália s/n, CP 474, 96203–900, Rio Grande, RS, Brazil**

³ **Fundação Centro Brasileiro de Proteção e Pesquisa das Tartarugas Marinhas, Reserva Biológica de Santa Isabel s/n, Centro, 49190–000, Pirambu, SE, Brazil**

* **Corresponding author Email: rpetitet@hotmail.com**

SUPPLEMENT 1. Results

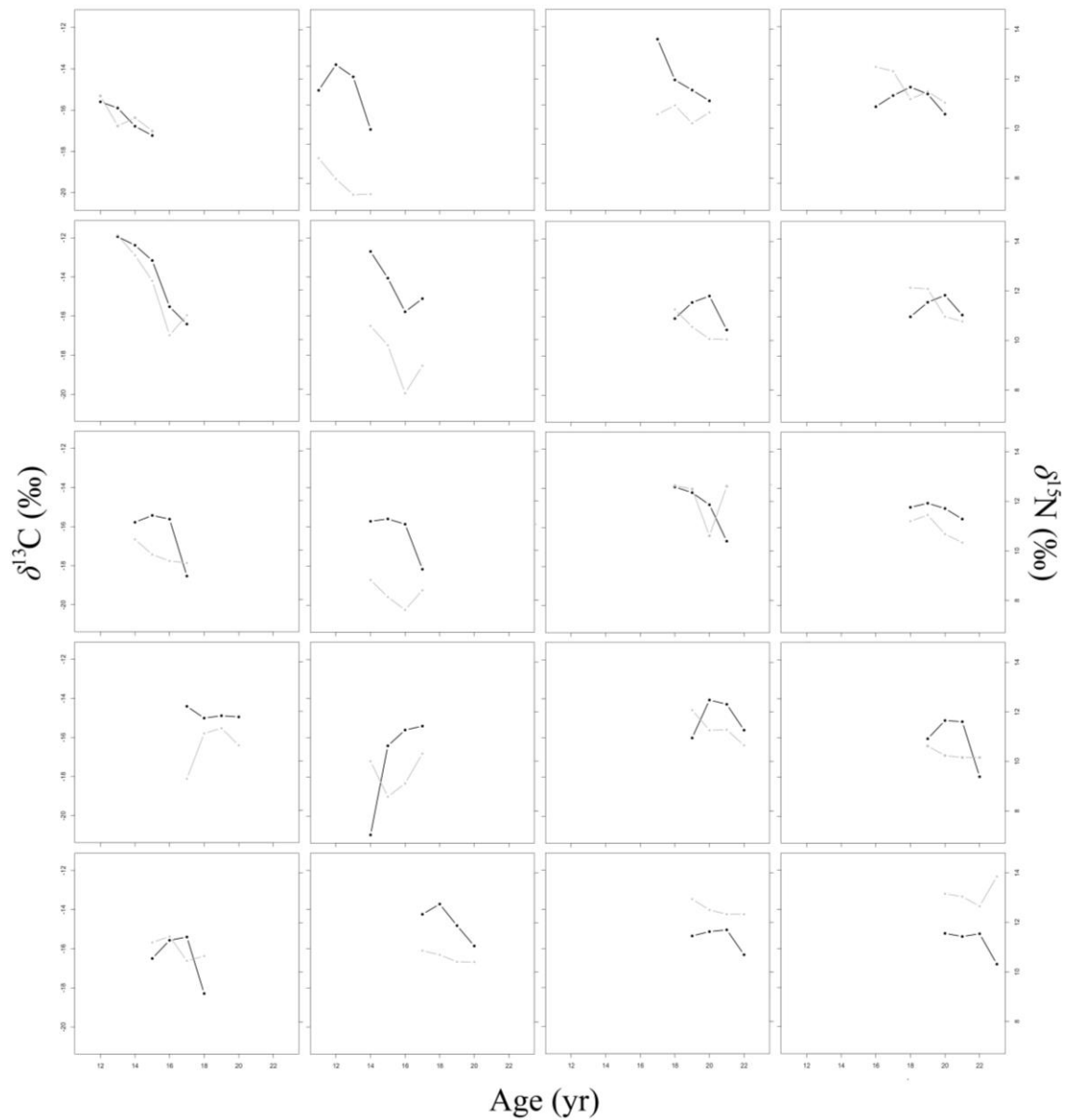


Fig. S1. $\delta^{13}\text{C}$ and $\delta^{15}\text{N}$ values related to each line of arrested growth (LAG) that it is referring to each age. Each plot is referred to each individual sampled, gray lines is the trajectory of $\delta^{15}\text{N}$ values and black lines also is the trajectory of $\delta^{13}\text{C}$ values from each LAG